# MASTER'S THESIS PROPOSAL

| | |
|---|---|
| study programme: | Civil Engineering |
| study branch: | Advanced Masters in Structural Analysis of Monuments and Historical Constructions |
| academic year: | 2017/2018 |

| | |
|---|---|
| Student's name and surname: | Pratik Gajjar |
| Department: | Department of Mechanics |
| Thesis supervisor: | Prof. Pavel Kuklik |
| Thesis title: | Nonlinear numerical evaluation of the wall bearing capacity and the structure stability of the St. Ann Church from the Broumov Group of Churches |
| Thesis title in English | see above |

Framework content:    The main objective of this thesis is the Finite element analysis and evaluation of current bearing condition of the St. Ann Church from Broumov Group of Churches. To accomplish this objectives, a site visit was done in which visual inspection of the church, rebound hammer test and thermography was carried out.FEM analysis of the wall samples were carried out to evaluate the bearing capacity.A 3D FEM analysis was perfromed to stimulate the differential settlements presents on the site. From this analysis it was concluded that structure is suffering from the differential settlements mainly due to the poor surface and groundwater drainage around the church and for that possible intervention techniques are presented.

Assignment date:  9/04/2018                    Submission date:    02/07/2018

If the student fails to submit the Master's thesis on time, they are obliged to justify this fact in advance in writing, if this request (submitted through the Student Registrar) is granted by the Dean, the Dean will assign the student a substitute date for holding the final graduation examination (2 attempts for FGE remain). If this fact is not appropriately excused or if the request is not granted by the Dean, the Dean will assign the student a date for retaking the final graduation examination, FGE can be retaken only once. (Study and Examination Code, Art 22, Par 3, 4.)

*The student takes notice of the obligation of working out the Master's thesis on their own, without any outside help, except for consultation. The list of references, other sources and names of consultants must be included in the Master's thesis.*

......................................................                    ......................................................
Master's thesis supervisor                                              Head of department

Date of Master's thesis proposal take over:      July 2018

......................................................
Student

# DECLARATION

Name:                           Pratik Gajjar

Email:                          pratik.gajjar@hotmail.com


Title of the                    Nonlinear numerical evaluation of the wall bearing capacity and the structure
MSc Dissertation:               stability of the St. Ann Church from the Broumov Group of Churches

Supervisor(s):                  Prof. Pavel Kuklik

Year:                           2017/2018


I hereby declare that all information in this document has been obtained and presented in accordance with academic rules and ethical conduct. I also declare that, as required by these rules and conduct, I have fully cited and referenced all material and results that are not original to this work.


I hereby declare that the MSc Consortium responsible for the Advanced Masters in Structural Analysis of Monuments and Historical Constructions is allowed to store and make available electronically the present MSc Dissertation.


University:                     Czech Technical University

Date:                           02-07-2018

Signature:
                                _____

This page is left blank on purpose.

To my friends, family and faculty members!

"दायरा हर बार बनाता हूँ ज़िन्दगी के लिए,

लकीरे वही रहती है,

मैं खिसक जाता हूँ."

This page is left blank on purpose.

## ACKNOWLEDGEMENTS

This dissertation thesis consumed huge amount of work, research and dedication. Still, implementation of this project would not have been possible if I did not have support of many individuals. Therefore, I would like to extend my sincere gratitude to all of them.

First of all, I am sincerely thankful to my supervisor Prof. Kuklik for his provision of expertise, and technical support in the implementation in this study. Without his support, knowledge and experience, the study would be deficient in quality of outcomes, and thus his support has been essential.

I am also indebted to Dr. Sněhota, Dr. Kovarova, Dr. Zalesky and Dr. Valek for their constant guiding and support, from which it was possible to know about the history, current state, material and modelling strategy employed in this case study.

I am also grateful to Dr. Pukl for his support, teaching and guidance with the ATENA software.

I would like to express my gratitude to Cervenka consulting and Fine Software, for providing us with the ATENA and Geo 5 software.

I would like to express my sincere thank towards Prof. Kabele and Ms. Alexandra, who help me in implementation of this project.

Nevertheless, I would like to express my sincere gratitude towards Mr. Jacopo and other SAHC colleagues for their constant support and facilitate to ponder on my project work any way possible by them.

This page is left blank on purpose.

## ABSTRACT

The Czech Republic is blessed with the rich history of events and as a consequence of these events, many architectural heritages came into existent and became a symbol of the rich history. Within this wide variety of monuments, baroque architecture can be considered as a heart of this region's legacy. One such case is the case of Broumov Group of Churches, which is very significant not only for its unique Baroque architecture but also for the short duration of construction and relation between the single client and a single family of architects. St. Ann's Chruch, which was built by the Killian Ignaz Dientzenhofer, is situated on the sloping ground of Viznov. The church which was built in a short duration in early 18th Century has witnessed many events in its life of 300 years. Due to its remote location and lack of maintenance over the decades, this church can be found in the damaged condition presently. This case of the study was aimed at providing the probable cause of these damages and some preventive intervention methods.

This report summarizes the visual investigation, structural investigation using ATENA 2D software, Geo 5 geotechnical FEM software and DIANA FEM software, to assess and verify the safety of the church walls regarding the damages it currently suffers. With regards to the material and sub-soil data available, micro modelling of different wall configuration in longitudinal and transversal direction was done with ATENA 2D software to evaluate the safe bearing capacity of the walls, from the analysis it was found that the current bearing capacity of the walls are higher than the values recommended by the Eurocodes. From this 2D FEM analysis, a set of homogeneous properties were also computed, which were later used in the geotechnical and 3D macro FEM analysis. In Geo5 software, the effect of sub-soil conditions was analyzed, and it was observed that, for the present condition of the soil, the church suffers from the differential settlements between the area where drainage water is accumulated and have a disintegrating effect on the subsoil. To analyse the extent of damage on the church walls due to the differential soil settlements, a 3D analysis was carried out considering the equivalent spring elements for the boundary interface. From the non-linear vertical pushover analysis, it was found the amount of soil settlements from 3D analysis and geotechnical analysis were within the tolerance limits and the crack strains induced at the different locations are matching with the cracks observed on the site. After finding the probable cause of differential settlements and its adverse effect on the walls, preventive measurements, such as, monitoring, execution of roof and ground drainage works, were proposed and for the long-term intervention, grout injection for walls and sub-soil, re-plastering of walls are proposed in this case study.

**Keywords:** Soil-structure Interaction, Nonlinear analysis, Wall Bearing Capacity, Micromodeling

This page is left blank on purpose.

## ABSTRAKT

Česká republika se honosí bohatou historickou minulostí, s kterou je spjato architektonické dědictví, jež ve svém důsledku tuto bohatou historii symbolizuje. Mezi všemi architektonickými styly pak barokní architektura hraje zcela výjimečnou úlohu. Jedním z takových barokní skvostů je Broumovská skupina kostelů, která byla postavena v krátkém období jedním stavebníkem a jednou rodinou architektů. Kostel Sv. Anny byl postaven Kiliánem Ignácem Dientzenhoferem. Je situován na svažujícím se území obce Vižňov. Kostel byl postaven během krátké doby na začátku 18. století. Během své třistaleté historie pamatuje mnoho událostí. Díky své vzdálené poloze a nedostatečné údržbě v průběhu několika dekád je v současnosti v značně poškozeném stavu. Tato studie si kladla za cíl stanovit pravděpodobné příčiny poruch a doporučená sanační opatření. Práce sumarizuje šetření na místě, analýzu konstrukce pomocí kódu ATENA 2D, geotechnického programu Geo5 MKP a DIANA MKP. Pomocí programů byla posouzena a ověřena bezpečnost stěn kostela z pohledu současného poškození. Z dostupných materiálových parametrů a dostupných dat  týkajících se podloží bylo provedeno určité mikromodelování rozdílných konfigurací modelů zdí, a to jak v podélném směru, tak i příčném. Programem ATENA 2D pro dané konfigurace byla odhadována únosnost a následnou analýzou pak stanovena únosnost zdí jako celku. Tato je větší než hodnoty doporučované Eurokódy. Z analýzy 2D MKP byly stanoveny homogenizované parametry, které později byly použity při geotechnickém I 3D makro MKP modelování. Podloží bylo analyzováno programem Geo5. Bylo shledáno, že současný stav kostela je způsoben nerovnoměrným sedáním způsobeným zejména akumulovanou vodou díky špatným drenážím, které navíc způsobí degradaci zeminy. Progrese poruch zdí byla analyzována ve 3D. Podloží bylo modelováno ekvivalentními pružinami na hranici. Byla provedena nelineární analýza svislého sedání a ověřeno, že 3D analýza a geotechnická analýza jsou v dobré shodě. Rovněž se ukázalo, že místa vypočtených porušení dobře kopírují trhliny na skutečné konstrukci. Po ověření příčin nerovnoměrného sedání základů a jejich nepříznivých účinků na stěny kostela, byla navržena kontrolní měření a monitorování, provedení spolehlivého odvodnění střechy i zemních drenáží. Z dlouhodobého hlediska pak byly navrženy injektáže stěn a podloží, rovněž tak nová omítka.

**Klíčová slova:** Interakce půdních struktur, Nelineární analýza, Nosnost na stěnách, Mikromodelování

This page is left blank on purpose.

## ઉપસંહાર

ઝેક પ્રજાસતાકને ઇતિહાસ ની ઘણી મહત્વની ઘટનાઓના આશીર્વાદ આપવામાં આવ્યા છે. અને આ ઘટનાઓના પરિણામે આ દેશ માં ઘણા મહત્વના પુરાતત્વ સંસ્થાપનો બનાવામાં આવ્યા હતા, અને હાલ માં આ દેશ એક સમૃદ્ધ ઇતિહાસ નું પ્રતીક બની ગયું છે. આ વિવિધ સ્મારકો ની અંદર, બરોક સ્થાપત્યોને આ ક્ષેત્રની વારસોના હૃદય તરીકે ગણવામાં આવે છે. આવોજ એક ઉદાહરણ બ્રોમોવ જૂથ ના ખ્રિસ્તી ગિરજાઘરો નો છે. આ જૂથ ખાલી તેના અનન્ય બરોક સ્થાપત્યો માટે જ નહિ પણ તેના બાંધકામ ના ટૂંકા ગાળા, અને એકજ ગ્રાહક અને શિલ્પકારના એકજ પરિવાર વચ્ચે ના સંબંધ માટે પણ જાણીતો છે. આ જૂથ નો એક ગિરજાઘર, મહાત્મા એન ના નામથી બનેલો છે, જે કિલિઅન ઇગ્નાઝ ડિન્ટેઝેનહોફર દ્વારા બનાવવામાં આવી હતી. આ ઇમારત વિઝનોવ ગામની ઢાળવાળી જમીન પર બનેલી છે. ૧૮ મી સદીની શરૂઆતમાં ટૂંકા સમયગાળામાં બાંધવામાં આવેલી આ ઇમારતે, ૩૦૦ વર્ષનાં તેના જીવનમાં ઘણી ઘટનાઓની સાક્ષી બની છે. તેના દૂરસ્થ સ્થાન અને દાયકાઓ સુધી જાળવણીની અછતને લીધે, આ ઇમારત હાલની ક્ષતિગ્રસ્ત સ્થિતિમાં મળી શકે છે. અભ્યાસના આ કિસ્સામાં આ નુકસાનોના સંભવિત કારણ અને કેટલાક નિવારક હસ્તક્ષેપ પદ્ધતિઓ આપવાનું લક્ષ્ય હતું.

આ રિપોર્ટ ATENA ૨D સોફ્ટવેર, GEO ૫ જીઓટેક્નિકેક એફ.ઈ.એમ સોફ્ટવેર અને DIANA એફ.ઈ.એમ સોફ્ટવેરનો ઉપયોગ કરીને પ્રારંભિક દ્રષ્ટિકરણ અને માળખાકીય તપાસનો સારાંશ આપે છે. બાંધકામમાં વપરાયેલા પથ્થરો અને જામીનની માટીની માહિતી ઉપલબ્ધ હોવાના સંદર્ભમાં, સમાંતર અને કાટખૂણા દિશામાં જુદી જુદી દીવાલ સંમિશ્રણની સૂક્ષ્મ મોડેલીંગ ATENA ૨D સોફ્ટવેર સાથે દિવાલની સુરક્ષિત ક્ષમતાનું મૂલ્યાંકન કરવામાં આવ્યું હતું, વિશ્લેષણમાંથી જાણવા મળ્યું છે કે દીવાલોની વર્તમાન ક્ષમતા યુરોકોડ દ્વારા ભલામણ કરાયેલા મૂલ્યો કરતા વધારે છે. આ ૨D એફ.ઈ.એમના વિશ્લેષણમાંથી, સમાન-સરખી ગુણધર્મોનો સમૂહ પણ ગણતરી કરવામાં આવ્યો હતો, જેનો ઉપયોગ પાછળથી જીઓટેક્નિકલ અને ૩D મેક્રો એફ.એ.એમ વિશ્લેષણમાં કરવામાં આવ્યો હતો. GEO ૫ સોફ્ટવેરમાં પેટા-માટીની પરિસ્થિતિઓની અસરનું વિશ્લેષણ કરવામાં આવ્યું હતું અને તે જોવા મળ્યું હતું કે, જમીનની હાલની હાલતથી, ઇમારત તે વિસ્તારના જમીન વચ્ચેના તફાવતથી પીડાય છે જ્યાં વરસાદનું પાણી સંચિત થાય છે અને તેના પર વિઘટનિત અસર કરે છે. ભૂગર્ભમાં વિભિન્ન જમીનની વસાહતોને કારણે ઇમારતની દીવાલો પર નુકસાનની હદનું વિશ્લેષણ કરવા માટે, ૩D વિશ્લેષણ હાથ ધરવામાં આવ્યું હતું, જેમાં ઇમારતના પાયાના સહારા તરીકે સ્પ્રિંગ બનાવવામાં આવી હતી. બિન-રેખીય લંબરુપ પુશોવર વિશ્લેષણથી, તે મળી આવ્યું હતું કે ૩D વિશ્લેષણ અને જીઓટેક્નિકલ વિશ્લેષણના પાયાના તફાવતોના મૂલ્યો સહનશીલતા મર્યાદાની અંદર હતા અને વિવિધ સ્થાનો પર પ્રેરિત તિરાડો સાઇટ પર જોવાયેલા તિરાડોથી મેળ ખાતા હોય છે. દિવાલ પર વિભિન્ન વસાહતોના સંભવિત કારણ અને તેની પ્રતિકૂળ અસર શોધવા પછી, નિવારક માપ, જેમ કે દેખરેખ, છત અને ગ્રાઉન્ડ ડ્રેનેજ કાર્યોનું અમલીકરણ, પ્રસ્તાવિત અને લાંબા ગાળાના હસ્તક્ષેપ માટે, દિવાલો અને પાયા માટે ગ્રાઉટ ઇન્જેક્શન અને દીવાલો ઉપર પાછો લેપ કરવાની દરખાસ્ત આ અભ્યાસ માં કરવામાં આવી છે.

This page is left blank on purpose.

## TABLE OF CONTENTS

## LIST OF FIGURES

## LIST OF TABLES

## LIST OF GRAPHS

# 1   INTRODUCTION



Figure 1.1 - Prague Skyline  **(Vinyl Silhouettes, 2018)**

Czech Republic, this small country is in the middle of Europe – surrounded by a ring of bordering mountains, settled by the Slavs and formed by the historical territories of Bohemia, Moravia, and Silesia – has been the crossroads of important trade routes and their accompanying economic and power struggles, as well as diverse cultural influences, since time immemorial. During and after the Premyslid dynasty, many constructions started to flourish around the country.  (Tourism, 2017)

Cultural heritage is a very integral part of Czech Republic's material and intellectual resources. Here, heritage is artistically and historically rich and diverse and highly authentic in nature. In addition to material heritage in form of such tangible cultural heritage, Czech cultural heritage can also well define by an intangible heritage. Different from the current construction practice, constructions from the past were typically designed based on a set of geometrical rules, established by the former generations of constructors. With the rational design practices were formulated only during the 17th Century, many of these formulations had limited knowledge of different construction material or subsoil properties. And therefore, many of the constructions were either under-designed or over-designed. The constructions, which are survived till today belongs to the latter category, yet they suffered greatly from the structural or non-structural damages and decays during their long history of standing. In the Czech Republic, the problem of deterioration of structures is very frequent, mainly due to the lack of maintenance because of the centralized state ownership of most of the properties during the communist regime. With many examples available of such kinds, the study of this report is subjected to the Broumov group of churches.

The Broumov region is in one of the northeast elongations of Czech by the border with Poland, surrounded by the bizarre natural rock formations. This region is consisting of various sandstones with the climate of high rainfall and cold weather. Due to same reason, this region witnesses subsoil degradation, a frequent phenomenon. In past construction practices, very little attention was paid to the subsoil properties and consequently, it was also difficult to assess the problems of differential settlements. This problem might cause either due to the degradation of subsoil material over course of time or due to the differential pressures implied upon the subsoil by the above structure. This report

will deal with the soil structure interaction modeling to evaluate the amount of settlements and cause of the cracks observed.

The construction of these churches was mostly funded by the local villagers, and with the limited funding opportunity, the churches were mainly constructed by various type of materials available locally and less skilled masons. Given the different properties of the materials used to build a wall and given the heterogeneous behavior of this material and the wall itself, many problems arise even when the wall is loaded with only self-weight. These behaviors cause lateral tension between the units and lead to the cracks or separation in case of three leaf wall. In this report, analysis of lateral and transversal cross-sections of the walls will be performed to observe the behavior.

## 2 HISTORY

To commence the study of the church, it is important to observe the setting on which the structure was built. The past geopolitical aspects reveal the journey of the structure through the history. These aspects help to determine the dominant power in the area at the time of construction, personalities involved in commissioning of the constructions, architects, builder, and masons. With these study, damage and decay process of the structure can be best understood and it helps in a conservation study by establishing the cultural, spiritual and economic importance of the monument and subsequently to build a hypothesis on damages of past and probable intervention techniques that can be adopted.

### 2.1 Bohemia
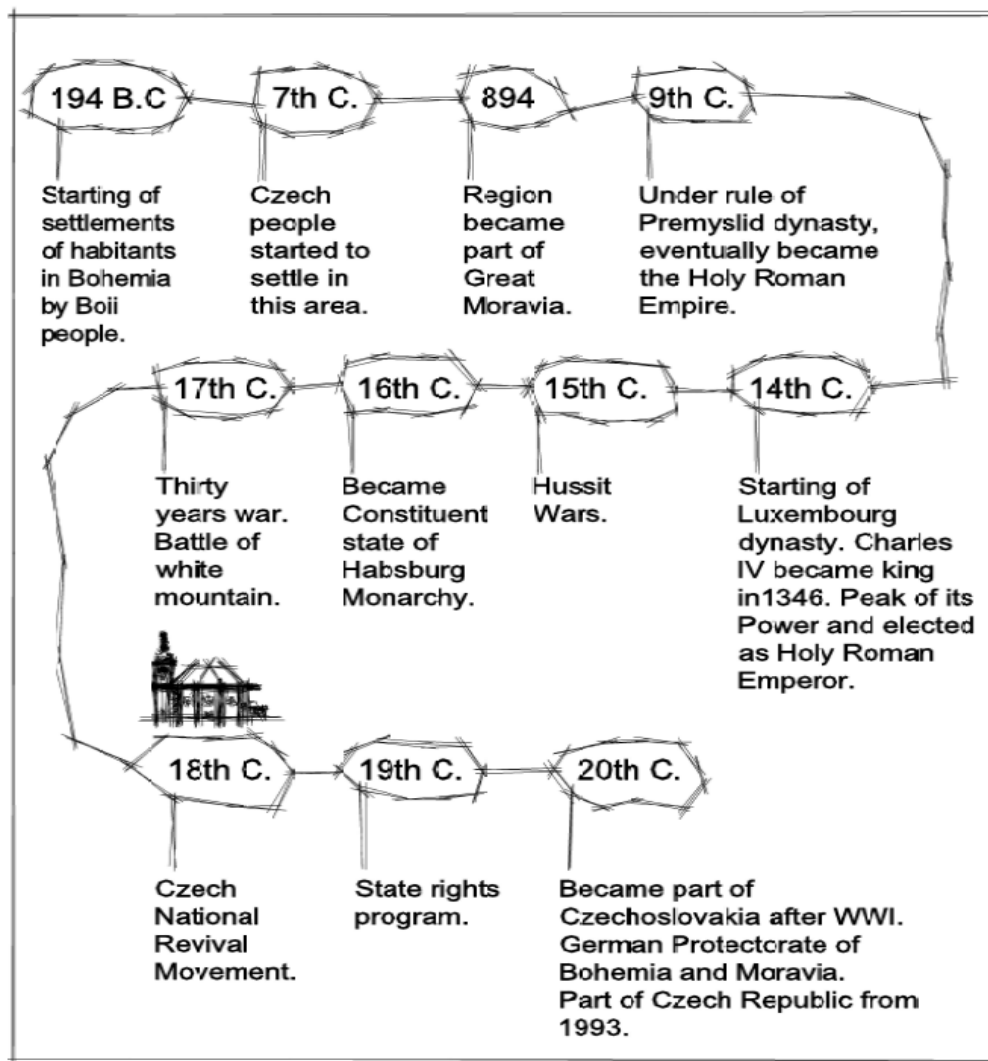


Figure 2.1 – Timeline of Bohemia Region

From going back to the ancient times of first migration in this region till now, Bohemia, a centrally located region in Europe is a very important place, not only considering its trade routes but also because of its rich history and beautiful landscapes.

Bohemia is the westernmost and largest region of the present-day Czech Republic.

In the beginning, Bohemia was part of the Great Moravia, later an independent region, a kingdom in the Holy Roman Empire, and subsequently a part of the Habsburg Monarchy and the Austrian Empire. Closing looking at the history of Bohemia, it can be observed that this region has witnessed many devastating events such as turning tides of the Rulers and wars.

After the world war 1, Bohemia became a part of independent Czechoslovakia and finally in 1993 with the dissolution of Czechoslovakia it became a part of Czech Republic. (Figure 2.1.)

The Broumov group of churches were built at the beginning of the 18th century as Bohemia started to recover from the damages wreaked by the war.

## 2.2　Baroque architecture and Dientzenhofer family



Figure 2.2 - Graphical Representation of Baroque Church in Bohemia

When the enormous round boulder set atop a rigid stone, sea of Renaissance finally moved, it brought down an avalanche of restlessness, changes, questions, and exploration. The history of mankind never witnesses an era that wished to alter the world and turn its face to God to such an extent as Baroque. (Tourism, 2016)

Baroque architecture in Bohemia initiates from Italy. Baroque architecture in Italy started in the early 17th century accompanying the Counter-Reformation that was intended to restore Catholic's popularity after challenges it had faced due to Protestant Reformations. As the Roman Catholic Church looked for a way to manifest its influence and regain lost souls all over Europe, it turned its attention to architecture in churches. The new style of church architecture shall be one that touches a human emotion, not just their understanding. The very act of approaching and stepping into a church had to

become more of an experience; one that would lure the believers into the grandeur of the church, but also one that would make them feel welcome and ultimately a strong attachment to the church.

Faith was reflected in the vast numbers of crosses, wayside crosses, chapel-shrines with deep niches or pillars, forest shrines and pilgrimage churches scattered around the countryside. Having once flowed like the ocean, suddenly the landscape was full of islets, landmarks and places, where just stopping or looking around would move the heart and spark a thinking.

Baroque style architecture differs from the previous Renaissance style which was very strict with rules. It allows very dynamic designs, employing a mixture of repetition, breaking-up, and distortion of Renaissance classical motifs. Typically, Italian Baroque architecture makes much larger use of abstracted or exaggerated elements to provide more dynamic interiors. The building interiors usually contain much decoration including frescoes, paintings, and ornaments. These exaggerated features coupled with large gold statues of Christian figures imposes a feeling of domination and protection.

While the early baroque period in Bohemia in the early 17th century was dominated by Italian architects, the high Baroque period later in this century witnessed the emergence of architects of Bohemian or Moravian birth and architects from Bavaria. One of the most significant architects of the High Baroque period is Christoph Dientzenhofer, who came to Bohemia from Bavaria and lived in Prague. Together with his son Kilian Ignaz Dientzenhofer, they are known for their style called "radical Baroque", which was inspired by examples from northern Italy, particularly by the works of Guarino Guarini, and which seeks to express movement. It is characterized by the curvature of walls and intersection of oval spaces. However, this was later adapted into a version of the style that Czech architects took further than most of Europe. One of their most important work includes the St. Nicholas Church in the Lesser Town of Prague which becomes one of the most important Baroque churches in Europe. (Figure 2.2)

## 2.3   Broumov Region
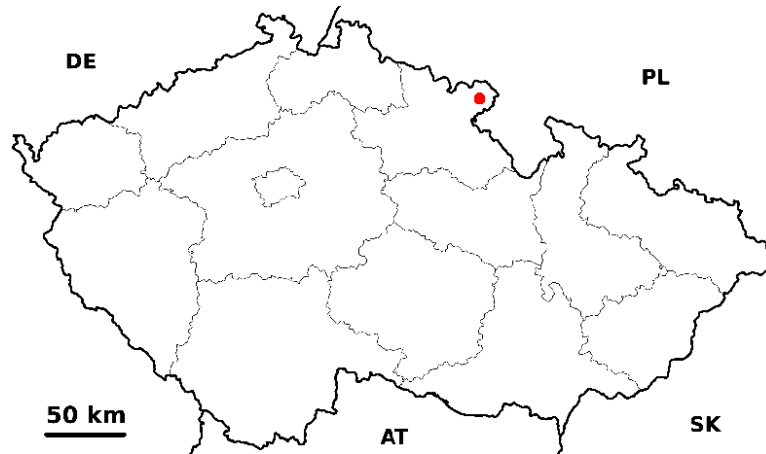


Figure 2.3 - Broumov region within the Czech Republic
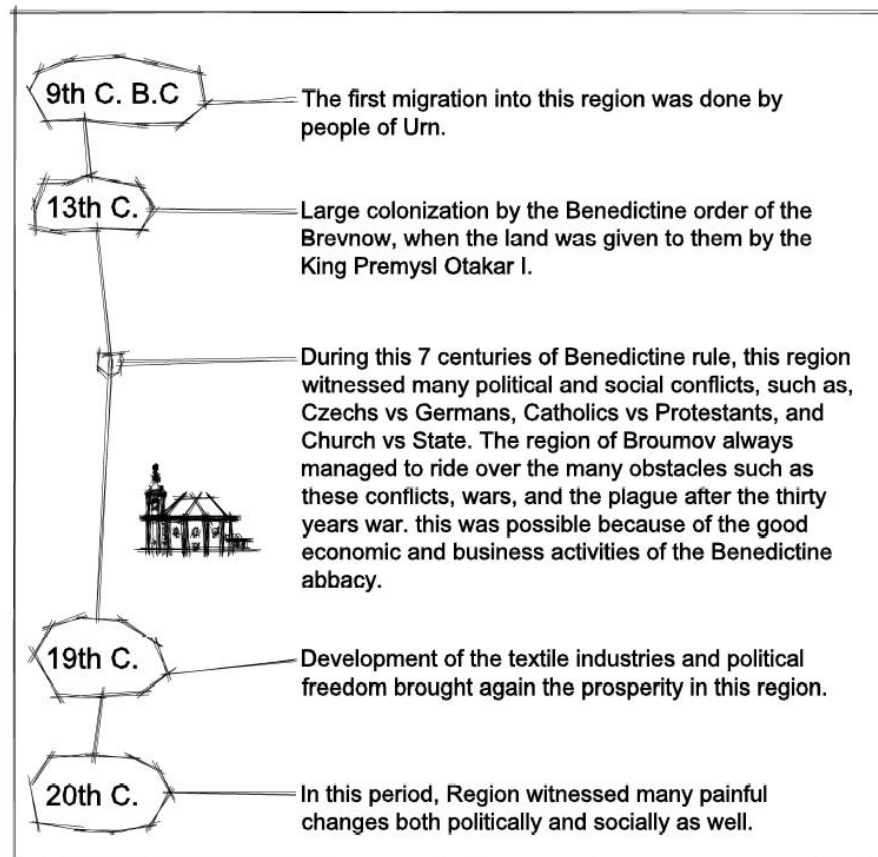


Figure 2.4 - Timeline of Broumov Region

The Broumov region is a poetic and romantic country, wedged into Poland at north-east part of the Czech Republic. (Figure 2.3). The landscape of this region is very diverse, with mountains, valley, bizarre rock formations, and also mazes of forest lands juxtaposed onto meadows and large grasslands. For many centuries this region was an important cultural center enriched by artistic

monuments and edifices, which were built during the admiration of the Benedictine monks. (Figure 2.4) (Czech Tourism, 2018)

This prosperity would not last in the 20th century. After the Munich Agreement in 1933, the Broumov region was divided - Broumov and Teplice, whose inhabitants were mostly of German origin, became part of Hitler's Third Reich and Police was part of the Protectorate Bohemia - Moravia. The German inhabitants who would not swear allegiance to Czechoslovakia were evicted from the country. The population of this area would be reduced by about two third deeming many buildings unnecessary as the residents were gone. This was made even shoddier by the nationalization of many buildings, leading to minimal or no maintenance of the buildings by the locals. This directs to the current damaged state of the buildings.

This region's unique location with its picturesque landscapes and the beautiful architecture, that can be found in the churches makes this area exceptional. These qualities mixed with folk monuments make the spirit of this ever-enchanting region.

## 2.4    Broumov Group of Churches
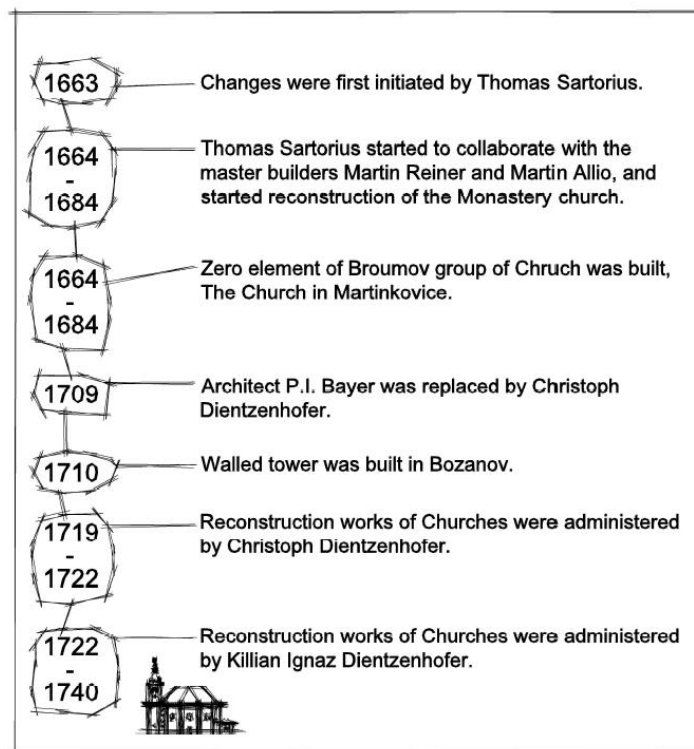


Figure 2.5 - Timeline of Broumov group of churches

Broumov group of churches represents a unique and interesting implementation of the typical Bohemian Baroque architecture, which includes numerous parish country churches, built in the villages of the Broumov-Brevnov abbey, rising high with the title of Archabbey. Another uniqueness of

this group of churches is the short construction period which lies on the first quarter of the 18th century, as a work of the only abbot Otmar Zinke and by the only family of builders, the Dientzenhofers.

The main purpose of this huge project was the renewal of unsatisfactory network of old wooden churches. The monastery owned 19 villages at that time, the older churches were small and at the end of their service life periodic repairs were demanding and therefore the abbot made the decision to replace all existing churches by new ones.

Although this group of churches is known for its short construction period, and it was indeed a rare instance, it was a result of a long-term process of the renewal of the many places in that region as mentioned in Figure 2.5. To execute this huge project, renewal of economic potential of the monastery was needed, which was seriously struck by the Hussite wars and the thirty years war. Two abbots of this monastery, Thomas Sartorius, and Otmar Zinke had merit in renovation and had a significant extension of properties in the region, which helped to convert this dream project into reality.

All the churches belonging to this group are connected not only by the names of the client and the builder but, before all, by their specific function of country churches. First of all, such a church had to meet a number of requirements; simple and general design of a single-nave church with a bell-tower was a must; moreover, it had to be cheap, feasible, without complicated technical features and complicated decorations. The solidity of the construction was more important than the artistic ambitions. There were logical reasons behind this; partly it was the less skilled local masons, partly it was the fact that the churches were built at the expenses of parishes and gatherings. The abbey lent necessary financial capital in the amount of maximum 50% of costs and provided movables such as the things that had been taken out of the service in other churches. For the same reason, the churches had false wooden ceilings with flat centerpiece covered with reed and mortared, imitating integrating segmental sail vaults, which also enabled to build the enclosure walls of smaller thickness.
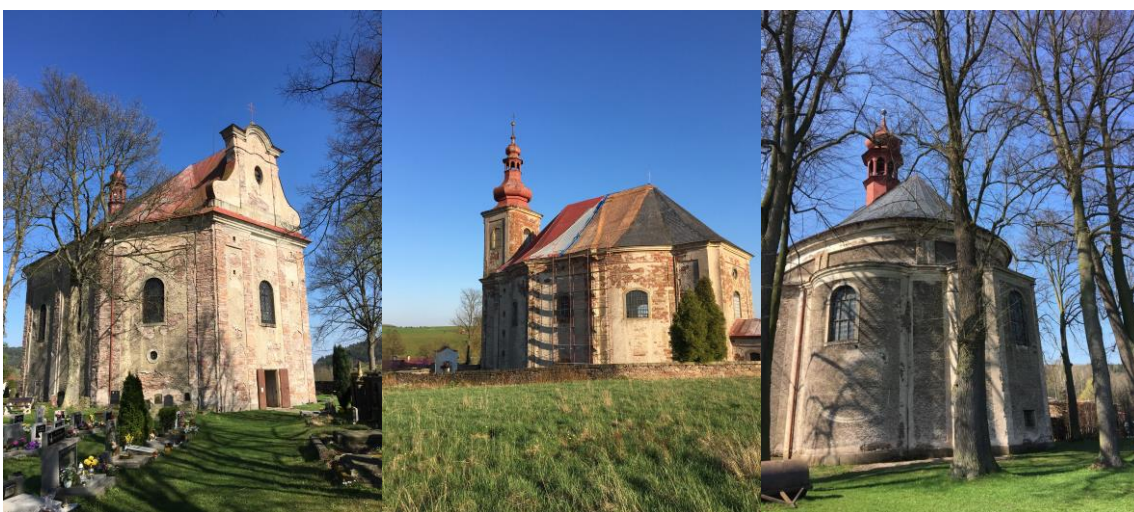


Figure 2.6 - (L) Church of St. Jacob (C) St. Ann Church (R) St. Barbara Church

## 3.    ST. ANN CHURCH, VIŽŇOV
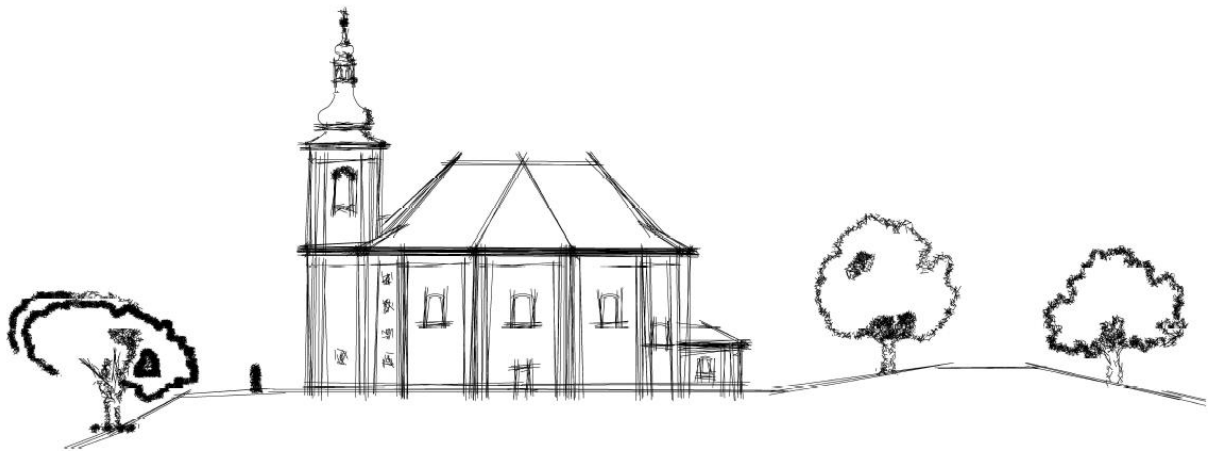


Figure 3.1 - Graphical representation of St. Ann Church

Viznov, this village was established in the mid-13th century; it was owned by the noblemen from Adrspach. Since 1434, it was administered by the Broumov monastery. Originally, this village consisted of two parts – Horni Viznov (now Viznov) and Dolni Viznov (now Mezimesti). Originally agricultural village became a center of canvas trade in the mid-19th century. Viznov has been a local part of Mezimesti since 1st January 1986.

### 3.1    Characterization of Chruch

The original gothic wooden church was reconstructed in 1708-09. In 1719, abbot Zinke initiated the construction of a new church, but it was interrupted for four years. Work started again in 1724-25 when the church was almost finished. The design was made by Killian Ignaz Dientzenhofer and built by a master builder from Broumov. Carpenter Josef Heinrich Opitz took part in the construction of the considerable high tower. The church was being finished until 1727, but the older wooden church was still next to the new one.

A dominant structure, seen from a long distance is situated on a moderate hill in the middle of a long village situated along a stream and a road leading to Mezimesti. The church faces this main road. Its axis aims to the top of Ruprechticky speak and the tower of the church is in optical contact with other churches. The church is surrounded by a cemetery with a gate axially situated towards the main facade.

Longitudinal octagonal central modifies the ground plan that had been used in Hermankovice. Unlike in that church, this church is characterized by radically curved outer walls, the church in Viznov is typical for its rounded walls shaped in a soft continuous line. The longitudinal axis is again characterized by several additional narrowing spaces logically connected into a series antechapel, tower, cornice, main nave, organ loft, and sacristy. Outer facades, accenting developed side facing,

are structured by simple side walls on cut edges and is topped with a massive stone cornice with accented overlap.

The interior is built in a deep oval with continuously curved walls, dividing high and shallow niches. Wooden organ lofts were built in a diagonal axis. Distinctive pilasters support an elegant curve of the crowning cornice; flat wooden vault with a cavetto centerpiece is placed on it. The chancel and space under the organ loft are segmental sail vaulted. A new solution of a ground plan was tested and adumbrated by Killian Ignaz Dientzenhofer here; he used it later in the design of a royal mint and in the design of an important church of St. Kliment in Odolena Voda.

In the framework of the group, this church represents a unique solution of dynamic build in the way represented Christoph's construction of the castle chapel in Smirice from the time before 1700 and subsequently by the best works of Killian Ignaz Dientzenhofer from the mid-1730s. The interior of the church is characterized by the continuous transition of segments of inner walls in a gracious counter movement **Figure 3.2**.



Figure 3.2 - Interior (Left) and Exterior (Right) of the St. Ann Church

## 3.2    Description of Geometry

The church of St. Ann is relatively smaller than other Broumov churches and has a unique design. At the front of the church, a large bell tower is characterized by the main façade and serves as an entrance to the large main nave. The walls of the church are composed of heavy three-leaf masonry. The ceiling of the main chamber is sail vaulted with timber, lathe, and plaster hanging from the heavy timber trusses. The timber ceiling, rather than vaulted masonry, allows for a much more shallow and wide ceiling and reduces the lateral thrust exerted on the masonry walls. This provides a lighter and more open feeling to the structure. The elliptical shape of the structure provides a basis for very subtle reliefs to be set into the walls as well as shallow choir lofts and a small organ balcony to be placed along the front half of the church without impeding the open feeling of the main chamber. The church is 43 meters long and 20 meters wide, including the bell tower and sacristy as can be seen in the floor plan in **Figure 3.3**. The masonry walls are on average 2.6 meters wide and the main nave is 24 meters by 15 meters. The walls are made up of the locally available stones which include but not limited to the red sandstones, grey sandstones, siltstones, basalt, green sandstones, bricks etc. The timber roof is mainly constructed with the European spruce (Picea abies) (Prokop, 2009). The organ loft set back into the tower on the eastern end of the nave is approximately 6 meters by 3 meters. The tower itself is 28 meters high. The detailed Floor plan and Elevations are provided in Appendix A.
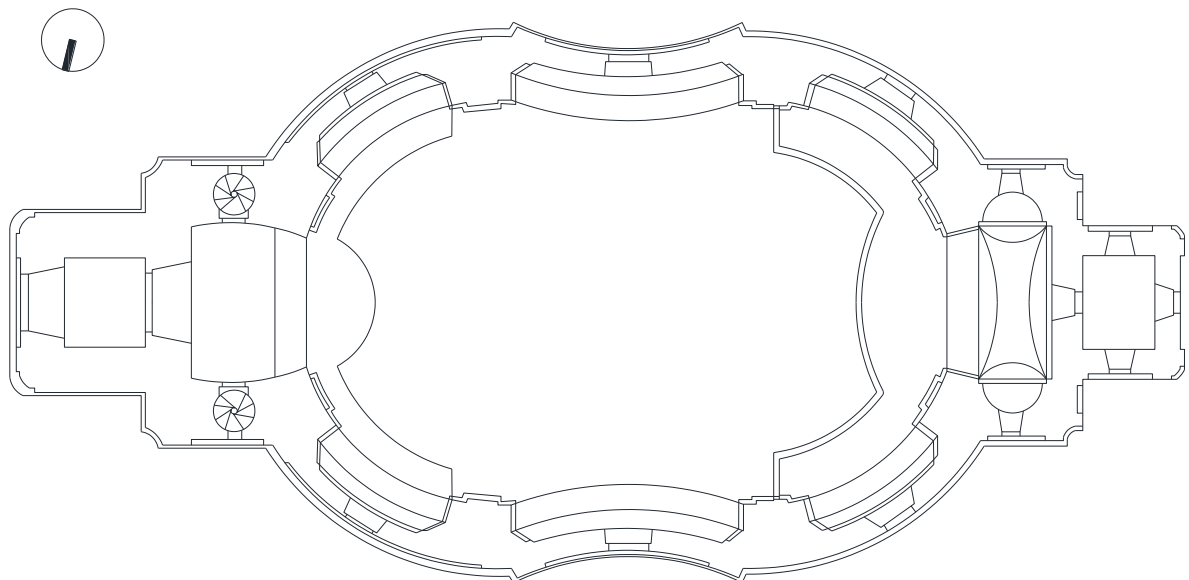


Figure 3.3 - Floor plan of St Ann Church

## 3.3 Damage Survey

A damage is the human perception of the loss of values due to decay, which can be due to a chemical or a physical modification. Three main classifications of damage are degradation, deterioration, and weathering. Degradation is the decline in condition, quality, or functional decay. Deterioration in the process of obtaining a lower quality, value or character. And weathering is any chemical or mechanical process that causes changes in character when weather exposure occurs, as defined by ICOMOS.

The Damage Survey aims to evaluate the actual state of St. Ann Church. The damages were classified according to ICOMOS Guidelines. The damage is classified into five principal categories, Cracks and Deformation, Detachment, Material Loss, Discoloration and Deposit, and Biological Colonization. (ICOMOS-ISCS, 2008)

### 3.3.1 Cracks and Deformation

A crack, defined by ICOMOS, is an individual fissure, clearly visible by the naked eye, resulting from the separation of one part from another. There are diverse types of cracks, including fracture, star crack, hair crack, craquele, and splitting. The façades of the church have several cracks which can be classified as fractures. These cracks are in mostly on the interior part of the church (**Figure 3.4**), but some cracks can be observed from the exterior of the church as well (**Figure 3.5**).



Figure 3.4 - Cracks on the Interior of the Church. Sacristy (Left) Main Nave (Right)

Figure 3.5 - Cracks on the exterior of the church. Sacristy (Left) Main Nave South side (Right)

Many observations regarding the deformation of the plinth stones can be observed on the exterior part of the church. In this case, it can also be observed that the major deformations are located on the northern part of the church while some deformations can be observed on the south side as well (**Figure 3.5**).



Figure 3.6 - Deformation of Northside (Left) Southside (Right)

### 3.3.2 Detachment

Detachment includes: blistering, bursting, delamination, disintegration, fragmentation, peeling, and scaling. The exterior of the Church shows some disintegration of the granite stone. Disintegration, as defined by ICOMOS, is the detachment of single grains or aggregates of grains (**Figure 3.7**).



Figure 3.7 - Detachment as scaling on plasters

### 3.3.3 Material Loss

The material loss includes alveolization, erosion, mechanical damage, microskarst, missing part, perforation, and pitting. The exterior of the Church presents erosion including loss of matrix and rounding of the edges close to the joints, these are due to the erosion of the stones at the exterior part mainly due to freeze and thaw cycles **Figure 3.8**. There are also some missing parts, as shown in **Figure 3.9**.



Figure 3.8  - Erosion of stones at the exterior side
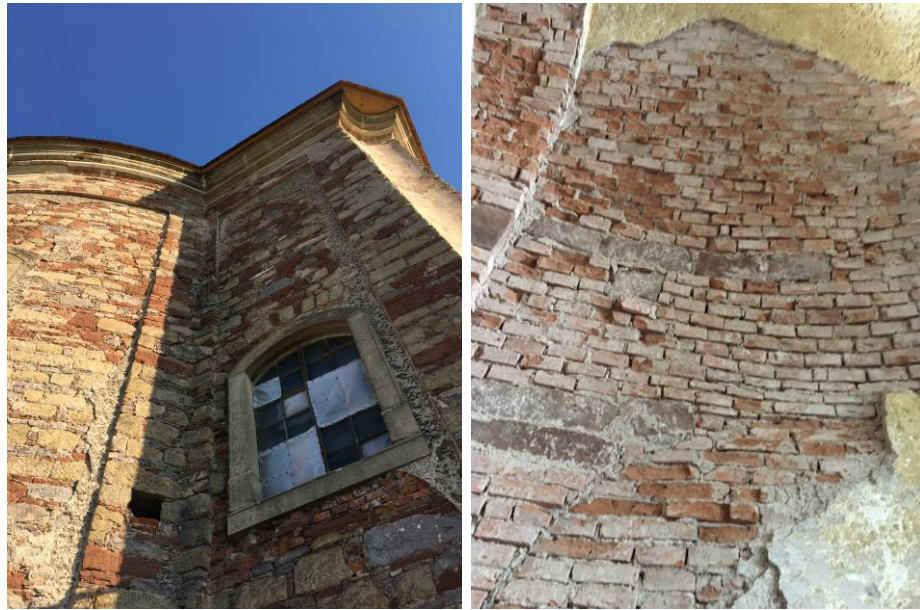
Figure 3.9 - Plaster loss at the exterior (Left) and Interior (Right)

### 3.3.4 Discoloration and deposit

Discoloration and deposits include coloration, bleaching, moist area, staining, deposits, crust, efflorescence, encrustation, film, glossy aspect, graffiti, patina, soiling, sub efflorescence. The exterior of the Church presents black crust on the North façade. Also, the exterior of the Church has patina and staining due to moisture, as shown in **Figure 3.10**.



Figure 3.10 - Patina and Staining on exterior part

### 3.3.5 Biological Colonization

Biological colonization, as defined by ICOMOS, is the colonization of the stone by plants and micro-organisms such as bacteria, cyanobacteria, algae, fungi, and lichen. It also includes influences from other organisms such as animals nesting on and in stone. Around the Church, several types of biological colonization were observed, including algae and lichens; as shown in **Figure 3.11**. Also, the biofilm is observed in the facades of the Church, especially in the North Façade, as shown in **Error! Reference source not found.**



Figure 3.11 - Biological colonization at interior of Church



Figure 3.12 - Biological colonization on exterior side

## 3.4  Thermography and Moisture

Thermographs are an important tool to measure the difference in the wall temperatures and to identify the superficial damage. Different materials present different temperatures as well as superficial damage. In the following images in **Figure 3.13**, it is possible to observe the difference in wall temperature at different parts of the church, from the images, it can be observed that the bottom one meter of the church suffers from the higher moisture content compared with the upper parts, this can be due to the capillary rise of the water from the ground.
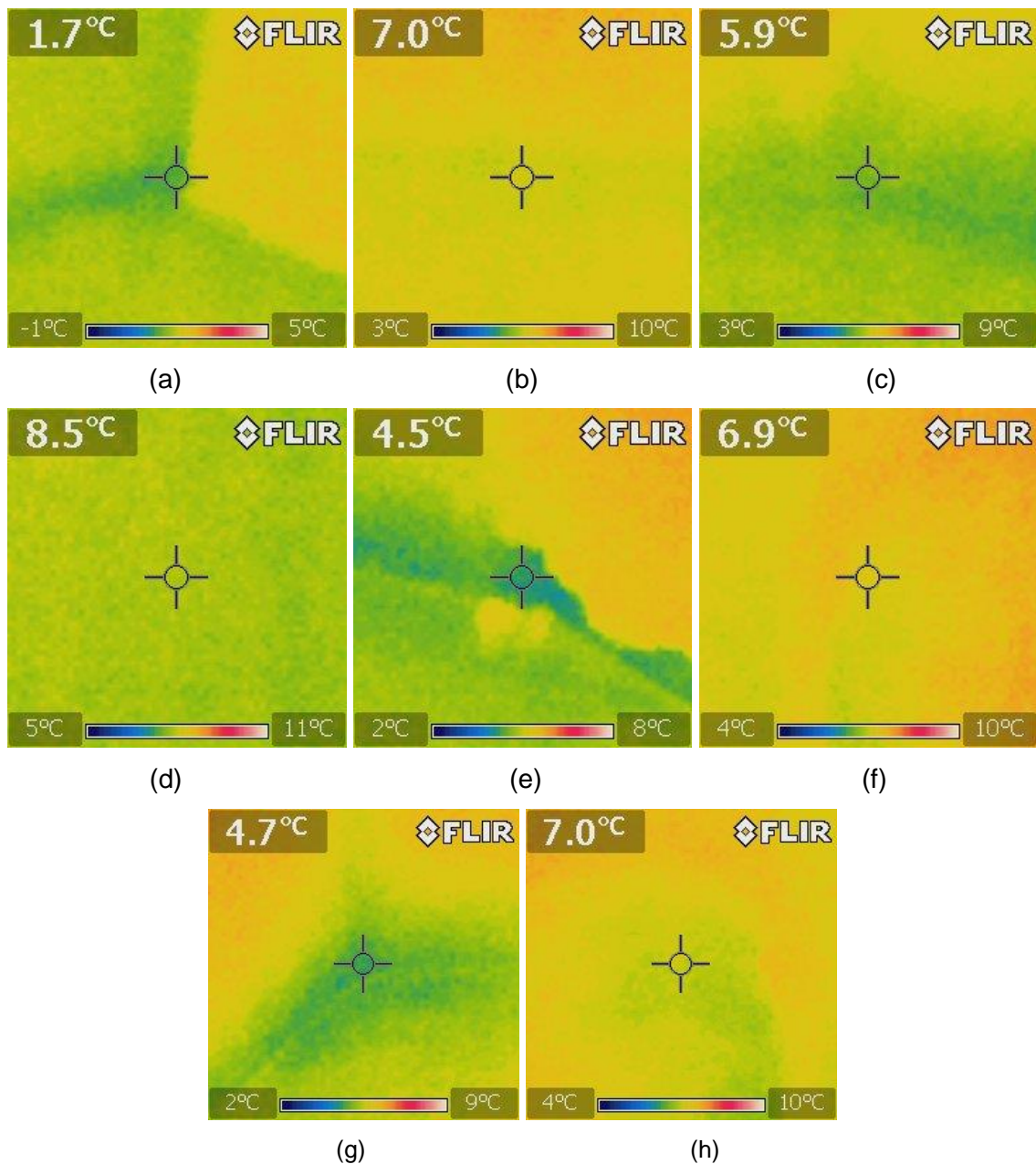


Figure 3.13 – Thermogrpahs at (a) east side bottom (b) east side top (c) south side bottom (d) south side top (e) north side bottom (f) north side top (g) west side bottom (h) west side top

## 3.5 Climatic Conditions



Figure 3.14 - Regional Climate map (VUMOP, 2018)

The region where the church is located falls into a slightly cold, humid climatic region. The average January temperature reaches the magnitudes of -3 °C to -4 °C, the average July temperature is 16 °C to 17 °C. The average annual precipitation in total is in the range of 700-800 mm.  The snow cover lies on an average of 80-100 days per year (AOPK, 2018).

## 3.6 Geological Conditions

It is a mountainous region with an average altitude of 495 m above sea level. Specifically, Viznov lies at an altitude of 470 m above sea level.
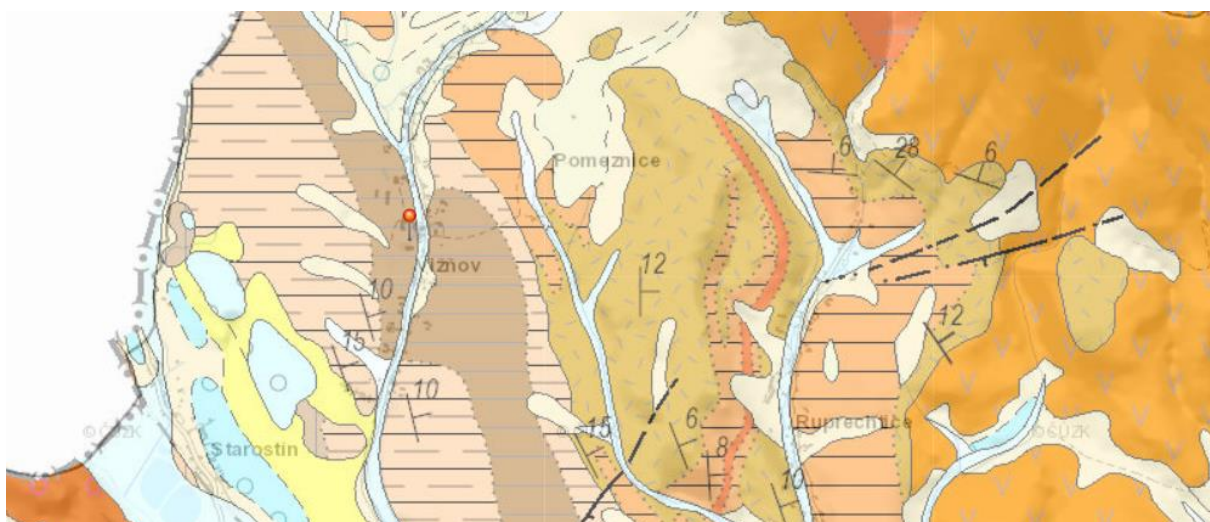


Figure 3.15 - Regional Geological map (Geology, 2018)

Viznov is located between the Broumov Highlands and the Javori Mountains. The geological territory belongs to the Bohemian Massif, namely the Bohemian massive-covering formations and the postvarian migmatites, which is referred to as the Vnitro-Sudet basin. The subsoil is made up of paved sediments, in particular, colorful aleuropelites, which are often limestone with an admixture of silicites (Czech Geological Survey, 2018).

## 3.7   Data Monitoring

A diploma thesis carried out by Oldřich Peleška focused on the assessment of the water transport in a soil-masonry system of the St. Ann Church, was a multidisciplinary research in which the movement of water in the masonry and soil in the surrounding of the church was investigated.

For the investigation work, a network of monitoring systems is installed on site, which consists of humidity sensors, strain gauges, and MPS-6 sensors. These sensors are located inside the church on the wall and outside in the soil as shown in **Figure 3.16** and **Figure 3.17**. From this research work, it was possible to observe the presence of the pressure water at the shallow depth in the soil and the capillary rise of the water in the masonry walls of the church. From the work, it was also concluded that the groundwater at the area is more affected by the water coming from the uphill than the water infiltrated from the precipitation directly on the site (Peleška, 2108).

This research work is found to be very informative regarding the subsoil condition with respect to the groundwater movement and the capillary rise of water in walls and its relations with the rainfall in the area (**Figure 3.18**).



Figure 3.16 - Sensors installed inside the church at north side **(Peleška, 2108)**

Figure 3.17 - Sensors installed in the surrounding soil at north side **(Peleška, 2108)**
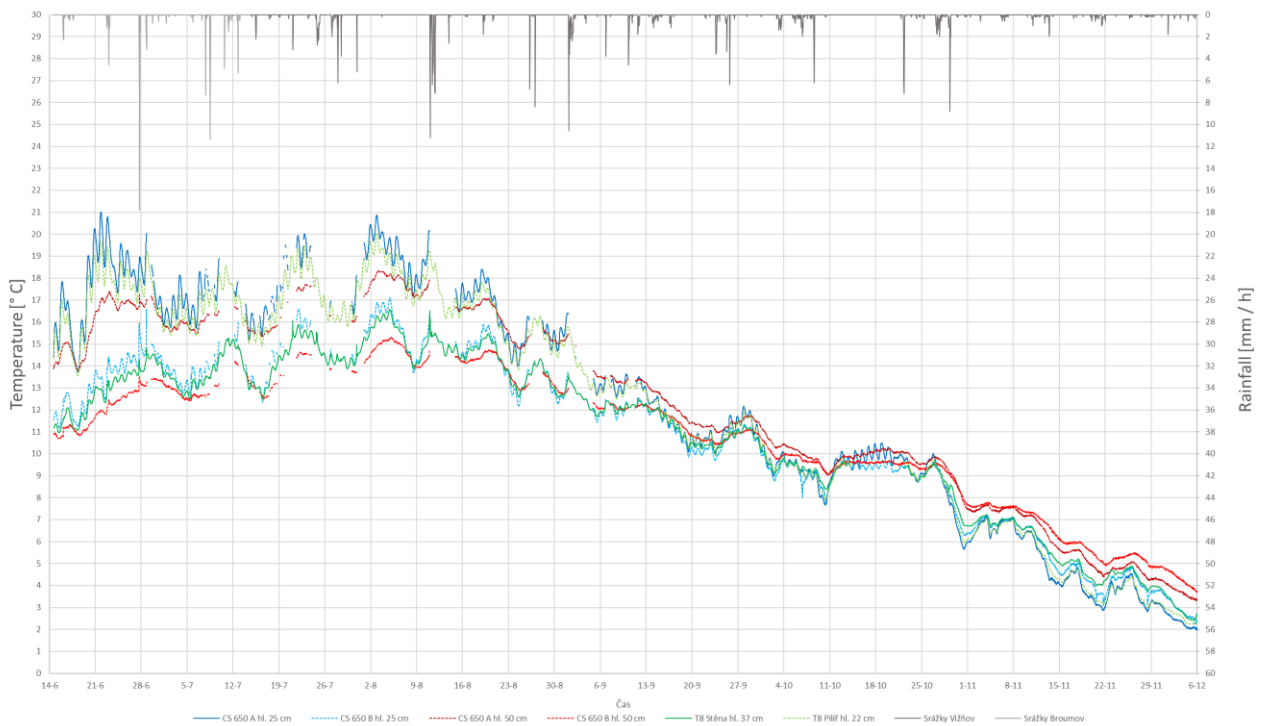


Figure 3.18 - Comparison of temperatures measured by the humidity sensors and the strain gauges in the church **(Peleška, 2108)**.

## 3.8   Damage Map

To assess the actual damage of the St Ann Church, Visual Inspection was carried out. This method is considered as one of the effective methods to qualify the real state of the structure, to the acquisition of data and its analysis. Due to the advantages previously mentioned, visual inspection can also be characterized as one of the most effective non-destructive methods for a preliminary analysis. In **Figure 3.19**, damage plan is presented for this case of study.
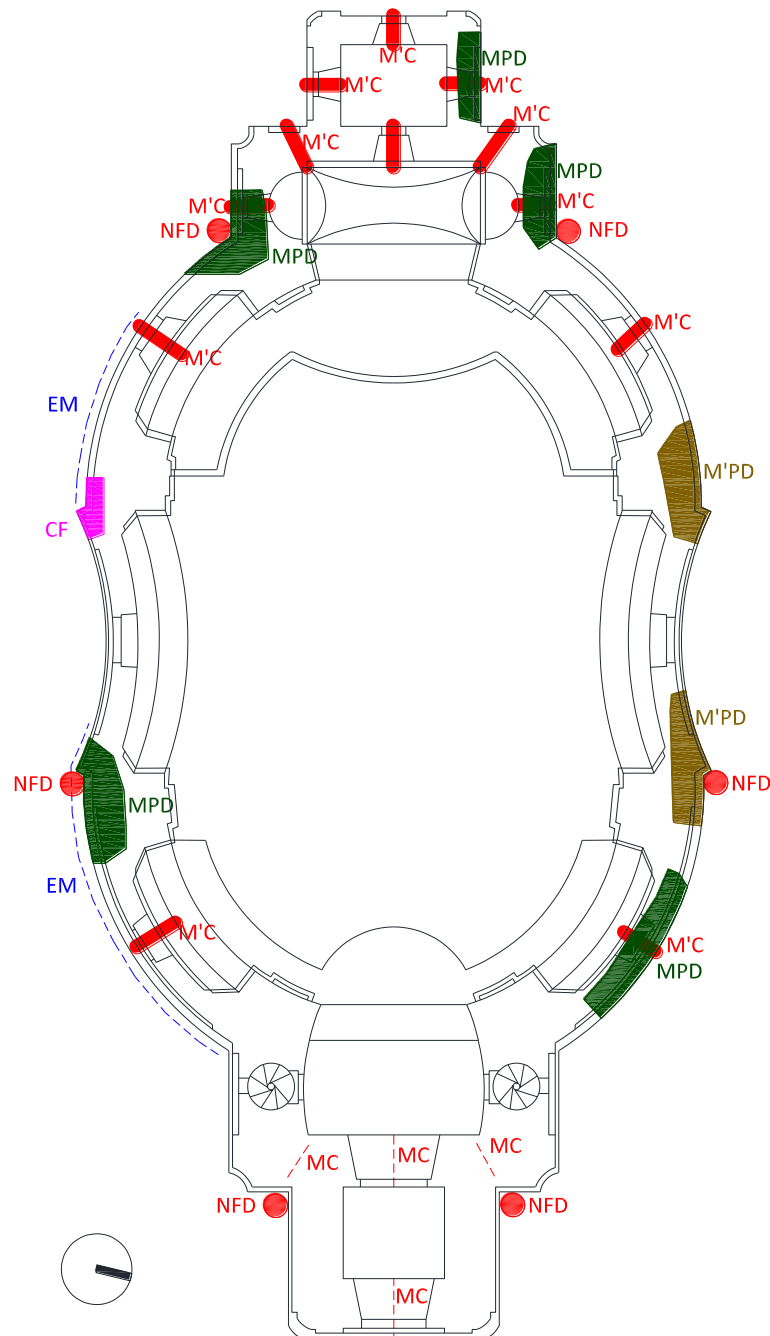


Figure 3.19 - Damage Plan

Table 1 - Table Showing the description of damage legends shown in damage plan

| Legend | Description of Damage |
|--------|----------------------|
| NFD | Non-Functioning Downspouts |
| MC | Minor Cracks |
| M'C | Major Cracks |
| MPD | Minor Plinth Damage |
| M'PD | Major Plinth Damage |
| EM | Erosion of Masonry stones |
| CF | Cornice failure at the top |

## 3.9   Conclusion on the visual investigation

### 3.9.1   The decay of stones and plaster due to groundwater infiltration

As described earlier, most of the decay of mortar, stones, plaster and extensive biological growth could be found at the lower part of the wall. A plausible explanation of this decay can be the groundwater infiltration causing a moist environment that is a suitable living environment for moss, algae, and fungi and creates an opportunity of freeze and thaw cycle.

### 3.9.2   Deterioration due to drainage system failure

However, during the site visit it was observed that the currently the work is carried out on the church roof to improve its suitability and improve the roof drainage system, but it was also observed that the downspout which was previously installed were found to be of inadequate for the rainwater drainage and the downspout end, there was no connection found to divert the water away from the walls. This can be one of the reasons, of observing the minor plinth damage near the downspout areas, which can happen due to the splashing of drained water from the downspout. Furthermore, it was also observed that given the topography surrounding the church, free rainwater can be naturally drained at the south side of the church which is not possible at the northside, which will create the circumstances for the rainwater infiltration near the wall and cause the decay of sub-soil near the downspout area.

### 3.9.3   Major deterioration and decay at the northern façade

As described in the previously, given the topography surrounding the church, groundwater coming from the uphill side and rainwater infiltration at the northern side of the church does not have a free passage of movement due to wall foundation and that water stay near the wall foundation, which creates the circumstances of capillary rise of water and soluble slats at the walls and cause the damage and decay of the wall masonry as well as the sub-soil. Also because of the orientation of the church, northern side of the wall receives less direct sunlight annually and it creates a breeding opportunity for moss and algae.

### 3.9.4   Major deterioration of the plaster at the southern façade

Annually, the amount of sunlight on the southern facade varies with respect to the sun path and accordingly the surface temperature receives more changes compared to the northern side, these changes in temperature create suitable environment for the increased intensity of freeze and thaw cycle, which will contribute to the accelerated deterioration of the plaster on the southern side compared to the northern side.

### 3.9.5   Damage due to the differential soil settlement

Combining the above hypothesis on the damage and deterioration of the church walls and the obstructed passage of the groundwater, paves way for the hypothesis of differential settlement of the soils on the location where the drainage of surface and groundwater is freely allowed and at the location where the movement of groundwater is obstructed which ultimately led to the deterioration of the sub-soil, further weakening the sub-soil and reducing its load carried capacity compared to the other region, which proved a way for the differential settlement on the church.

# 4 STUDY ON THE BEARING CAPACITY OF WALLS

Most of the walls present in the historic structures can be described as made up by the stones or brick unites and bonded together with or without the mortar. In this case of study, it can be observed that the walls are made up of the different stone units and bonded together with the lime mortar. As described in earlier chapters, the walls are built by the locally available stones which are varying in many different parameters such as, materials, size, shape, color etc. Furthermore, it was also observed from the site that the average width of the walls is 1.2 meters. Considering all these parameters, estimating the homogeneous mechanical properties of the wall by prescribed code's guidelines become inappropriate and more studies become necessary to achieve the same homogeneous mechanical parameters from the given combination of the stone units and the mortar.

To predict the mechanical properties of the masonry wall, many different testing procedures and code guidelines are available, of which may involve the minor or major destructive testing to be carried out on the walls. Now, given the historical and cultural importance of this monument, such testing procedures are impossible to perform, which makes the wall categorization very difficult. Hence, modeling representative parts of the wall to obtain its mechanical paraments become necessary.



Figure 4.1 - Enclosure wall masonry from the exterior shows non-uniform combination of stones building up the outer layer

## 4.1   Surface hardness test and strength of stones

The surface hardness and superficial strength of the stones can be tested by a non-destructive test performed by the Schmidt hammer. This test can yield the useful value of the superficial strength of the stones through the available transformation criteria provided by the hammer manufacturer. To best describe the strength of the different stones, present in the outer layer of the masonry wall, it was necessary to describe the strength of these different stone units.

For the same reason, two different spots were chosen to perform the Schmidt hammer test on different types of stones. The wall samples which were chosen are of size 1 meter by 1 meter at two different locations in the church and these two locations of the sample represent the different combinations of the stones to build the masonry as shown in **Figure 4.2**
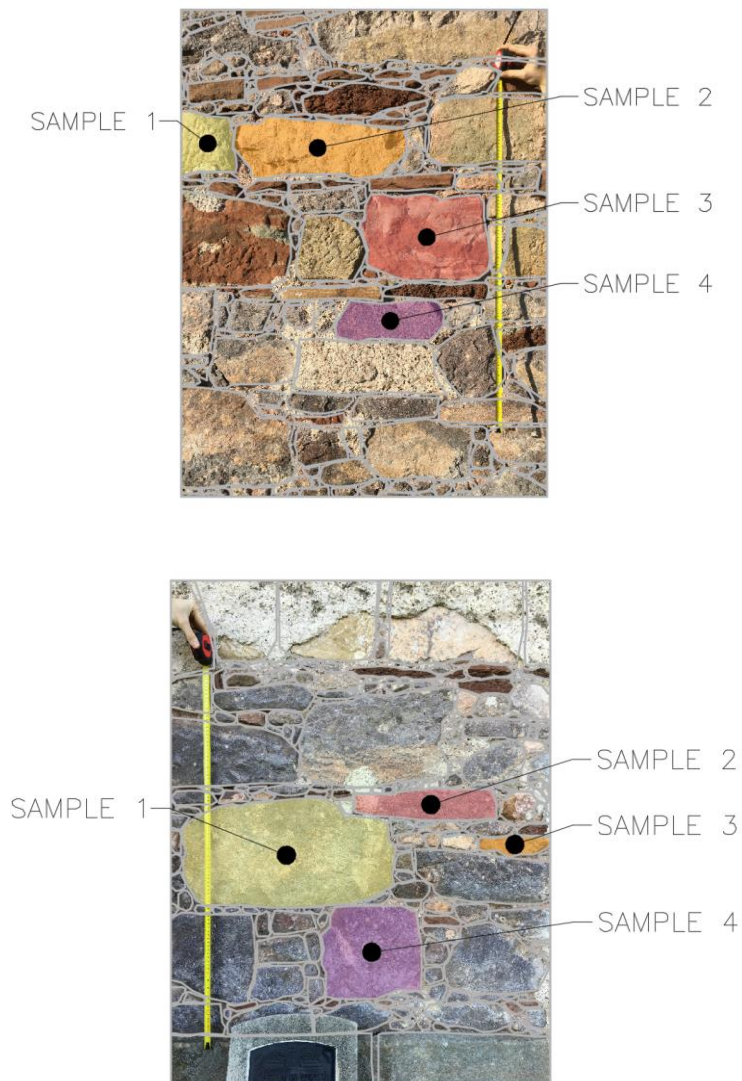


Figure 4.2 - Wall samples considered in the analysis. Wall sample 1 (top) wall sample 2 (bottom)

As it can be observed from the above figure, on each wall samples, four different types of stones were chosen to perform the superficial strength test. On each stone sample the rebound hammer was performed for 10 times and then the average value of the rebound number was chosen, this average number of rebound number was transformed into the equivalent strength values from the formula provided by the manufacturer of the equipment (Proceq, 2017). Following are the tables showing the strength of these sample stones.

Table 2 - Table showing the superficial strength of the stone samples in Wall 1

| Wall Sample 1 | | | |
|---|---|---|---|
| Stone Sample | Average rebound hammer value | C.O.V (%) | Equivalent Strength (MPa) |
| Sample 1 | 52.48 | 9.45 | 41.48 |
| Sample 2 | 52.83 | 8.80 | 41.96 |
| Sample 3 | 43.20 | 10.14 | 29.81 |
| Sample 4 | 49.45 | 12.00 | 37.47 |

Table 3 - Table showing the superficial strength of the stone samples in Wall 2

| Wall Sample 2 | | | |
|---|---|---|---|
| Stone Sample | Average rebound hammer value | C.O.V (%) | Equivalent Strength (MPa) |
| Sample 1 | 40.70 | 7.69 | 26.99 |
| Sample 2 | 50.65 | 11.51 | 39.03 |
| Sample 3 | 43.90 | 6.51 | 30.63 |
| Sample 4 | 53.20 | 13.76 | 42.46 |

These values of the strength of the stones are superficial values and it does not represent the true strength of the stone samples but provide with the reliable values of the strength which are useful while categorizing the stone properties for the finite element analysis of the wall samples.

## 4.2   Mechanical parameters of the materials used in modeling

The walls are modeled as the combination of various stone units, lime mortar, and rubble masonry infill. From the different available stone units, mainly three different types of stones were observed to be present in the walls outer leaf, namely red sandstone, grey sandstone, and basalt. These stones are bonded together with the lime mortar. While for the internal leaf, rubble masonry was considered. Here the values of the mechanical parameters used are derived from both the typical values of such stones and the values obtained by the Schmidt hammer test. Observing the degraded state of the outer leaf, it was considered to use the lower bound value as a general for these types stones present in the wall, which will be a conservative approach and will result in the lower bearing capacity of the wall.

Furthermore, for modeling of the longitudinal wall section, since only a single layer of masonry can be modeled in this 2D model, to account for the effect of the multi-leaves wall, reduced parameters are applied on the outer wall masonry blocks that are modeled. The reduction factor is obtained by modeling only the outer leaf in the sectional wall. subjecting this wall to the same uniform loading, a load-displacement curve is obtained. The Young's modulus and the yield strengths are modified such that a load-displacement curve that is comparable to that obtained from the three-leaves wall model. The ultimate reduction factor used is a factor of 0.33 for Young's modulus and 0.8 for the yield strength and the shear strength.  (Drdácký M., 2008) (J. Válek, 2005)

The mechanical parameters considered in the analysis are listed in the table below.

Table 4 - Mechanical properties of elements used in the analysis of wall

| Material Type | Young's Modulus E | Poisson's ratio V | Tensile Strength | Compression strength | Fracture Energy in tension (Gf) | Peak compressive strain | Unit Weight |
|---|---|---|---|---|---|---|---|
| | GPa | - | MPa | MPa | N/m | - | kN/m3 |
| Lime Mortar | 0.126 | 0.17 | 0.1 | 1.5 | 10 | 0.0119 | 20 |
| Red Sandstone | 20 | 0.2 | 1.5 | 30 | 43.5 | 0.0015 | 21 |
| Grey Sandstone | 13 | 0.2 | 2 | 20 | 58 | 0.00154 | 21 |
| Green Sandstone | 8 | 0.2 | 1.2 | 12 | 34.8 | 0.0015 | 21 |
| Rubble Masonry | 0.7 | 0.2 | 0.1 | 2 | 10 | 0.00286 | 20 |
| Steel Plate | 200 | 0.3 | - | - | - | - | 0 |

## 4.3    The geometry of the wall sample considered for the analysis

From the two wall samples considered for the Schmidt hammer test, same samples have been considered for the finite element analysis. To take into the effect of infill masonry, two different set of analysis was chosen to be performed, namely the longitudinal section of the outer leaf of the masonry and the transversal section of the walls which include all three leaf of the masonry wall. While for the longitudinal section, the arrangement of the stone units and lime mortar are modeled based on the on-site element measurements and observation from the photographic documentation of the walls which were exposed. While for the arrangement of the transversal section, some assumptions have been made to consider the effect of the internal rubble masonry, from different arrangements the arrangement with some stone interlocking between the leaf but without any through-stones was considered to neither underestimate or overestimate the bearing capacity of the walls.

The arrangement which has been used in the analysis are shown in **Figure 4.3** and **Figure 4.4**
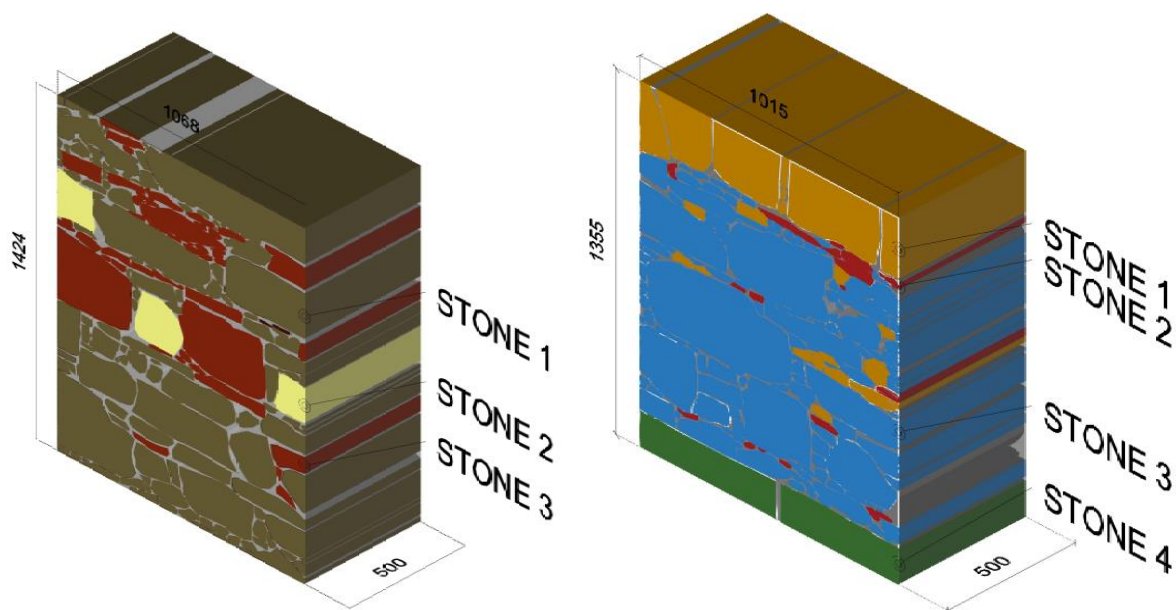


Figure 4.3 - Longitudinal section considered for the numerical analysis, Sample 1 (Right) Sample 2 (Left)

From the figure 4.3, it can be observed that the longitudinal sections considered for the analysis are approximately square in the cross-section and the thickness of the section considered is 0.5 m.

While from the figure 4.4, it can be observed that the transversal sections considered in the analysis are of 2 meters height and 1.2 meters in width and 0.5 meters in thickness. Here, considering the relatively large width of the wall, it was assumed that the effect of slenderness on the wall is less and hence the sample with a height of 2 meters was considered.
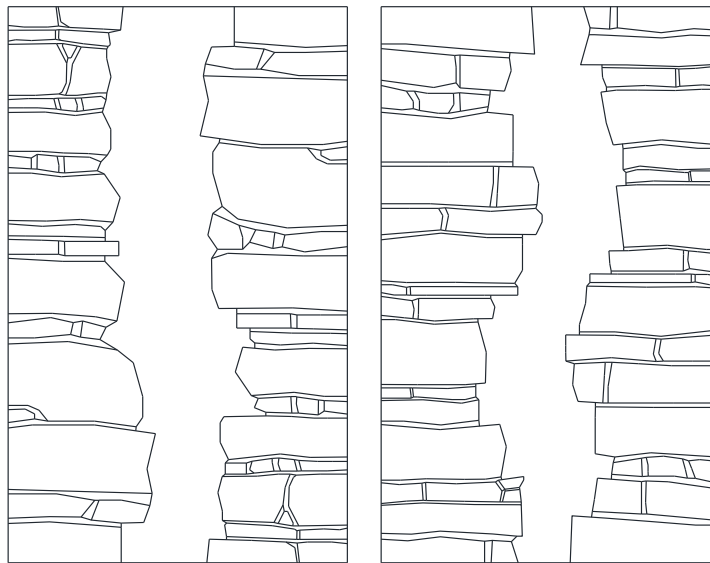
Figure 4.4 - Transversal sections considered for the numerical analysis Sample 1 (Left) Sample 2 (Right)

## 4.4   Modeling assumptions

Geometrical and material nonlinearity is considered in this numerical analysis of the wall models. Taking into account of the less tensile strength of the stones and mortar and as well as the crushing behavior of the materials in compression, material non-linearity has to be considered into the modeling. The easier way to explain these is the direct relation of the stress to the strain induced in the material, unlike the perfect elastic material, with an increase in applied stress levels, strain generated into the materials are tending to go beyond the elastic limit of the materials and then some non-linearity in the material is exhibited. In addition, the scope of this finite element analysis is to compute the maximum load-bearing capacity of the wall, it is also expected that the different material will undergo the different amount of strains and will be subjected to significant displacement. Considering this aspect, the loads are applied as a set of small prescribed deformation of 0.5mm per steps. With this strategy, it will be possible to compute the non-linearity of the wall configuration beyond the elastic limit as well.

The interface between the elements is considered to be rigid, which means that the sliding between the elements is restrained. This assumption is not true in the real behavior of the masonry elements, but it does not deviate much from the true behavior of the masonry as the surface of the stones used is not smooth. This results in the increased friction between the elements. Also, it is observed from the site inspection that the stones are either in contact with the mortar of with the infill material, which exhibits lower tensile strength compared to the stones, which will result on to the tensile failure of that material, which is more possible that the failure at the interface.

Also, in the analysis of this wall configurations, to apply the uniform displacement at the top and have the uniform reaction at the base, a thin rigid steel plate was modeled at the top and bottom of the wall configuration. In addition to that for the longitudinal wall configuration, plane stress model was adopted and for the transversal configuration, plain strain model was considered. In longitudinal wall configuration, the wall sample was restrained to move in horizontal directions to stimulate the real condition of the enclosure wall.

## 4.5 Material Constitutive Model

Material model in this numerical analysis is 3D nonlinear Cementitious 2, which is a type of fracture-plastic constitutive model available in ATENA 2D. The fracture-plastic model combines constitutive models for tensile (fracturing) and compressive (plastic) behavior of the material. The fracture model is based on the classical orthotropic smeared crack formulation and cracks band model. It employs Rankine failure criterion, exponential softening, and it can be used as rotated or fixed crack model. The hardening/softening plasticity model is based on Menetrey-William failure surface. The model uses return mapping algorithm for the integration of constitutive equations. This model can be used to simulate material cracking, crushing under high confinement, and crack closure due to crushing in other materials, which is ideal for the numerical analysis of the walls. This model supports the conversation of parameters for the plane strain idealization, which is the case for the analysis of the transversal wall sections.  (ATENA, 2018)
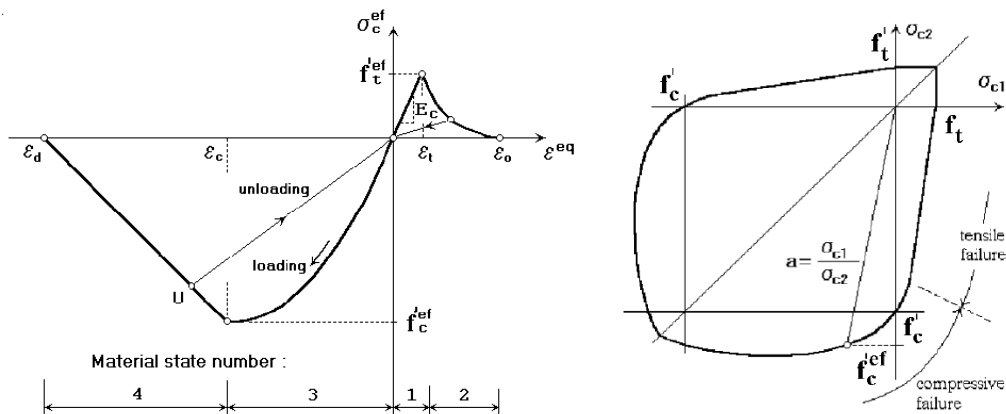


Figure 4.5 - Uniaxial stress-strain law (left), biaxial failure function (Right) used in the model (ATENA, 2018)

## 4.6 2D Analysis

For the analysis of the wall configurations, two longitudinal sections, and two transversal sections, ATENA 2D software was used. The modeling strategy, material parameters and material constitutive model used in these analyses are the same as described in the previous chapters. Furthermore, the solution parameters used for the analysis of the finite element problem was performed by using the

Newton-Raphson solution method with tangent stiffness and line search option. And for the convergence tolerance, energy error tolerance of 0.0001 was used.

### 4.6.1 Longitudinal Wall Configuration

As mentioned in this chapter earlier, two different configurations of the walls with the different build up were used and performed in the analysis, as shown in **Figure 4.6**
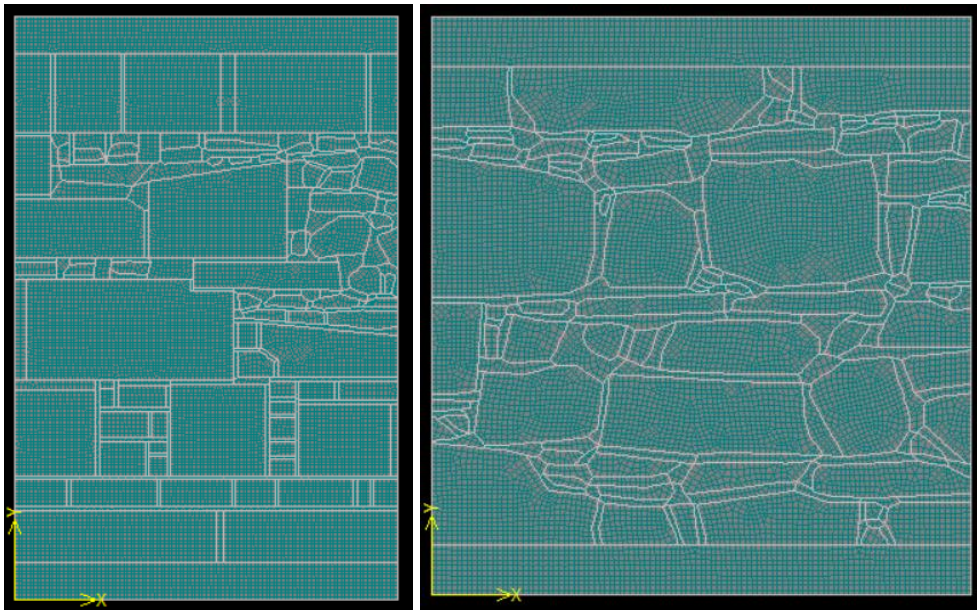


Figure 4.6 Longitudinal wall configuration 1 (left) configuration 2 (Right)

After performing the analysis, to observe the damage and performance of the wall under the compressive stress applied as the deformation, cracks and the maximum principal stress was observed on the section as shown in **Figure 4.7** and **Figure 4.8**.

From this analysis it is possible to observe the damages occurred in the walls, which can be defined as the tensile failure of the lime mortar near the joints and at some isolated locations, crushing of stones which are concentrated at the sharp corners.
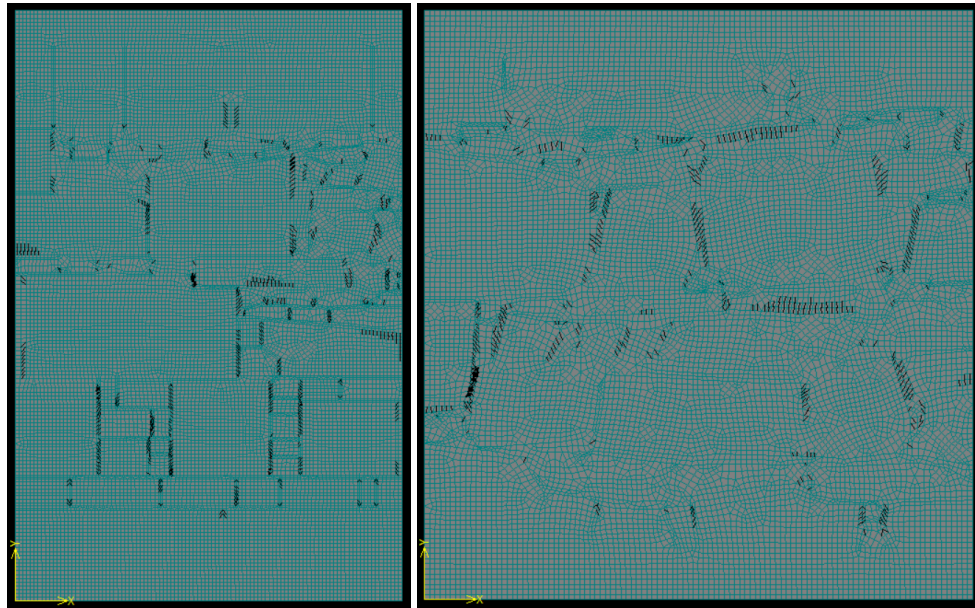
Figure 4.7 - Crack pattern in longitudinal wall configuration 1 (Left) configuration 2 (Right)
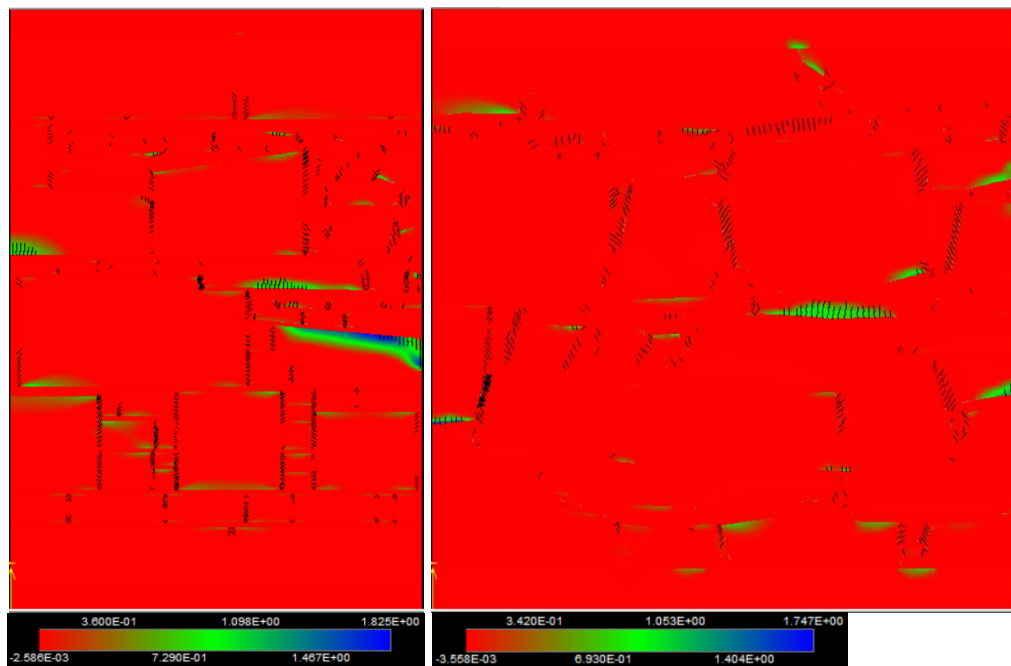


Figure 4.8 - Maximum Principal stress in the wall configuration 1 (Left) configuration 2 (Right)

From this analysis, a stress vs strain curve can be plotted as shown in Graph 1, from the graph it can be observed that after achieving the maximum stress, the stress level with increasing strain level is declining but it is not brittle, this type of failure can be explained by the confined boundary condition of the wall configurations, which does not allow the horizontal global movement of the elements, which ultimately results into the crushing and crack closing of the mortar and stone units.
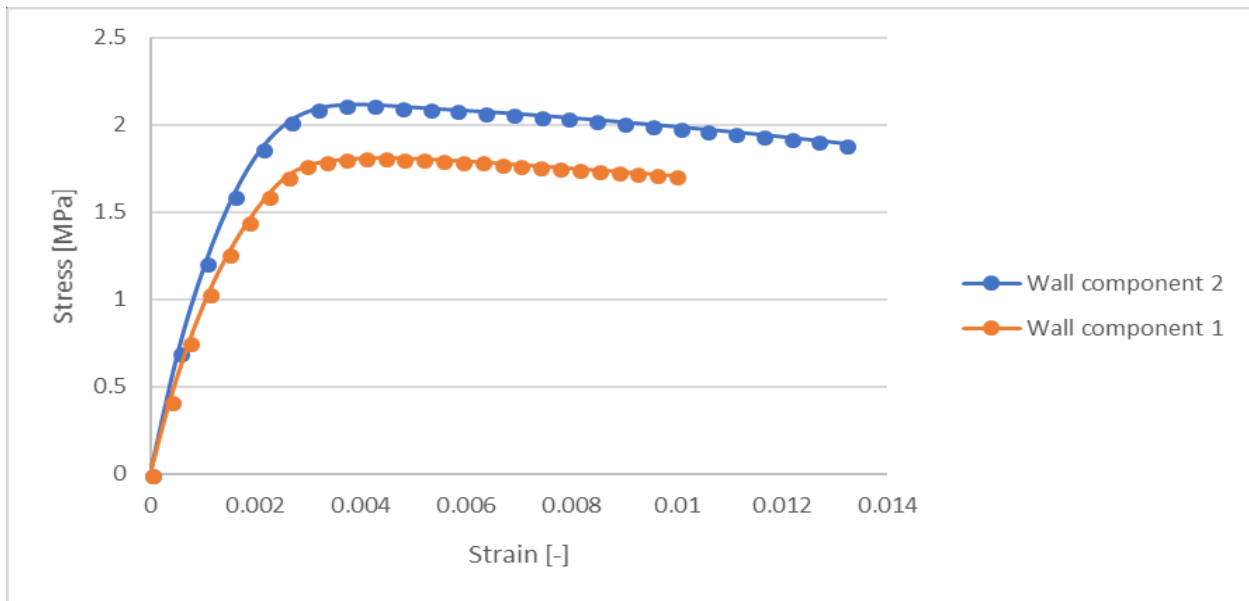
**Graph 1 - Stress vs Strain plot of longitudinal wall configurations**

From this analysis, results can be plotted in the table as shown in Table 5, where the tensile strength of the wall as a homogeneous material is considered as 1/10th of the peak compressive strength.

**Table 5 - Table showing the peak compressive strength and corresponding other parameters for longitudinal wall configurations**

| Wall Configuration | Peak compressive stess [MPa] | Estimated Tensile strength [MPa] | Global Vertical displacement [mm] | Global Vertical strain [$10^{-3}$] | Young's modulus [GPa] |
|---|---|---|---|---|---|
| 1 | 1.81 | 0.18 | 6.00 | 4.43 | 0.94 |
| 2 | 2.11 | 0.21 | 3.50 | 3.70 | 1.01 |

### 4.6.2 Transversal Wall Configuration

As mentioned in this chapter earlier, two different configurations of the walls with the different build up were used and performed in the analysis, as shown in Figure 4.9

After performing the analysis, to observe the damage and performance of the wall under the compressive stress applied as the deformation, cracks and the maximum principal stress was observed on the section as shown in Figure 4.10 and Figure 4.11.
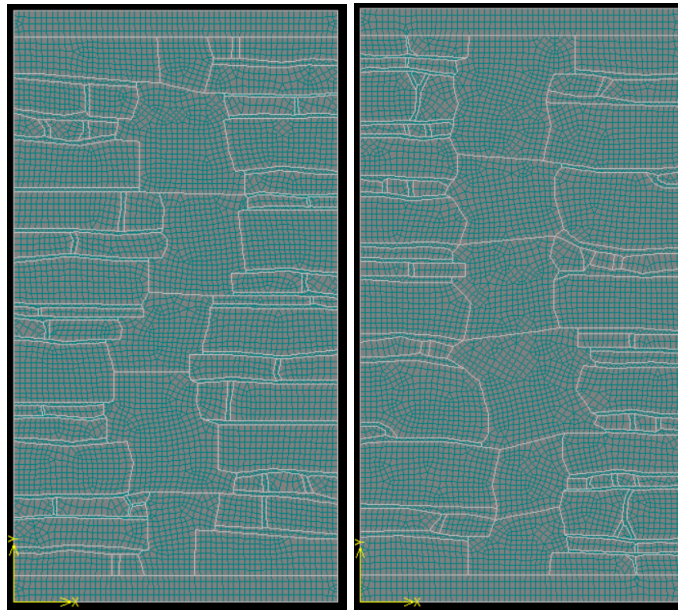
**Figure 4.9 - Transversal wall configuration 1 (Left) configuration 2 (Right)**
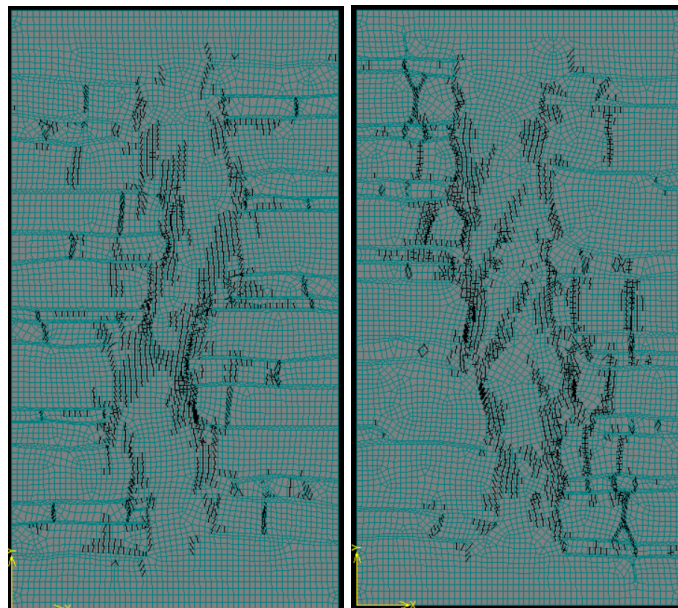


**Figure 4.10 - Crack pattern in a transversal wall configuration 1 (Left) configuration 2 (Right)**

From this analysis, it is possible to observe the damages occurred in the transversal walls. Here with an increase in the compressive stress, it can be observed that the wall undergoes the damage, which starts to occur near the infill rubble and outer leaf from both sides, these cracks separate the infill from the external masonry and relatively high transversal deformations can be observed in the wall. With further increase in the load, cracks in the lime mortar and crushing of stones can be observed at some locations. From this analysis, a stress vs strain graph can be plotted which is shown in Graph 2.
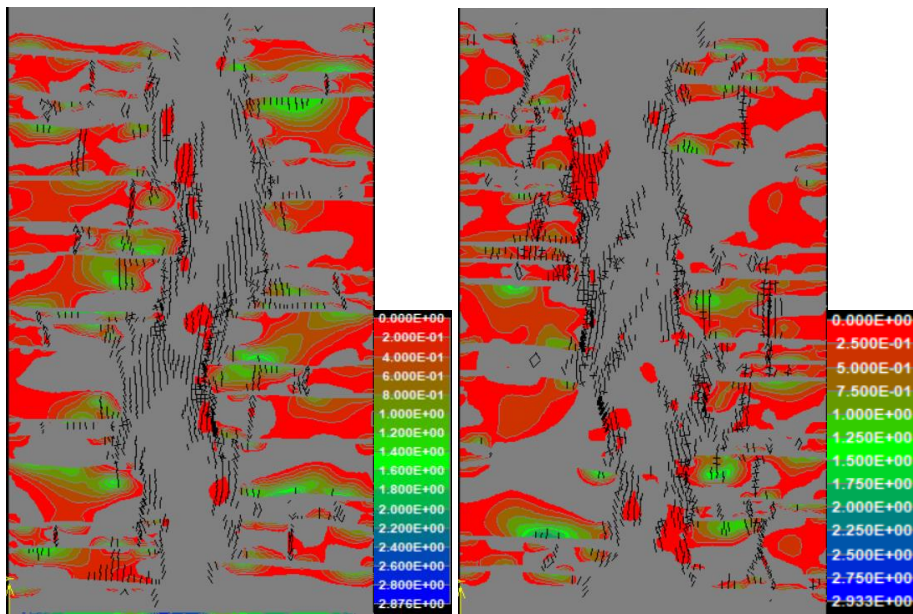
**Figure 4.11 - Horizontal tensile stress in transversal wall configuration 1 (Left) configuration 2 (Right)**
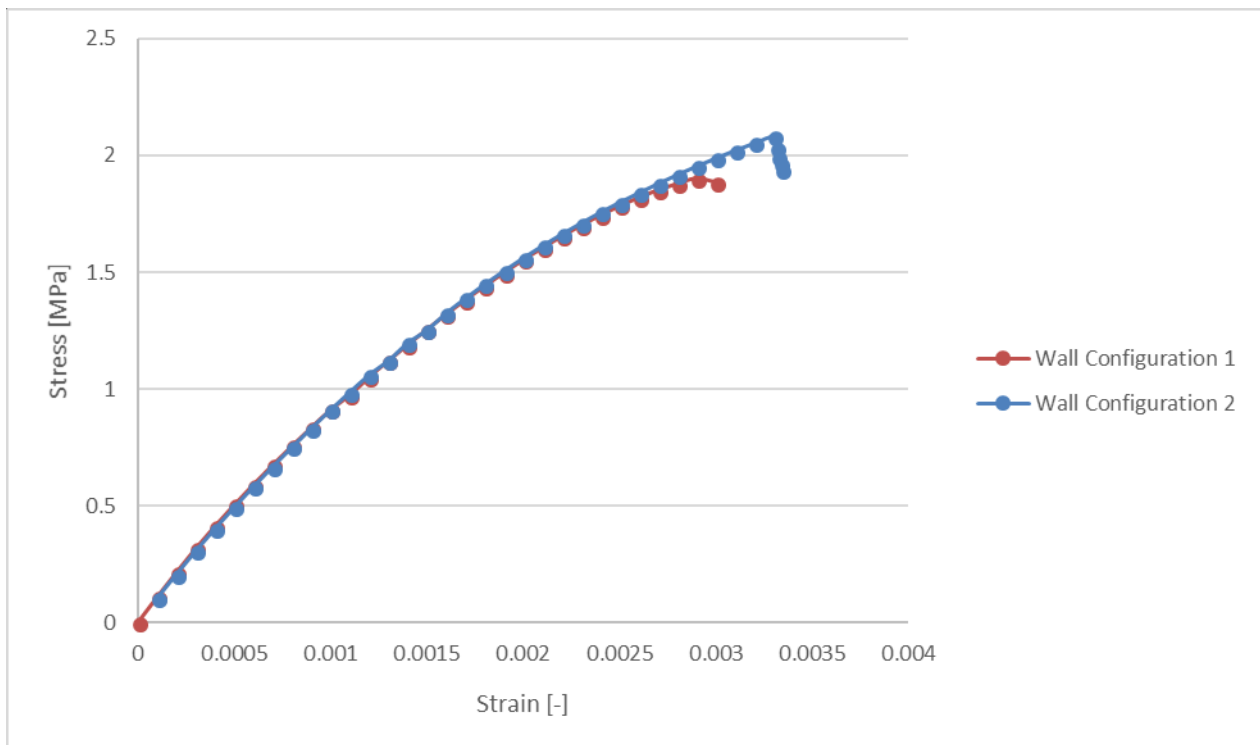


**Graph 2 - Stress vs Strain plot of transversal wall configurations**

From this analysis, results can be plotted in the table as shown in Table 5, where the tensile strength of the wall as a homogeneous material is considered as 1/10th of the peak compressive strength.

**Table 6 - Table showing the peak compressive strength and corresponding other parameters for transversal wall configurations**

| Wall Configuration | Peak compressive stess [MPa] | Estimated Tensile strength [MPa] | Global Vertical displacement [mm] | Global Vertical strain [$10^{-3}$] | Young's modulus [GPa] |
|---|---|---|---|---|---|
| 1 | 1.90 | 0.19 | 5.8 | 2.9 | 1.08 |
| 2 | 2.08 | 0.2 | 6.6 | 3.3 | 1.03 |

## 4.7  Loading condition of Structure

To compute the bearing capacity of the masonry walls, it is important to consider the state of different loading that the structure is supporting such as self-weight, live loads, wind loads, snow load, seismic acceleration in the event of an earthquake. To consider the effect of this loadings separately and in combination with each other is complex in the context of historical structures as there are adequate guidelines available for the same, but Eurocode 5 provides a basis for the consideration of the state of loadings. From the Eurocode 5, it is also possible to consider the combination of different loadings which is shown in Table 7

**Table 7 - Load combination according to Eurocode 5**

| # | ULS Loading Combinations |
|---|---|
| 1 | 1.35DL + 1.5LL |
| 2 | 1.35DL + 1.5SL |
| 3 | 1.35DL + 1.5(Sl or LL) + 0.75WL |
| 4 | 1.35DL + 1.5WL (pressure) + 0.75SL |
| 5 | 1.0DL + 1.5WL (suction) |

In this analysis, only the vertical components of the loading are considered. The detailed calculation of this is mentioned in the Appendix B. In Table 8, the state of loading due to the load combination and the safety factor from the previous analysis of longitudinal and transversal loads is mention.

**Table 8 - Table showing the safety factor from the numerical analysis against different load combinations**

| Load Combination No. | 1 | 2 | 3 | 4 | 5 |
|---|---|---|---|---|---|
| Load at foundation level for ULS [MPa] | 0.54 | 0.52 | 0.55 | 0.53 | 0.38 |
| Longitudinal Wall 1 | 3.33 | 3.46 | 3.30 | 3.42 | 4.81 |
| Longitudinal Wall 2 | 3.88 | 4.04 | 3.84 | 3.98 | 5.61 |
| Transversal Wall 1 | 3.49 | 3.63 | 3.45 | 3.58 | 5.04 |
| Transversal Wall 2 | 3.82 | 3.97 | 3.92 | 4.70 | 5.52 |

From the table it can be observed that the all the numerical analysis for the walls have the higher safety factor against different load combination which shows that the structure itself is safe for the current state of loading and the damages that can be observed from the site is due to the external factors rather than the wall's capacity of transfer the static loads.

# 5 SOIL STRUCTURE INTERACTION AND EFFECT OF SETTLEMENTS ON CHURCH

## 5.1 Soil structure interaction

In the structural design of the new structures, often the superstructure is designed in detail and the sub-soil structure is simplified as the pinned or rigid supports. This strategy of designing is valid in the most cases of the new structure as the foundation is designed from values of those support reactions and the available soil data which is simplified in terms of soil bearing capacity including many safety factors. These assumptions are acceptable when the sub-soil is relatively stiff, and the superstructure is light. But in the case of historical structure, which is mainly the load bearing structure with a large thickness of wall and shallow foundation depth, this strategy or assumption does not apply mainly because of the effect of soil settlement and differential settlements are neglected. So, it is important to consider the effect of the soil deformations and its effect on the superstructure. To incorporate the deformations in the structure, which are consistent with the deformations in the sub-soil, some soil-structure interaction methods can be employed, which treats the superstructure as a beam and the sub-soil as a set of vertical springs.

To model the soil structure interaction, there are two methods that can be used, one is modeling the structure as beam element on elastic subsoil layer and the other is continuum approach using numerical analysis method. In these methods, deformation of subsoil layer and structure which finally determines settlement are analyzed. While the first method is simple, as it requires only two input parameter which is the modulus of subgrade reaction and shear modulus of a shear layer, however, to obtain these parameters, a series of estimations must be done when the subsoil within influence zone consists of many layers of soil. While the first method will be discussed in this study and used as a calibrating method to ensure that the finite element analysis method does not deviate too far from the analytical method, the some of the analysis will be done in finite element modeling also.

### 5.1.1 Winkler Model

The aim of the Winkler foundation model is to idealize the soil as a series of springs which displaces due to the load applied to it. While the approach of this method is very simple the disadvantage of this model is the non-consideration of the interaction between the springs. The soil is also described according to the linear stress-strain relation. This linear behavior makes the calculations easier but, this is not the case, soil behave in a nonlinear way. (Brénousky J.S.)

While in reality this model does not yield the realistic value of soil-deformations, but it still gives an indication about the settlement, which might occur in reality. The main advantage of this model is the simplicity which is given by the one parameter (i.e. modulus of sub-grade reaction) to represent the soil as shown in Figure 5.1.
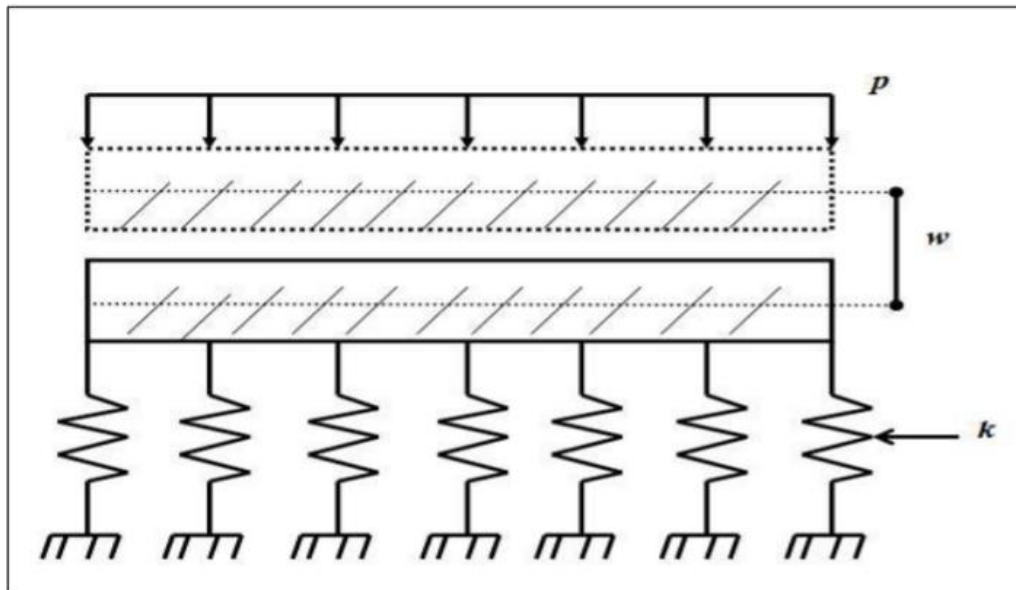
**Figure 5.1 - Winkler Model**

P = w*k

Where P = pressure, W = settlement and k = modulus of subgrade reaction

The modulus of subgrade reaction is a model parameter that describes the stiffness of the soil. This parameter is not a soil property. This value is determined by dividing the pressure by the settlement. The settlement can be determined by different methods. A few methods are given by the Koppejan and Terzaghi. This parameter does not only depend on the nature of soil but also it depends on the dimensions of the foundation area and the type of loading applied.

### 5.1.2    Pasternak Model

To overcome the shortcoming of the Winkler model, some improved versions of the model have been developed. One of these versions is the Pasternak foundation model. In this model, the springs are coupled with each other. This model is also simple as it depends on only two paraments, modulus of subgrade reaction and another shear parameter. Physically, this parameter represents the interaction due to shear action between the spring elements. With this extra parameter, the displacement of the model can be more realistic compared to the earlier model. (Figure 5.2) (Brénousky J.S.)
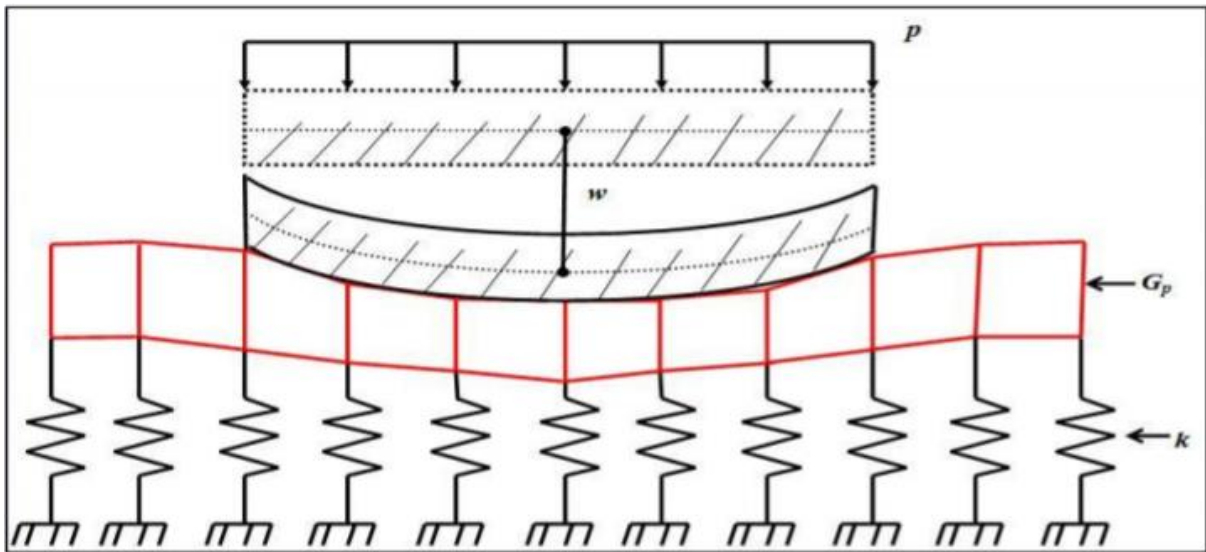
**Figure 5.2 - Pasternak model**

### 5.1.3 Continuum Approach

In continuum approach, the subsoil layers are modeled as continuously distributed objects through space. The various constitutive model can be used to represent the soil properties. The simplest one being linear elastic isotropic material. A continuum model can be analyzed with numerical methods which include Finite Element Method (FEM) and Boundary Element Method (BEM). FEM is a preferred to solve the model with non-linear soil properties, while BEM is more compatible with semi-infinite linear elastic analysis. Since modeling of a shallow foundation is not a problem of semi-infinite structure, FEM is more relevant in the course of this study and hence will be discussed in more detail. (Susanti, 2017)

Several analytical solutions for this continuum approach have been developed. One of the most well-known approaches is Boussinesq theorem. In his theorem, the sub-soil is assumed as a semi-infinite, homogeneous, isotropic, linear elastic matter. The analysis was carried out for point loads and infinite strip loads regardless of Poisson's ratio. The self-weight of the soil is disregarded in this approach.

Another proposed method of estimating the vertical stress is Westergaard's analysis. Westergaard's analysis assumes that subsoil is reinforced by thin, horizontal sheets of negligible thickness. Westergaard's formula is especially useful to model subsoil with alternating layers of stiff and soft material. Vertical stress increases below a stiff soil stratum calculated using this method had been shown to be less than that of Boussinesq's method. In this paper, however, since the subsoil does not consist of layers of very different soil, Boussinesq's method will be sufficient to perform calibration of the results obtained from the other program.

### 5.1.4    The depth of Influence Zone

The extent to which a structure or the surface load applied influences the subsoil below it is termed as the influence zone. The concept could also be used as a tool to assess the volume of soil actively supporting the foundation and superstructure.

One of the most common methods of assessing the depth of influence zone is to use the Boussinesq or Westergaard equations and evaluate the depth at which the stress in the soil becomes one-tenth of the stress applied on the surface. Depending on the experience and confidence of the analyst, this depth can be increased or decreased by considering 15 or 20 percent of the stress applied on the surface. The lateral width of the influence zone, on the other hand, needs to be found by trial and error due to the shape of the pressure bulbs obtained from Boussinesq's equation. Different values of z (depth) can be used, until the maximum value of the horizontal distance is obtained indicating the maximum horizontal distance at which the stress from the foundation is significant. (Susanti, 2017)

In this analysis, the depth of influence zone was calculated using a program which uses Winkler Pasternak and the Theory of Structural Strength as a basis for its calculation. It also provides the values of the constants $C_1$ and $C_2$. (Kuklik, 2 July 2016)

This program exploits the loading history of soil and its capacity to memorize the highest load it has been subjected to represented by over-consolidation ratio along with the initial voids ratio. Since the deformability of virgin soil is relatively high, the subsequent unloading and reloading result in minimal deformation, making the soil behave as an almost incompressible layer until the highest stress is reached again. It defines the depth of influence zone as the point in soil at which the effective vertical stress due to surcharge becomes equal to the value of      where h is the depth of excavation carried out. (Figure 5.3) This is based on the concept that the orginal stress state in the soil undergoes a change on being subjected to excavation due to a change in the highest stress level recorded in the loading history of the soil, often refered to, as the preconsolidation pressure. (Kuklik, 2010)

**Figure 5.3 - Concept of dthe epth of influence zone (Kuklik, 2010)**

Mathematically, the closed form of the expression used to estimate the depth of influence zone is based on the deformation of an elastic layer. Additionally, the horizontal displacements have been neglected, like in the Westergaard assumptions leading to a stiffer response than reality. The expression of the depth of influence zone (H) presented below is the result of loading from a uniform strip of width 2a. (Kuklik, 2010)

$$H = \frac{\pi a}{2}\left(\frac{2-2v}{1-2v}\right)^{\frac{1}{2}} \frac{1}{\ln\left(sin\frac{\pi\gamma h}{2f_z} + 1\right) - \ln\left(cos\frac{\pi\gamma h}{2f_z}\right)}$$

It is to be noted that H deepnds directly on the width of the strip load (2a) and is independent of Young's modulus of soil. The Poisson's ratio ( ) however plays a significant role where    is the value of the surcharge in kN/m. (Kuklik, 2010)

The Theory of Structural Strength offers a similar yet alternative method for assessing the depth of influence zone using a coefficient of structural strength called m. The influence zone is defined as the depth at which the increment in vertical stress (   ) is used as a standard to equate with the original structural strength of soil (    ) multiplied by the coefficient (m) expressed as    = .     and the settlement is expressed as   = (   ,  ,    ) (Figure 5.4) The value of m s determined on the basis of the fundamental type of soil, consistency, consolidation and deformation modulus.  (˘Sejnoha, 2009)

**Figure 5.4 - Depth of influence zone based on theory of structural sthe trength (Geo5)**

## 5.2   Sub-soil data

The geological condition on a global scale is described in chapter 3.6. That chapter described the geology of the sub-soil condition on a global scale, which does not include the mechanical parameter and different soil layers present in the case of study. To analyze the effect of sub-soil degradation and the present condition of the various sub-soils it is necessary to carry out the local test on the soil with bores.

In this case study, two different boreholes of about 10 cm diameter were bored next to the church wall outside. One borehole was installed near the east side of the church (entrance) and another borehole was installed at the west side of the church (Sacristy). Borehole locations and the description of sub-soils are mentioned in Appendix C.

In general, the extracted soil from both the borehole exhibited the average condition of the soils but it was also observed that the soil present at the east side is relatively inferior to the west side. From the bore-logs it was possible to observe the depth of foundation present at the site, as boreholes were bored near the wall, it was possible to notice the presence of fragments of sandstone and other building stones to the depth of foundation which was observed to be up to the 1.8 meters deep.

In the subsoil, it is also possible to observe the quality of different layer and derive some mechanical parameter of the soil layer. Figure 5.5 Shows the depth of different layers of soils from the foundation levels and Table 9 shows the estimated mechanical parameters of those soil layers which are used in the later analysis.
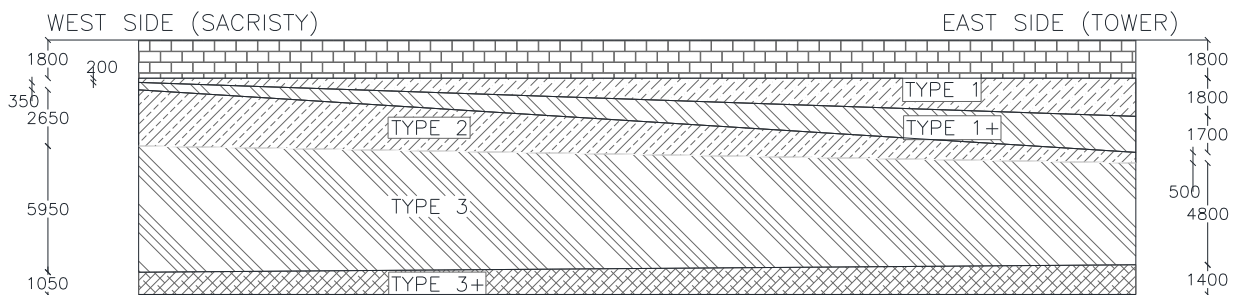


**Figure 5.5 - Linear idealization of different soil layers between boreholes**

**Table 9 - Table showing the different mechanical parameters of the soil types**

| "Soil Type" | Edef [MPa] | Poisson's Ratio v [-] | Friction angle ' [°] | Cohesion c' [kPa] | Density kN/m$^3$ |
|---|---|---|---|---|---|
| 1 | 20 | 0.35 | 25 | 30 | 19.5 |
| 1+ | 25 | 0.35 | 25 | 30 | 19.5 |
| 2 | 5 | 0.35 | 30 | 30 | 20 |
| 3 | 30 | 0.35 | 30 | 40 | 20.5 |
| 3+ | 35 | 0.35 | 30 | 50 | 20.5 |

### 5.2.1 The conversation of subsoil layer properties into spring constants

The modulus of the deformation k, of the subsoil as a homogenized parameter can be obtained by transforming the soil into the two Winkler Pasternak constants C1 and C2. This transformation is done using Program Depth as described earlier in this chapter. The limitation of this program is that it is only able to do the transformation for a single layer of subsoil. To overcome this limitation, an equivalent value of Young's modulus, Poisson's ratio and unit weight of the subsoil is obtained at the different location of the church. This equivalency is done for subsoil within the depth of influence. Similarly, the influence depth is also obtained from the Program Depth. Hence, an iteration process has to be performed such that an influence depth value that gives an equivalent value of unit weight and Poisson's ratio, that ultimately generates the same influence depth for the sub-soil.

**Table 10 - Table showing the depth of influence at different locations**

| Location | Influence depth [m] |
|---|---|
| West Side | 7.398 |
| MiddleWest Side | 7.398 |
| Middle Side | 7.398 |
| MiddleEast Side | 7.4 |
| East-Side | 7.4 |

For the estimation of soil-layers as a homogeneous property, a simple triangular force attenuation is assumed. For this deformation caused by a unit load (1 kN) is assumed to be acting at the ground level on a unit area. From the triangular attenuation of load into the sub-soil the deformation caused by each layer is computed and then the total deformation of sub-soil is computed by adding values together. And from this, the equivalent value of Young's modulus can be computed. Equivalent young's modulus, Poisson's ratio, density and C1 and C2 parameters are presented in Table 11.

**Table 11 - Table showing the idealised parameters on the sub-soil layers**

| Location | Equivalent Youngs modulus [MPa] | Poisson's Ration [-] | Unit weight [kN/m³] | c1 [MN/m³] | c2 [MN/m] |
|---|---|---|---|---|---|
| West Side | 26.88 | 0.35 | 20 | 8.681 | 6.82 |
| Middle-West Side | 26.26 | 0.35 | 20 | 8.481 | 6.662 |
| Middle Side | 25.7 | 0.35 | 20 | 8.3 | 6.52 |
| Middle-East Side | 25.19 | 0.35 | 20.5 | 8.136 | 6.391 |
| East-Side | 24.59 | 0.35 | 20.5 | 7.942 | 6.239 |

Analytical solution of Pasternak model, that expresses the stress experienced by sub-soil as a function of C1 constant, C2 constant, displacement, w, and change in displacement, Δw, could be expressed in the equation below:

$$f = w\left(2\sqrt{c_{1w} \cdot c_{2w}} + c_{1w}b\right)$$

Where f (kN/m) represents the total load acting on subsoil, c1w and c2w are Winkler Pasternak constants, b (m) is the width of the foundation modeled. Considering that the deformation modulus, k, of the subsoil is defined as the settlement, w, that a load, f, causes. This modulus of deformation, k, could be represented as:

$$k = 2\sqrt{c_{1w} \cdot c_{2w}} + c_{1w}b$$

Based on the above-mentioned equation, the modulus of deformation that would be used as spring constants for the 3D modeling is tabulated below.

**Table 12 - Idealised spring constant at different locations**

| Location | k [MPa] |
|---|---|
| West Side | 25.81 |
| Middle-West Side | 25.21 |
| Middle Side | 24.67 |
| Middle-East Side | 24.19 |
| East-Side | 23.61 |
| West Side (Degraded) | 7.74 |
| Middle-West Side (Degraded) | 7.56 |
| Middle Side (Degraded) | 7.40 |
| Middle-East Side (Degraded) | 7.26 |
| East-Side (Degraded) | 7.08 |

Here for the computation of subgrade modulus, k, at the degraded location, the reduction factor of 0.3 was used to mimic the poorer conditions of the soil.

## 5.3 2D Model

This study of analysis of walls with different soil layers was conducted by using finite element analysis module of software FINE Geo 5.

Geo5 is a 2D Finite Element software that can analyze the behaviour of soil with surcharge using continuum soil approach. Even if the 2D model does not represent completely the behavior of the church's 3D problem due to soil settlement, this is deemed sufficient as a preliminary model study to assess the magnitude of stresses that the wall is subjected to due to these different soil condition.

### 5.3.1 Modeling assumptions

For the 2D analysis for the soil-structure interaction, modeling of the transversal wall was done as the Geo5 consider the soil layers as the plane strain problem and also the transversal wall section at the different location of the church can be idealized as the plane strain 2D elements. For that reason, the modeling of church wall to the full height and different soil-layers for various locations were modeled in the software.
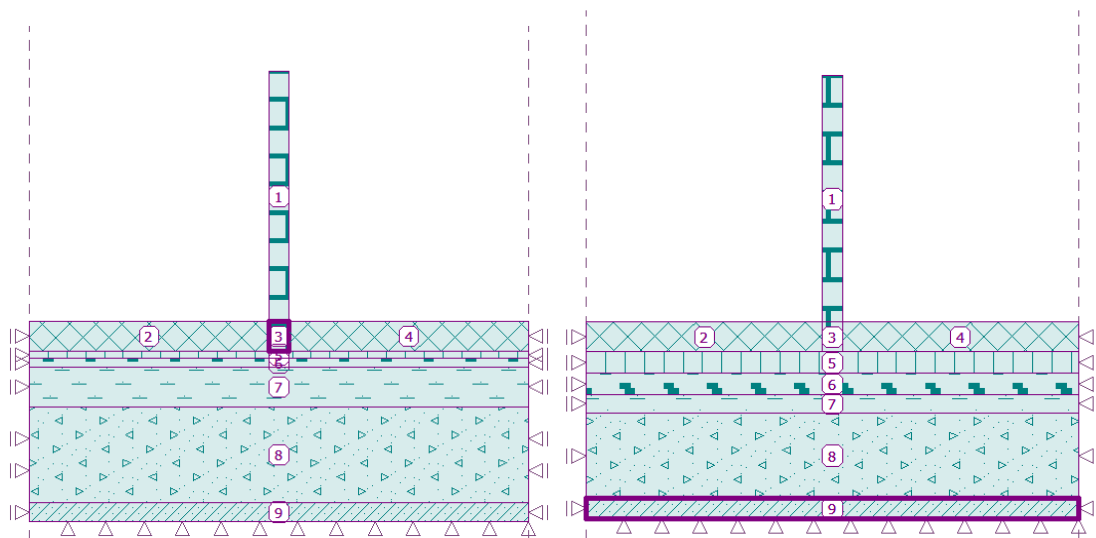


**Figure 5.6 - Modelling of the transversal wall and soil layer at West Side (Left) at East Side (Right)**

### 5.3.2 Material Model

Some contexts of the material model are available in Geo 5. In general, they can be divided into two categories namely, linear and non-linear. In Geo 5, two models are available for the linear material model including elastic and modified elastic model. The elastic model assumes a secant Young's modulus during the loading, unloading, and reloading. The modified version introduces one more parameter, Young's modulus for unloading and reloading to differentiate loading of the consolidated and virgin soil as shown in Figure 5.7. This modified version is especially useful for modeling of series loading and unloading of the surface load.

However, in this analysis, the material model employed for soil was the elastic model only, mainly due to the fact that there is the only limited amount of information is known for the different soil types. Hence, it would not yield useful results in the analysis by estimating more advanced soil properties as it requires in the modified elastic model or in non-linear soil model. However, using the elastic model to estimate the deformation yields the results on the conservative side in terms of the settlements which is the main objective of this case study.

**Figure 5.7 - Stress-strain diagram for Modified Elastic Model; real behavior of soil(left) and simplified depiction(right)**

Mechanical parameters were the same as described in this chapter earlier for that locations and load applied on the structure were in terms of the self-weight of the materials and additional surcharge due to the roof load was also applied as described in earlier chapters.

### 5.3.3    Result

Results from the analysis of the transversal wall sections in terms of soil settlements are tabulated in Table 13.

Also, from the analysis with geo 5, it is possible to observe the influence zone as well as the distribution of deformation in the different soil layers.

**Table 13 - Settlements at different locations**

| Location | Settlement [mm] |
|---|---|
| Sacristy | 5.5 |
| Sacristy Degraded | 17.7 |
| Middle West | 17.3 |
| Middle West Degraded | 54.3 |
| Middle | 17.6 |
| Middle Degraded | 55.4 |
| Middle East | 17.9 |
| Middle East Degraded | 56.2 |
| Tower | 30.6 |
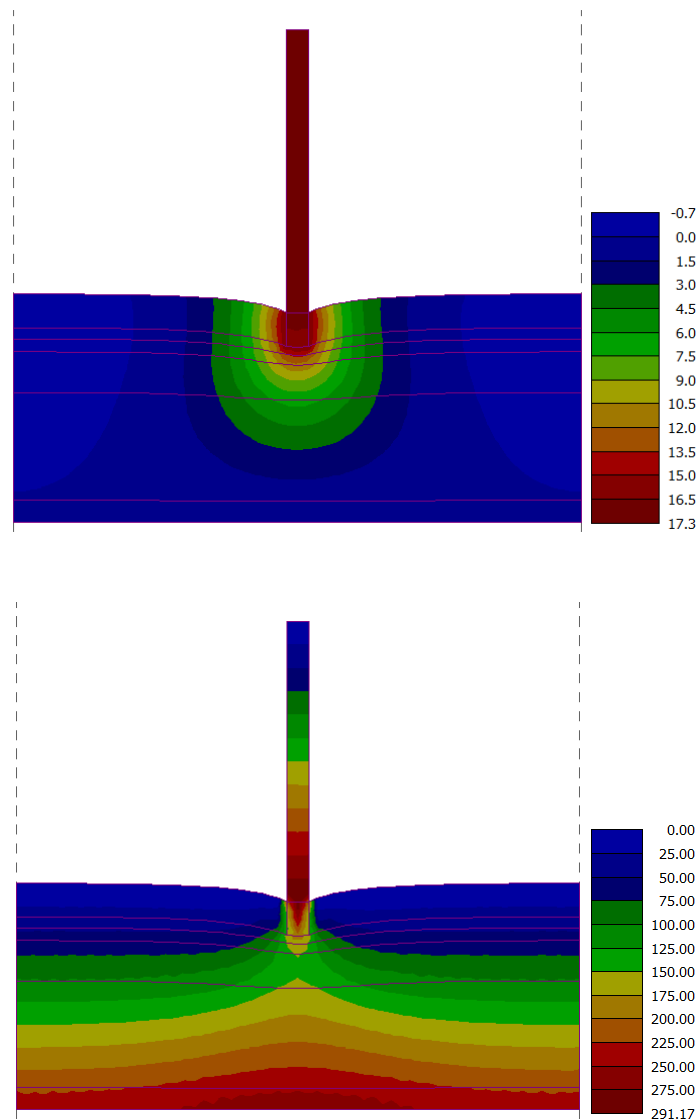
**Figure 5.8 - Settlement at the westside wall for the present soil condition [mm] at top and distribution of vertical compressive stress in soil layer [kPa] at bottom**

As shown in the case of backside wall it is possible to observe the distribution of settlement and stress in the soil layer for both conditions namely, at present state of sub-soil condition and at the location where the sub-soil is assumed to be degraded. For the degradation of soil, a reduction factor of 0.3 in terms of Young's modulus was applied in the analysis.

The analysis results for the settlement in degraded soil at west side is presented in, while the other results are shown in Appendix D.
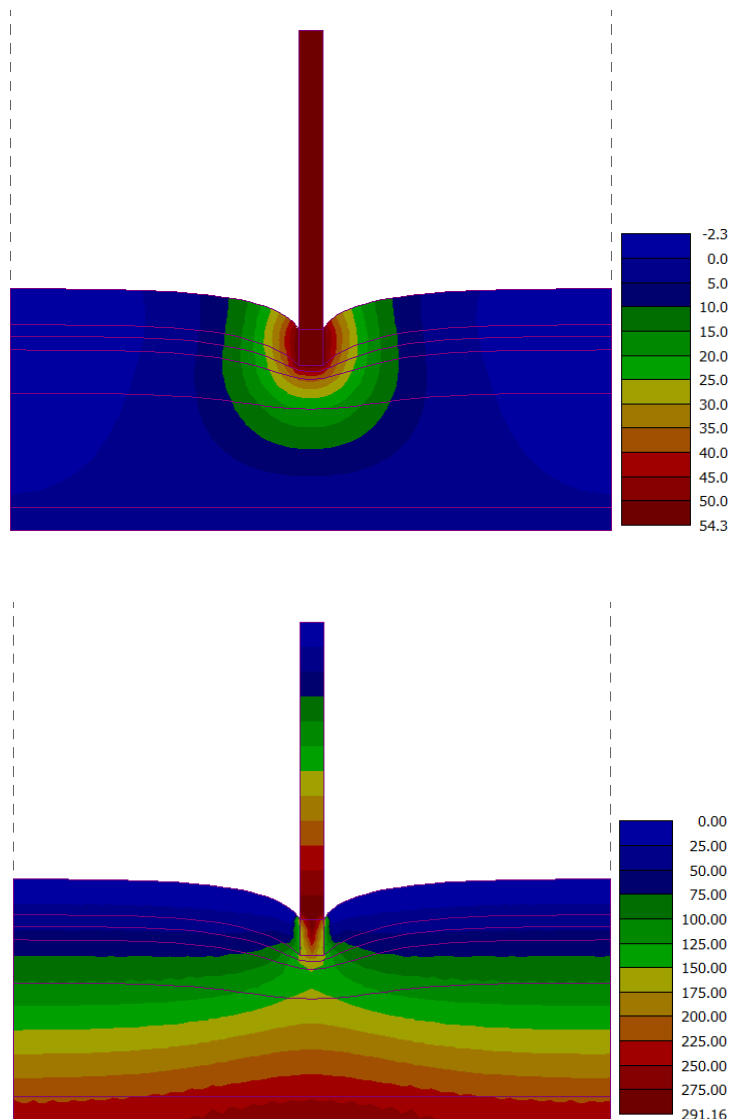
**Figure 5.9 - Settlement at the westside wall for the degraded soil condition [mm] at top and distribution of vertical compressive stress in soil layer [kPa] at bottom**

From the analysis results of the settlement using Geo 5, it is possible to observe that the differential settlement from westside to the east side of the church for the present state of soil is negligible [0.6 mm] but in the change of sections such as near the tower and sacristy where the applied load on soil is different than the man nave higher differences between the settlements can be observed for the present state of soil. While from the site observation it was observed that at many locations of the church foundation is degraded, and to evaluate the condition of foundation at those level, analysis was carried out considering the degraded condition of the soil at those locations, the amount of settlement observed at that location was much higher compared to the settlement in the present soil, which strongly suggest that the damages observed on the site can be related to the problems of differential soil settlement and a study is required to be carried out to analyse such effect by using 3D model.

## 5.4   3D Model

As discussed in the earlier in this chapter, from the 2D analysis of the transversal walls, it is evident that the structure on a global scale suffers from the problems of differential settlements and for the same reason, to evaluate the extent of damage in the structure a 3D analysis of the church shall be carried out.

In DIANA, a numerical model was built using solid structural elements to observe the behavior of structure in nonlinear material and geometrical conditions. The assumptions, support conditions, load, material properties, and results are discussed in following sections.

### 5.4.1   Assumptions

Some assumptions that made while developing the numerical model is listed here. It was considered that the roofing system of the church was not considered in the modeling part, only the equivalent loading for the roofing was considered. The architectural elements present in the church geometry were not considered into much detail but only the equivalent assumptions to make the simple orthogonal geometry was assumed. Also, the main focus of the study was to assess the damages due to the settlements in the main nave only the main nave part of the church was considered in the analysis as shown in Figure 5.10.
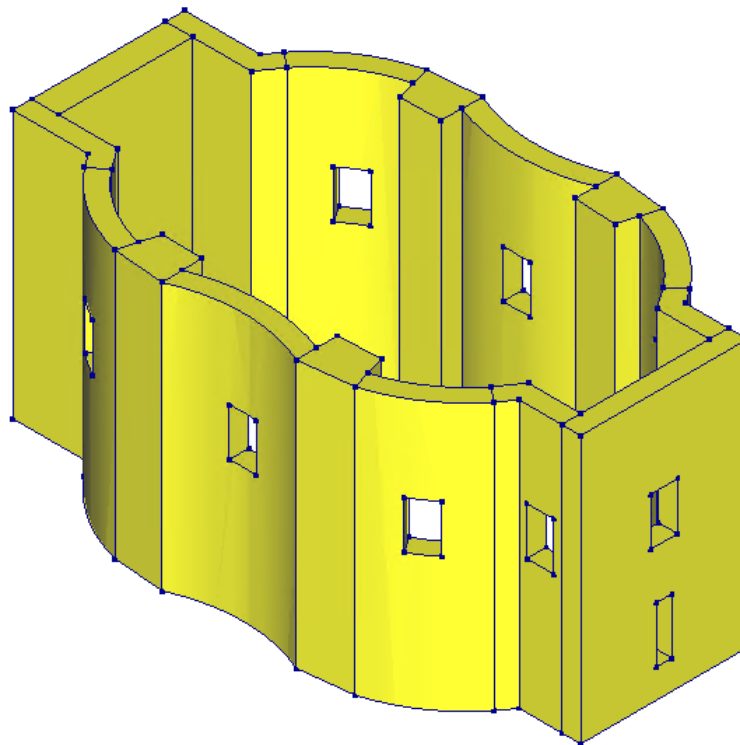


**Figure 5.10 - a Numerical model considered in the analysis**

### 5.4.2 Material properties and constitutive model

The definition of mechanical properties is the crucial and difficult part of the modeling phase. Since in heritage structures destructive tests are not accepted in most of the times, the most appropriate way to determine these properties are the non-destructive tests. However, non-destructive tests provide usually qualitative information which can be utilized to have a range of possible properties. A combination of a variety of tests can aid in the selection of the most suitable and realistic values. From the 2D numerical analysis of the wall configurations, it was possible to evaluate the material properties. From that analysis, it is possible to obtain the values of Young's modulus and peak compressive strength of the wall as a homogeneous element.

Afterward, the tensile strength can be computed as a percentage of the compressive strength. A ratio between the tensile and compressive strength can range between 3% to 10% (Angelillo M., 2014). A value of 10% of the compressive strength was chosen for the tensile strength. To compute the compressive fracture energy a ductility index (d) of 1.6 mm was used following Model Code 90. However, for the tensile fracture energy higher values are chosen in order to avoid convergence problems. All the mechanical parameters chosen for modeling are presented in Table 14.

**Table 14 - Material properties used in the 3D analysis**

| Youngs Modulus | 2 | Gpa |
|---|---|---|
| Poisson's Ratio | 0.2 | - |
| Mass Density | 2 | T/m3 |
| Crack Orientation | Rotating | - |
| Tensile Curve | Exponential | - |
| Tensile Strength | 0.2 | Mpa |
| Tensile Fracture Energy | 70 | N/m |
| Compressive curve | Parabolic | - |
| Compressive Strength | 2.9 | Mpa |
| Compressive Fracture Energy | 9100 | N/m |

For the analysis of the Church, in DIANA, total strain based crack based constitutive model was used for the analysis by applying above parameter while assuming rotating crack assumptions. The behaviours of the constitutive model can be observed graphically in Figure 5.11.
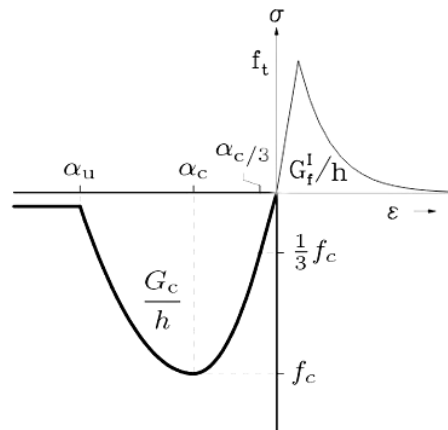
**Figure 5.11 - Graphical representation of the constitutive model used**

### 5.4.3 Supports and gravity loads

As the aim of this case study is to evaluate the extent of the damage on the structure due to differential settlements, supports were provided in a form of boundary interfaces which assumes the pinned supports with the spring elements at the nodes of elements, the spring modulus used here was the as it was evaluated in the chapter earlier. Here is the model these parameters were applied for the present state of soil only and to analyze the structure for the differential settlements, a prescribed deformation was applied at the location where it was suspected to have degraded soil conditions. Moreover, the loading due to the masonry wall was applied in the software as the dead weight and additional load due to the roof was applied at the top of the wall/
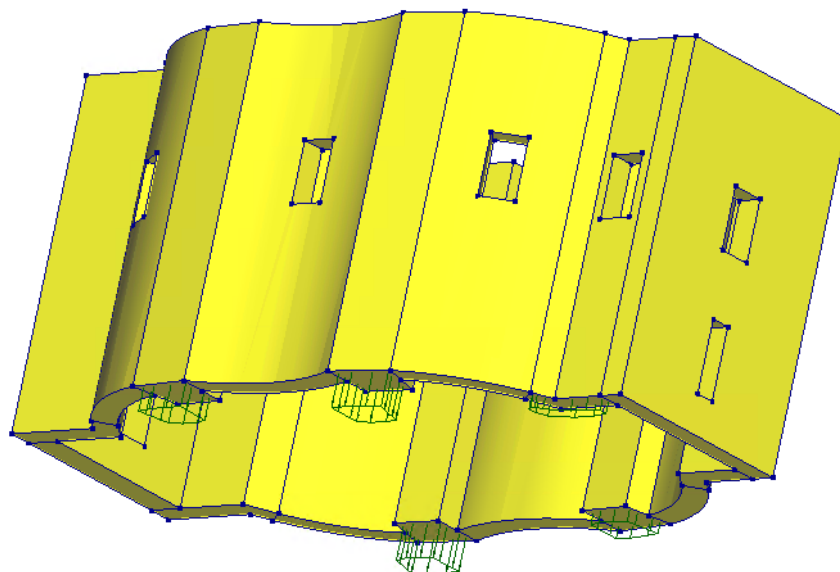


**Figure 5.12 - Graphical representation of prescribed settlement applied**

### 5.4.4 Results

To perform the analysis a nonlinear analysis in the vertical direction was carried out, the strategy used in the analysis was to apply the load of the structure on the boundary elements in an incremental manner to observe the occurrence of any damages due to the self-weight and roof load only. For this, the vertical load was applied in 10 steps until it reached the full weight and then the amount of settlement was observed. The deformation of the church in the vertical direction is shown in the Figure 5.13
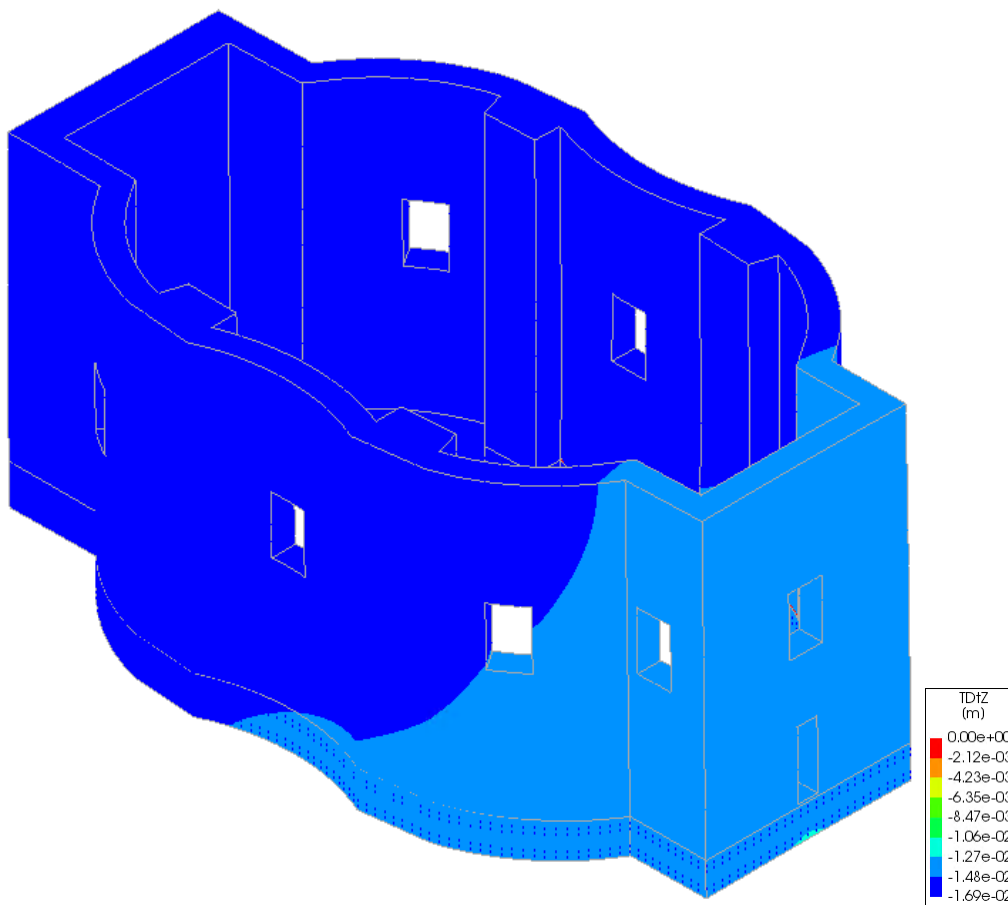


**Figure 5.13 - vertical deformations in the structure at full gravity load**

From the non-linear analysis for the gravity loads only it can be observed that the settlement values in the structure vary from the 14.8 mm to 16.9 mm from west to east side which is within the limits of the settlements values achieved from the 2D analysis using Geo 5.

After the application of the self-weight on the structure, the prescribed settlements of 30 mm and 15 mm at the locations of major foundation decay and minor foundation decay was applied respectively. These deformations were applied in the incremental manner of 0.05 times per load steps. The final deformation of the structure is shown in,
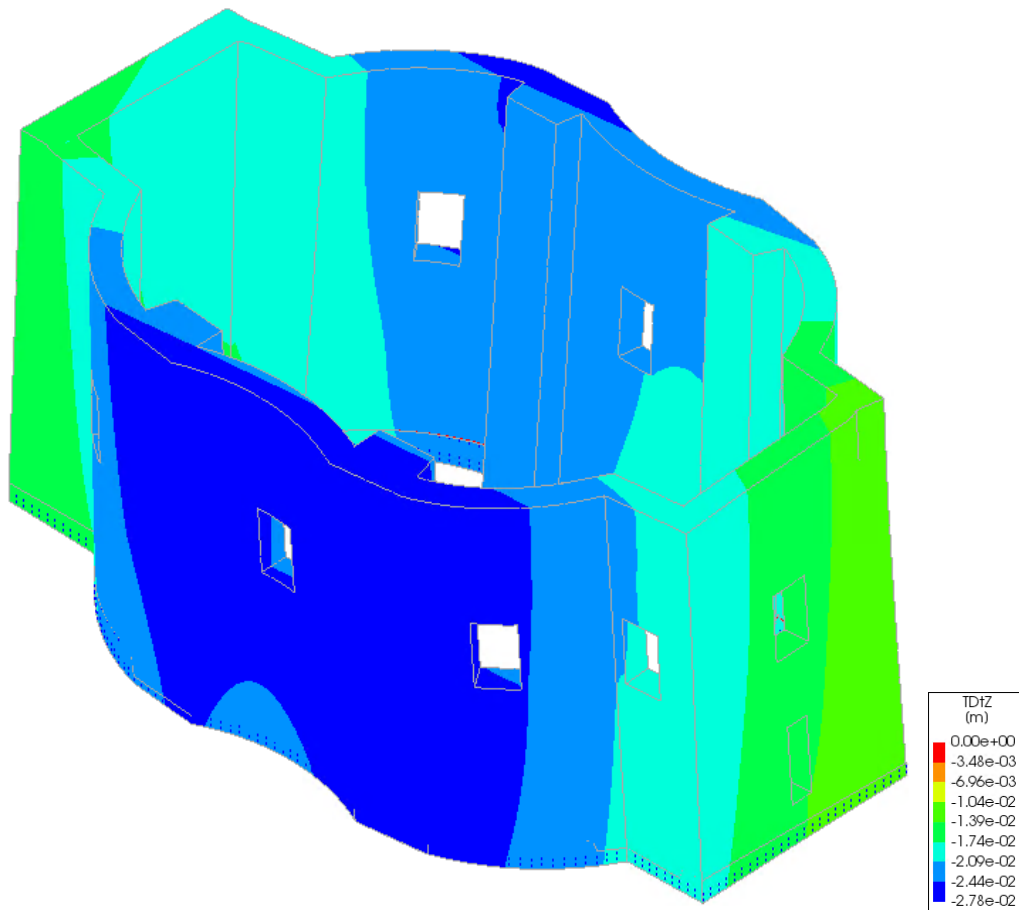


**Figure 5.14 - Deformation in the structure after implication of settlements in the structure**

Form the above figure it is possible to observe the settlement of the structure at the final stage of analysis. The load-step vs settlement plot can be observed in the Graph 3, at the different location in the structure. From the plot it is possible to observe that the until step 10, all the location went through the same settlements approximately, which was the case where the springs were applied for the good soils conditions throughout, but when the effect of differential settlements was mimicked, it is possible to observe the evolution of settlements at different locations.
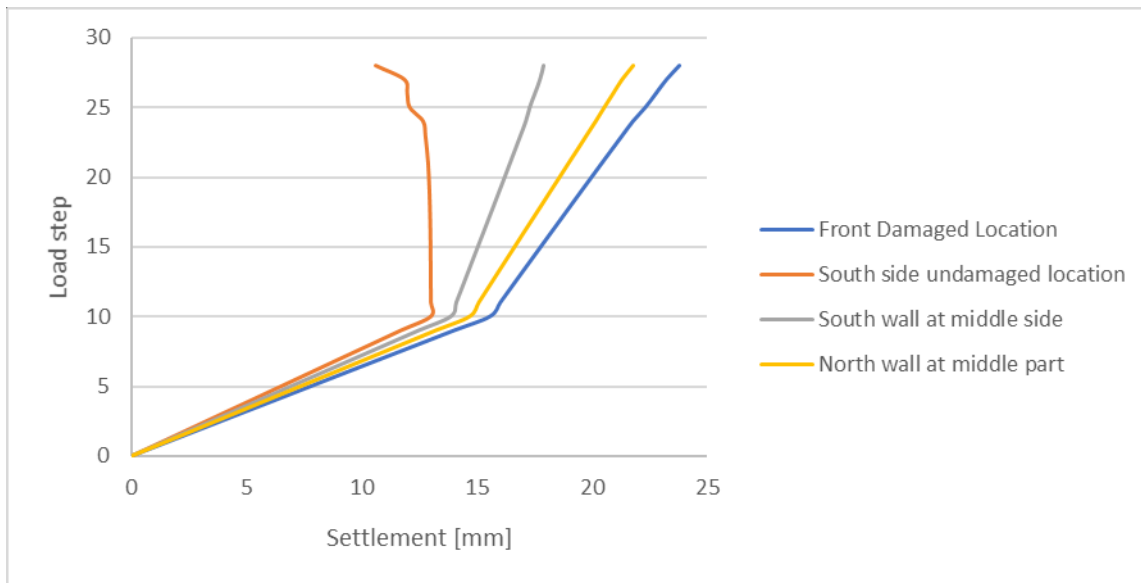
**Graph 3 - Plot showing evolution of settlements at different locations with load steps**

From the analysis it is also possible to observe the evolution of crack-width at the southern part of wall with respect to settlements at that part, from the Graph 4, it is possible to observe that until the soil settlement of 15mm, the crack was not formed and after the further increase in the settlement the crack was formed and the width is increasing with increasing settlement values.
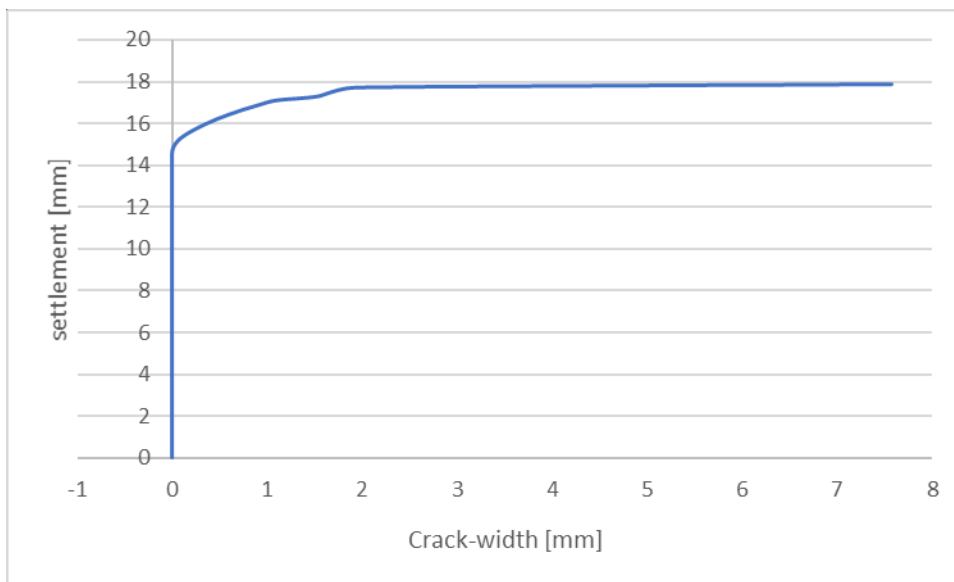


**Graph 4 - Evolution of crack-width with respect to soil-settlement**
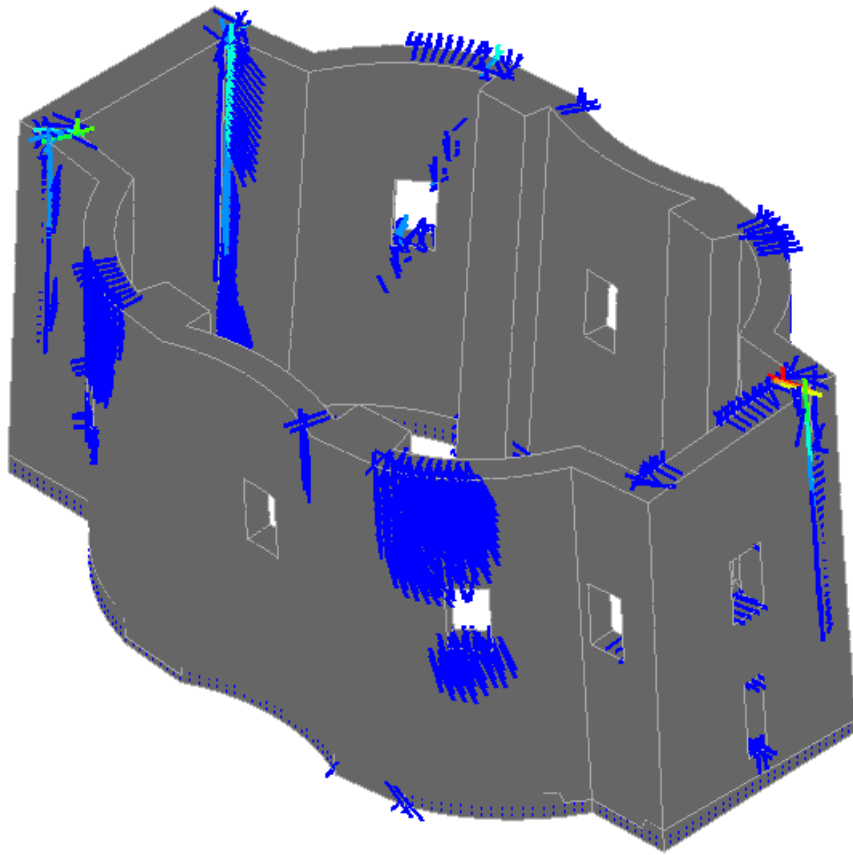
**Figure 5.15 - Crack strains in the 3D view**
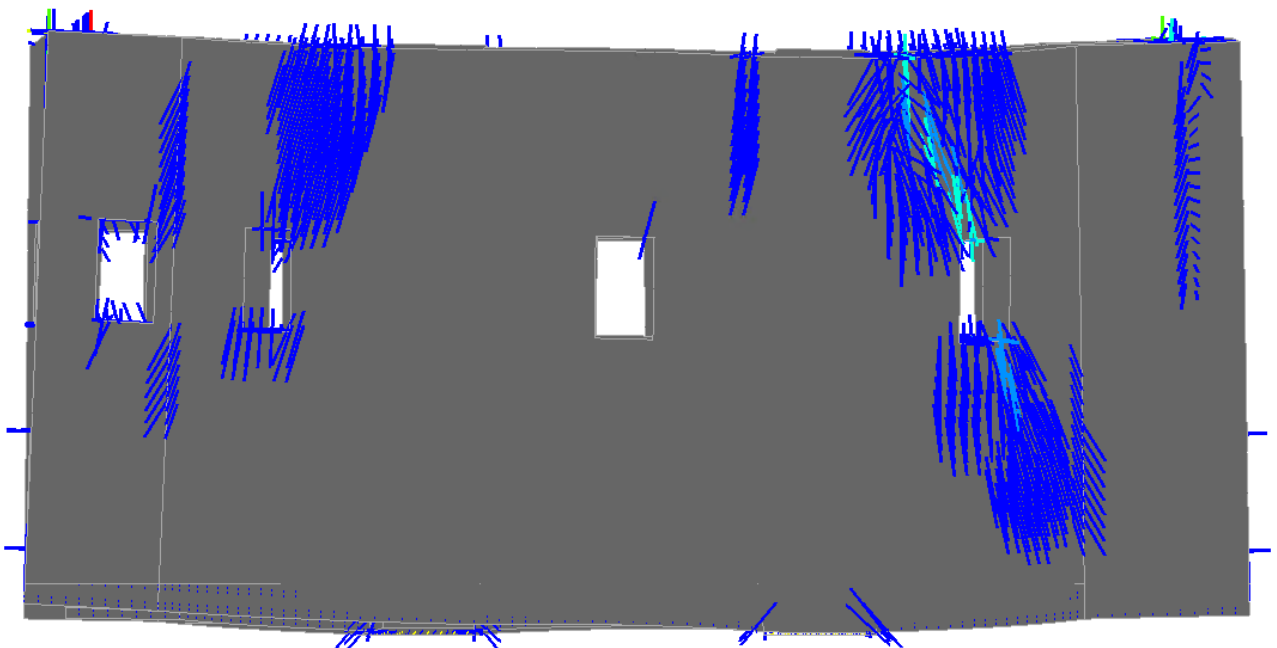


**Figure 5.16 - Crack strains at the north facade**
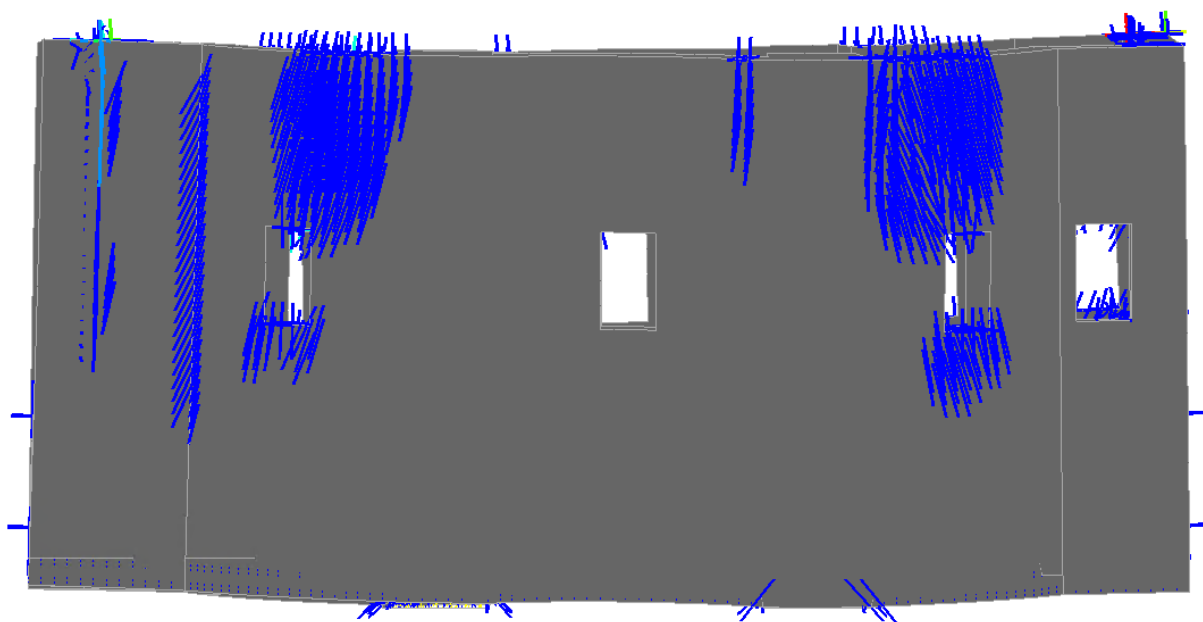
**Figure 5.17 - Crack strains at south facade**
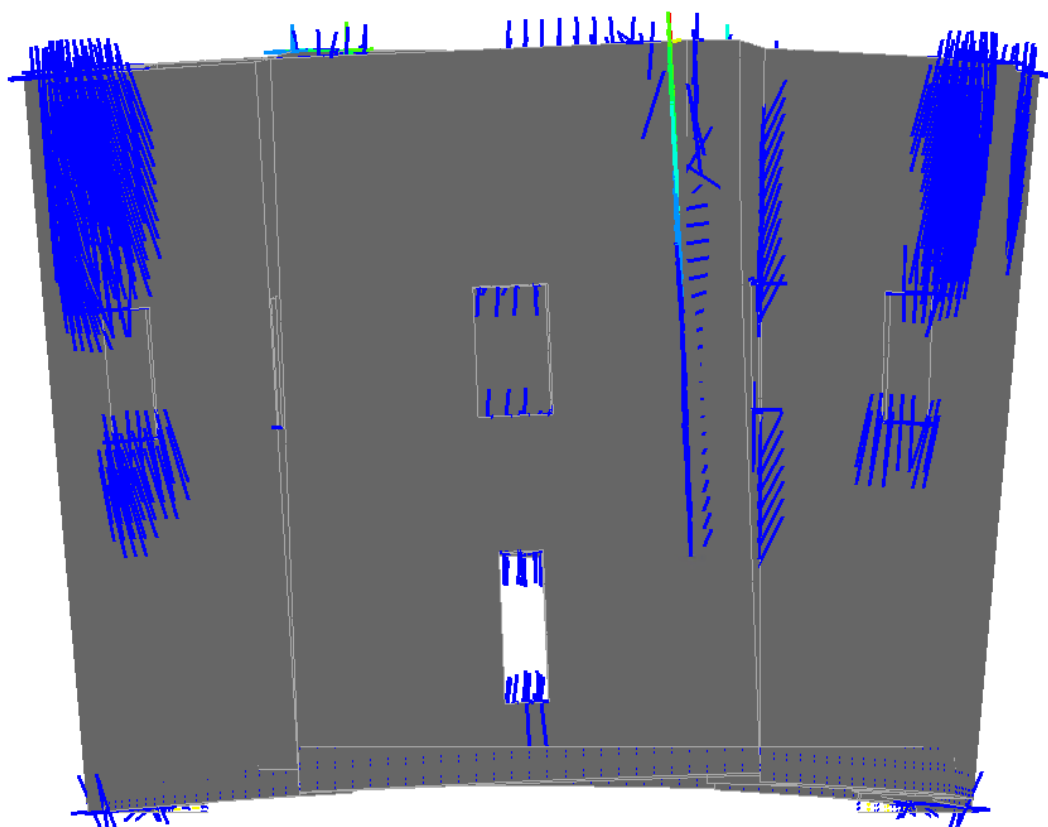


**Figure 5.18 - Crack strains at the West facade**
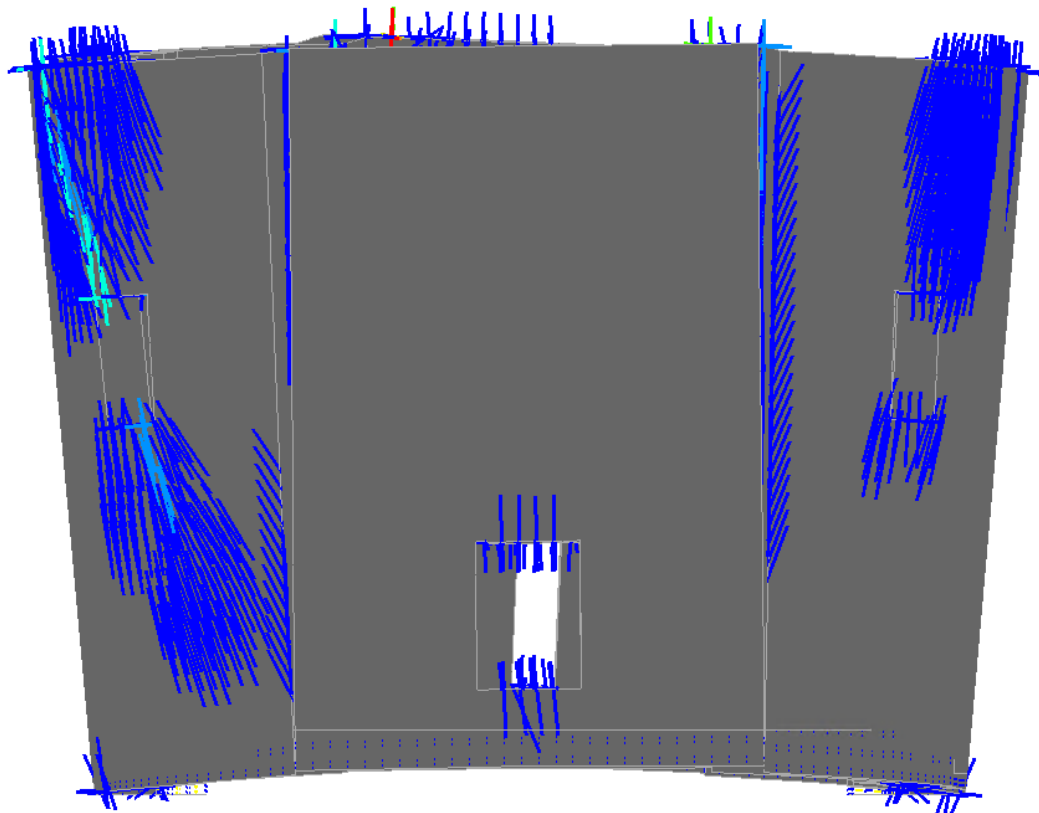
**Figure 5.19 - Crack strains at the east façade**

From the above figures, the crack strain obtained in the structures can be found which occurred due to the increased differential settlements. Here it is interesting to notice the that most of the crack strains that can be observed here were found to be in accordance with the damage observed on the site. From this, it supports the considered hypothesis behind the occurrence of damages (i.e. differential settlements).

# 6 CONCLUSIONS

From the works done on the St. Ann's church in Viznov, it is possible to arrive at the following conclusions.

From the previous works done on this church and as well as from the current visual inspection it was evident that the damage and decay of walls are due to groundwater infiltration, drainage system failure, due to the orientation of walls, and different settlements

The main source of differential settlement is an accumulation of ground and rainwater near the walls and its adverse effect on the sub-soil. From the research, it was also possible to observe that the problem of settlements is intensive at the northern side of the church. And the main source of damage is due to the incoming of groundwater from the uphill.

From the 2D analysis performed on the longitudinal and transversal wall configuration, it is possible to observe the failure patterns, which are mainly due to the failure of lime mortar at the joints in case of longitudinal wall sections and separation of leaves at the transversal wall sections.

From the same 2D analysis it is also possible to derive the safe load-bearing capacity of the walls in both longitudinal and transversal directions. From the analysis, it is possible to notice that the walls of the church are same for the current state of loadings as per the European standards.

Furthermore, from the 2D analysis, it is also possible to derive the homogeneous properties of the walls which are used afterward in the settlement and 3D analysis.

From the transversal analysis of soil-structure interaction using Geo 5, it is possible to observe the number of settlements at various locations of the structure where the soil is good or damaged. From this analysis, it is observed that without considering the damaged soil, structure have almost uniform settlement of 17.3 mm at west side to 17.9 mm settlement at the east side. When the effect of damaged sub-soil is considered at different locations the amount of settlement is much higher than the anticipated values.

With the 3D analysis of the church using spring foundation and mimicking the effect of the differential settlements as observed on the site, it is possible to correlate the damages observed on the site and a hypothesis can be derived that the damages observed on the site are mainly due to the differential soil settlements.

From this analysis, it is also possible to provide some short term and long term intervention methodologies along with the application of more tests and monitoring on the structure, which are listed in the below chapter.

# 7   RECOMMENDATION

The St. Ann church was constructed at the beginning of 18th century and even though some degradations and settlements can be observed from the overall assessment of the church, its condition can be stated as stable for the current state of damage and decays. Nevertheless, a monitoring system is recommended to be installed for a better understanding of the behavior of the church over a longer period of time. Maintenance is also a crucial factor in the longevity of the structure, postponing the need for major interventions. Furthermore, some proposals are given in order to take some preventive measurements for the safety of the church.

## 7.1   Further studies

However, the studies on the safe bearing capacity of the church walls have been performed in this case study with the help of numerical micro modeling which assumes the average properties of the material present in the masonry. To evaluate the actual state of the capacity of the structure, it is recommended to perform some non-destructive or minor-destructive tests on the structure to evaluate the mechanical parameters of the materials. Furthermore, it is also of the utmost importance to observe the behavior of the structure for a longer period to observe the damage and decay process with respect to the time which will allow for the better and minimal interventions.

### 7.1.1   Tests

In this case, study to evaluate the mechanical properties of the building stones, rebound hammer test was performed, from which, the mechanical parameter such as compressive strength can be correlated. But this test yields the superficial strength of the stone which is valid for only the 30-50 mm from the surface of the material, which does not give the properties of the inner materials. Moreover, the surface strength of the materials can be affected by the environmental decay and carbonation which makes the values of rebound hammer unreliable. To evaluate the material properties with a degree of confidence following NDT/MDT tests can be performed on the site.

**Georadar**

Ground penetrating radar is a non-destructive technique that employs radio waves by emitting a pulse and recording echoes that results from subsurface objects. The objectives for its use in the assessment of the St. Ann church can be used to understand the inner constitution of the wall, identify and quantify the damages and to assess the walls constitution.

**Sonic and Impact echo test**

The sonic and impact echo test is based on the principle of the speed of the sonic waves traveling through the materials, which can be useful to understand the quality and degree of damages of the materials. With the help of sonic test, it is possible to obtain the dynamic elastic modulus of the material which can be further used to predict the material properties of the material with some degree of confidence. Impact echo test can be used to evaluate the wall leaf thicknesses and also to predict the elastic modulus of the material, this test can be a complimentary test that can be performed with the sonic and georadar test.

**Core cutting and Single/double flat jack test**

While the above tests are non-destructive tests, which will not destroy the fabric of monument, the test will yield only the qualitative assessment of the material not the quantitative. To increase the level of knowledge about the church, it is necessary to have quantitative values of mechanical parameters of the materials with some minor-destructive tests, which is difficult to perform on a historical structure. But if these tests are allowed to execute on the walls, it can yield the quantitative values of parameters such as Young's modulus. Poisson's ratio, compressive strength, tensile strength, and density of the material. Two tests can be performed, first one is core-cutting, with which, it is possible to obtain the sample from the wall and perform the above-mentioned tests in the laboratory and the other one is single/double flat jack test, which can be performed in-situ and can yield the compressive strength and Young's modulus.

### 7.1.2   Continuous monitoring for a longer period
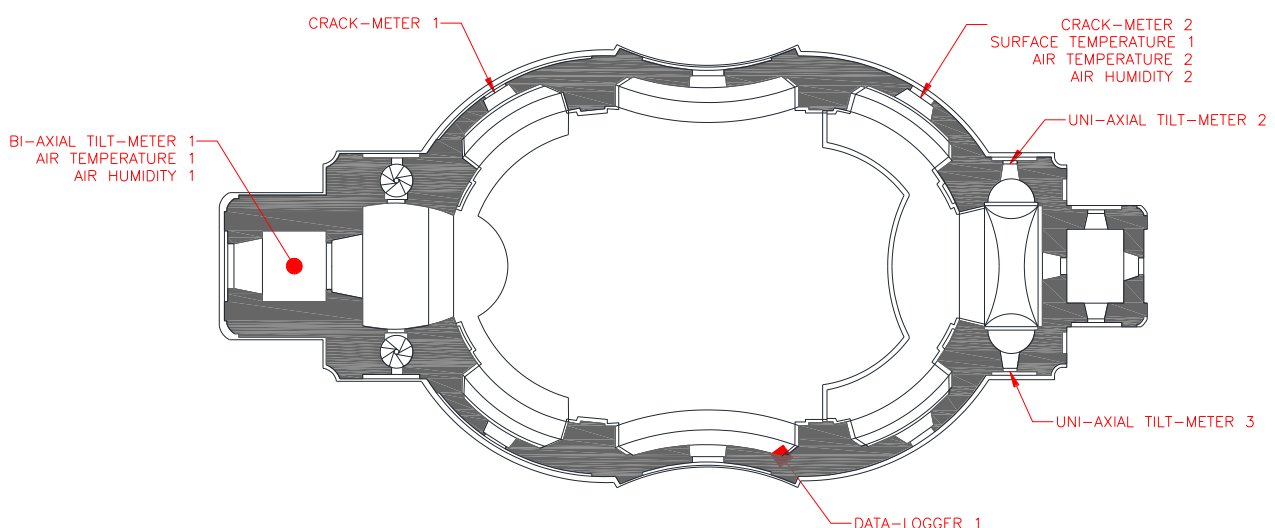


**Figure 7.1 - a Schematic diagram showing the location of proposed monitoring sensors**

To observe the current behavior of the structure and effectiveness of the proposed interventions, following monitoring techniques are proposed also shown in Figure 7.1.

The proposed system is composed of,

> One bi-axial tiltmeter to be installed at the top of the tower to observe the behavior of tilting of the tower due to differential settlement if any.
>
> Two uniaxial tiltmeters to be installed one each at the northern and southern wall as shown in above figure to observe the tilting of walls due to settlements if any.
>
> Three crack meters as shown in a plan to monitor the behavior of cracks with respect to environmental factors and due to the settlements.
>
> One surface temperature sensor near crack-meter 2
>
> Two combined sensors to measure air temperature and relative air humidity, one in the tower and another near crack meter 2.
>
> One datalogger for data acquisition, data record and remote communication.

From the installed monitoring system, it will be able to analyze the behavior of the structural damages in a long period of time, which will yield important information regarding the cause of the damages, whether that variations are due to environmental factors or structural damages. This monitoring system can also be useful after the intervention works are done to observe the post-intervention behavior and effectiveness of the executed interventions.

## 7.2 Immediate repair

From the current site inspection, it was possible to observe the current state of damages and decay of the walls and overall structure, from this observation, it was observed that the structure is in dire need of some immediate repair to consolidate the further damage and decay process occurring on the site. Some of the repair techniques are mentioned below, that can be employed on the structure as an emergency measure.

### 7.2.1 Drainage (Roof and Ground)

Major contributing factor regarding the current decayed state of the structure was observed to be due to the non-performing roof and ground drainage system, which allows rain and groundwater to accumulate near the walls and increases the decay process in both, the walls and sub-soil. This phenomenon is found to be the prime cause of the differential settlement which the structure is currently suffering from. As shown in Figure 7.2, it can be observed that the downspout to drain away the rainwater is not adequate and also the damages it can cause in walls due to capillary rise of water from the ground on walls.

**Figure 7.2 - non-performing rain water downspout (Left) damage in walls due to ground water in walls (Right)**

While it was also observed from the site that the works to upgrade the roof system and roof drainage is currently under progress, thus the proposed intervention method only focuses on the groundwater drainage the system can be observed in Figure 7.3.
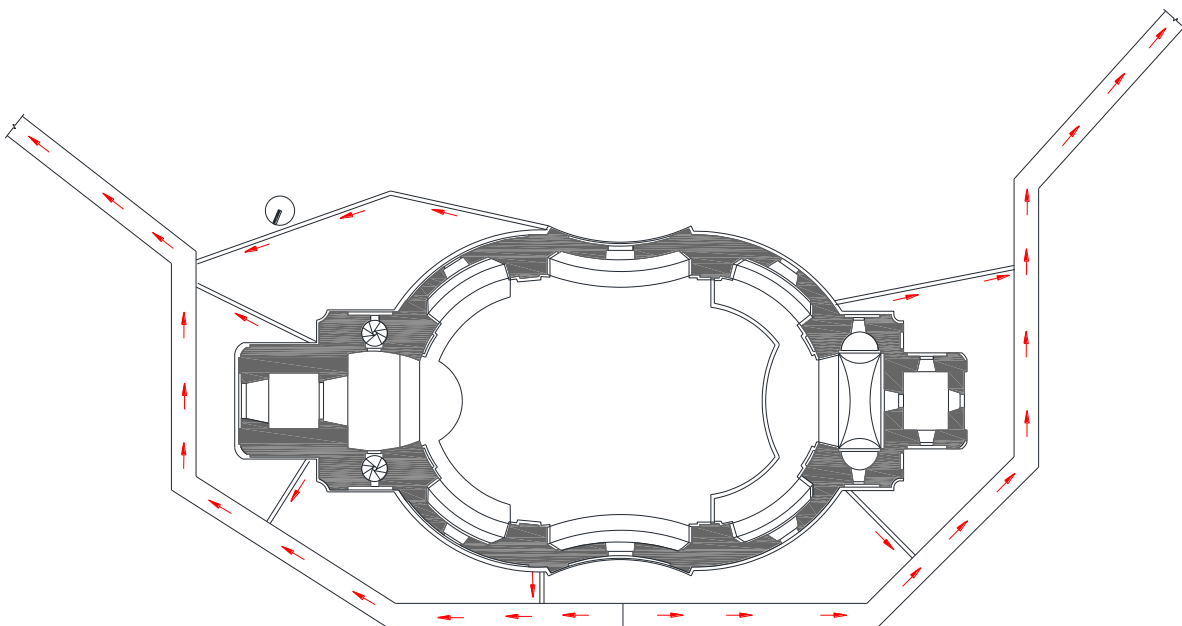


**Figure 7.3 - Schematic drawing showing proposed layout of the ground drainage system**

The idea behind this proposed groundwater drainage system is to drive away the drainage water as far as possible from the walls of the church. As it was observed from the previous studies and present study on this structure, the main problem of groundwater accumulation is at the north side where the groundwater comes from the uphill side as well as due to rainwater downspouts, the proposed system is designed to drive away the water from the walls, the detailed sections of the proposed drainage system can be observed in Figure 7.4.
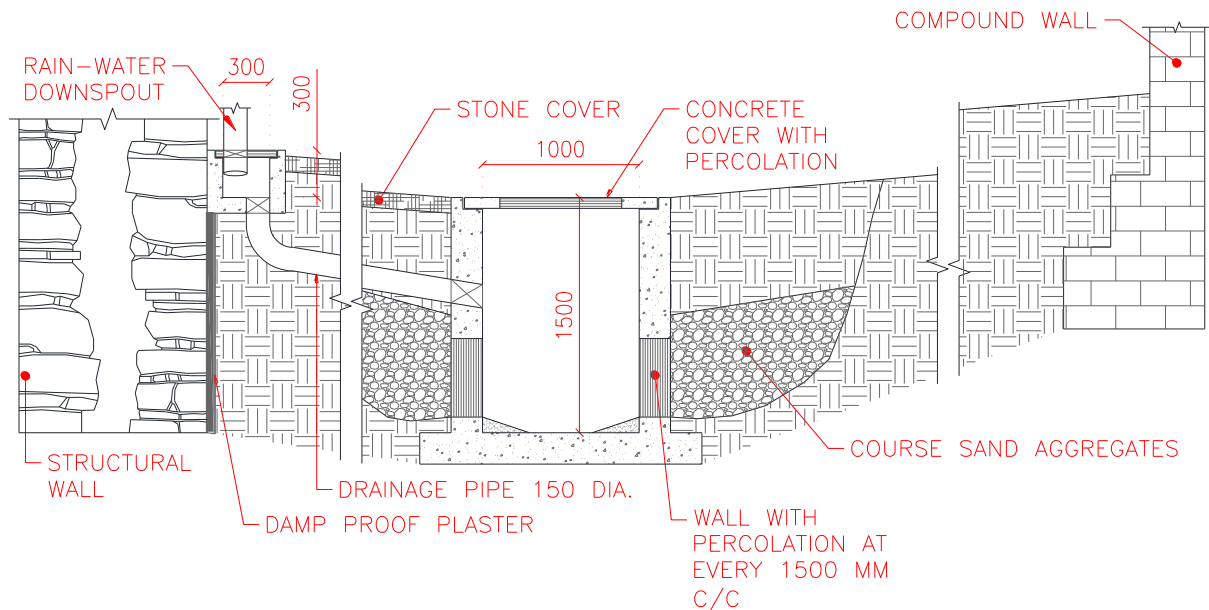


**Figure 7.4 - Section of Proposed rain and groundwater drainage system**

The philosophy behind this design was the drainage of not only the rainwater coming from the roof or the direct precipitation around the church wall but also to collect and drive away the groundwater coming from the uphill places. There are two elements of the design, one is the rainwater collection and drainage pit at every downspout and plinth protection along the outer side of wall in terms of damp proof plaster and stone cover to drive away the precipitated water, to collect the groundwater and maintain the level of groundwater, so that further decay of sub-soil can be stopped, a series of course sand aggregates is proposed on both side of the drainage line so that the groundwater could be filtered out and collected into the pit and any unwanted variation in the groundwater level can be stopped.

### 7.2.2    Re-pointing of masonry joints

From the visual inspection of the structure, it was observed that at many locations, especially at the lower part of southern wall, lime mortar was found to be missing as shown in Figure 7.5, which can be due to erosion of mortar, which ultimately allows the water ingress and expedites the process of

freeze and thaw cycles inside the masonry. To stop this disintegrating effect to happen further, it is recommended to re-point the mortar at the masonry joints, using suitable low-strength lime mortar.



**Figure 7.5 - Outer masonry wall showing missing mortar at some locations**

### 7.2.3    Re-Plastering on outside

As discussed in chapter 3.3, at many locations it was observed that the external rendering and plaster were either decayed or missing, which can be caused by the freeze and thaw cycles and capillary rise of water from the ground, this missing plaster, especially outside of the walls, can cause the further decay of masonry stones and mortar, due to its increased exposure to the atmosphere, to warrant this action, it is recommended to do re-plastering work using lime paster of low strength.

## 7.3    Long-term repair after monitoring

To have a proper intervention on the structure which is cost effective as well as the minimal intrusive, it is recommended to propose the major intervention works other than the one discussed earlier, after the long duration of continuous monitoring. From the continuing monitoring as proposed in the earlier chapter, it is possible to observe the on-going phenomenon of structural damage and its intensity. From those result, an effective measure of intervention can be chosen. However, here in following sections, some interventions that can be used are explained.

### 7.3.1 Grout injection in the walls infill and crack sealing

From the site inspection and 3D analysis of the structure, it is evident that the structure has some cracks that are the results of the differential settlement, it is also assumed here that in the effect of differential settlement and because the wall is made of the three leafs, there will be some separation between the leaf as well. To homogenize the wall once again it is recommended to use the ground injection and crack sealing after it is assured that the further problems of settlements are stopped.
The schematic and procedure of grout injection are illustrated in below figure. Here it is recommended to use the lime-based grout with low shrinkage and low water content.
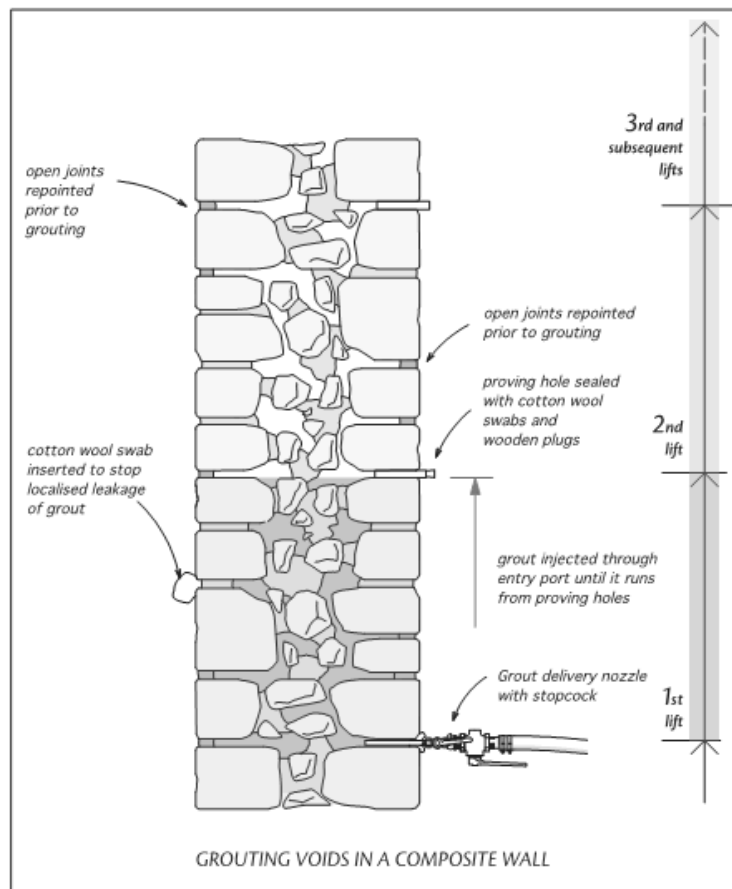


**Figure 7.6 - Grout injection procedure (building conservation, 2018)**

### 7.3.2 Micropiling or grout injection in soil at the degraded location

As from the analysis of this structure, it is evident that the structure is suffering from the problem of the differential settlement mainly due to the degradation caused by the groundwater and rainwater. To stabilize the further degradation of the subsoil, it is proposed to do the micro-piling operation or grout injection in degraded soil areas. The idea behind this method is to stabilize the sub-soil after the problems of groundwater are stopped with the implementation of groundwater drainage system as

proposed in this chapter earlier. The schematic of these intervention techniques can be observed in below figures.
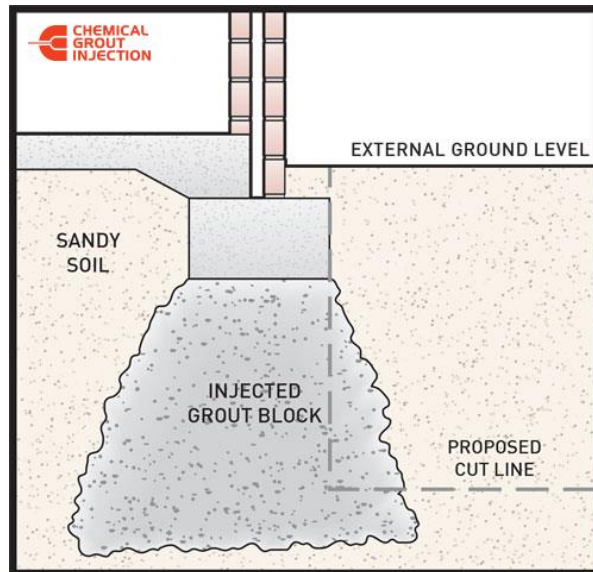


**Figure 7.7 - Schematic for grout injection of sub-soil (chemical grout injection, 2018)**
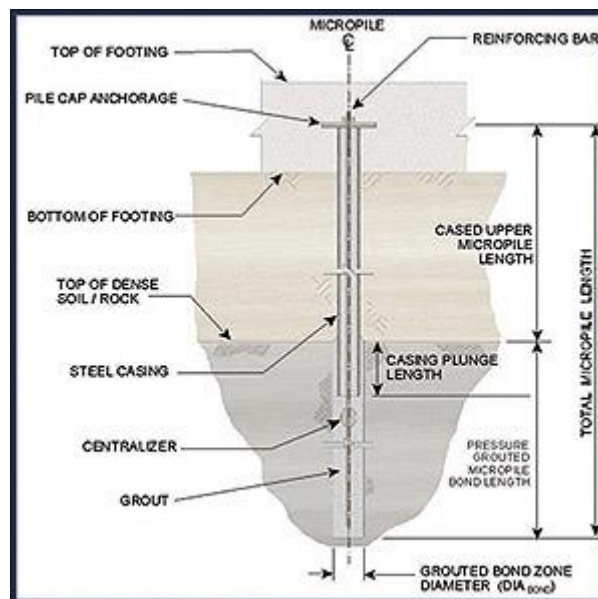


**Figure 7.8 - Schematic for micro-piling (engineered foundation, 2018)**

### 7.3.3    Periodic Maintenance plan

To maintain the good state of condition of the church it is also recommended to have a detailed maintenance plan which covers every aspect of the church be it structural or architectural elements. The advantage of this plan is to prevent the need for major intervention in longer durations, which are often intrusive and costly. To save the cultural and economic aspect of the heritage it is advantageous to have a detailed maintenance plan which can be divided into following parts.

Data information

Characterization; including past interventions, furniture, and other elements

Diagnosis; including damage mapping and management

Interventions; related mainly to the superficial problems

The plan can be defined as a very detailed, which includes every aspect of the church. Apart from this, it is also recommended to have a periodic inspection of the structure at every 6 months and at the same time minor interventions like cleaning of drainage routes, cleaning of biologically colonized area etc. shall also be performed. And if some structural problems are noticed, a more detailed inspection can be carried out and a probable intervention can be designed and implemented.

# REFERENCES

ˇSejnoha, M. (2009). *GEO FEM - Theoretical manual.* GEO FEM.

Angelillo M., L. P. (2014). *Masonry behaviour and modelling.*

ATENA. (2018). *ATENA Engineering Documentation.* Cervenka Consulting Ltd.

Borri, A. C. (2015). A method for the analysis and classification of historical masonry. *Springer Science*, 2647-2665.

Brénousky J.S., B. B. (n.d.). *Modelling the Interaction between Structure and Soil for Shallow Foundations.* Delft University of Technology.

CEN. (2005). *Eurocode 6: Design of masonry structures.* European Committee for Standardization.

Drdácký M., M. D. (2008). Compression tests on non-standard historic mortar. Historical Mortars Conference.

Duinker, P. (2009). *First and second order analysis of St. Anns' church timber roof in Viznov, CZR.* SAHC Dissertation.

ICOMOS-ISCS. (2008). *Illustrated glossary on stone deterioration patterns.* ICOMOS.

J. Válek, R. V. (2005). Characterisation of mechanical properties of. *Structural Studies, Repairs and Maintenance of Heritage Architecture IX*.

Peleška, O. (2108). *ASSESSMENT OF THE WATER TRANSPORT IN A SOIL-MASONRY SYSTÉM* Prague: CTU in Prague.

Proceq. (2017). *Operating Instructions SilverSchmidt & Hammerlink.* Proceq.

Susanti, E. (2017). *Numerical evaluation of the bearing capacity of the All Saints Church walls in Broumov, CR.* SAHC Dissertation.

Tourism, C. (2016). *Baroque - Czech Republic Through all the senses.* Czech Tourism.

Tourism, C. (2017). *Regions of the Czech Republic.* Czech Tourism.

Tourism, C. (2018). *Czech Tourism*. Retrieved from Czech Tourism: http://www.czechtourism.com/c/group-of-broumov-churches/

Vaconcelos, G. L. (2008). Experimental characterization of tensile behaviour of granites. *International Journal of Rock Mechanics and Mining Sciences*, 268-277.

Vasconcelos, G. &. (2008). Experimental Characterization of the compressive behaviour of granites. *Revista da Associação Portuguesa de Análise Experimental de Tensões*, 61-71.

*Vinyl Silhouettes.* (2018). Retrieved from Vinyl Silhouettes: http://www.vinylsilhouettes.com/prague-czech-skyline-decals
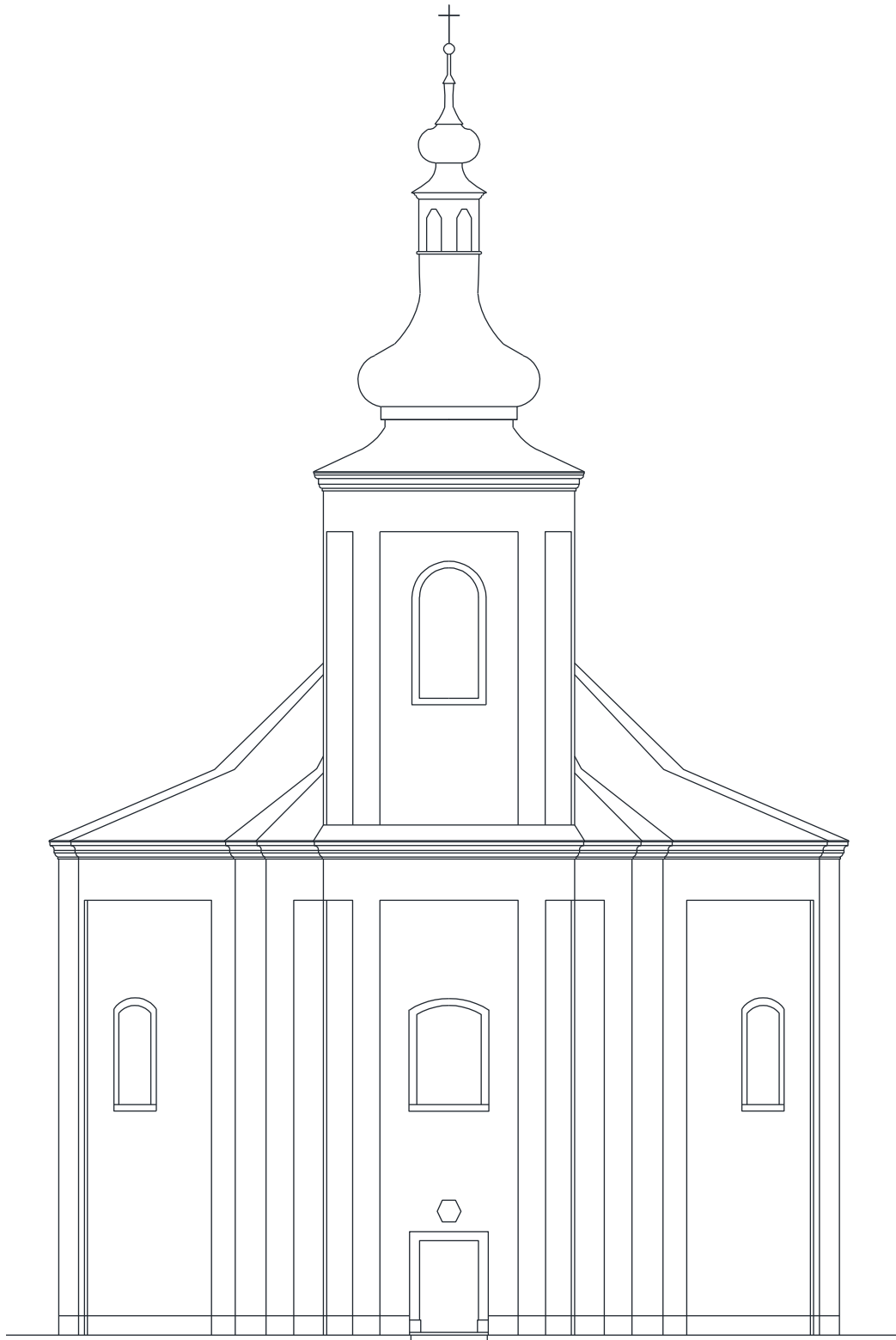
## APPENDIX A



**Figure A.1 - East Facade of the church**
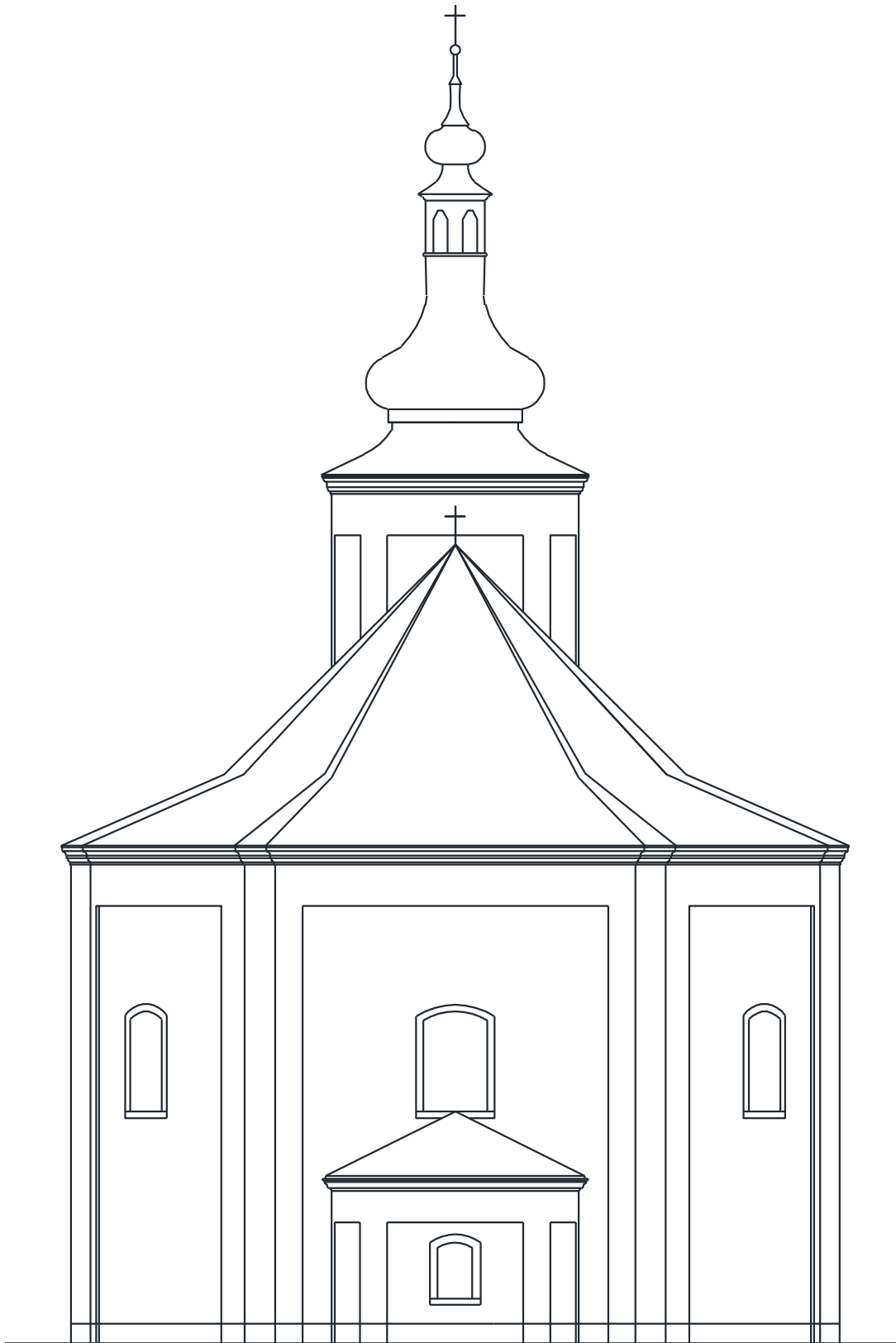
**Figure A.2 - West Façade**

**Figure A.3 - South Façade**

**Figure A.4 - North Façade**

## APPENDIX B

To calculate the current state of loading on the structure, the SAHC dissertation by Peter Nanning Duinker was referred. (Duinker, 2009)

From his assessment of loading on the structure, it is possible to come up with the state of loading on the structure from different loadings as shown in below Table.

**Table A - Table showing intensity of loading considered due to different load cases**

| Load | Value | Unit | Load on Unit Masonr (MPa) |
|---|---|---|---|
| Self-Weight (DL) | 20 | kN/m$^3$ | 0.336 |
| Roof Dead (DL) | 2.5 | kN/m$^2$ | 0.025 |
| Ceiling Dead (DL) | 2 | kN/m$^2$ | 0.02 |
| Roof Live (LL) | 1.5 | kN/m$^2$ | 0.015 |
| Ceiling Live (LL) | 0.5 | kN/m$^2$ | 0.005 |
| Snow Load (SL) | 0.62 | kN/m$^2$ | 0.0062 |
| Wind Pressure (WL) | 0.79 | kN/m$^2$ | 0.0079 |
| Wind Suction (WL | -0.26 | kN/m$^2$ | -0.0026 |

## APPENDIX C

**Table B - Borehole data of West side borehole**

| Distance from surface (m) | Description | Note | "Soil Type" |
|---|---|---|---|
| 0,00 - 0,50 | sandy soil with sandstone fragments above foundation masonry | | |
| 0,50 - 1,80 | ignimbrite fragments, 10 % of plate through the borehole diameter, sandstone fragments (size 40 mm to 80/100 mm) | **Footing Level at 1.80 m below ground** | |
| 1,80 - 2,00 | sharply disintegrating core, sediment | | **1** |
| 1,80 - 2,20 | grey-green sediment (siltstone to claystone), weathered, compact core | F1791, 325 kPa | **1+** |
| 2,20 - 2,35 | red-brown sharply disintegrated soil | 325 kPa | **1+** |
| 2,35 - 2,55 | greyreddish brouwnish layered claystone, plate-disintegrated, hard consistency | | **2** |
| 2,55 - 3,00 | sharply disintegrated rusty-brown silty claystone - disintegrated core, layered | | **2** |
| 3,00 - 4,00 | horizontal layers, sharply disintegrated, rusty-brown | > 500 kPa | **2** |
| 4,00 - 4,15 | as above, smudged, thiny layered, variable coloring, significantly lighter | | **2** |
| 4,15 - 4,80 | as above, hard consistency, sharply disintegrated core | | **2** |
| 4,80 - 5,00 | lighter rusty-brown color, soft consistency | | **2** |
| 5,00 - 5,50 | lighter rusty-brown color, harder consistency | > 500 kPa | **3** |
| 5,50 - 5,75 | aquiferous layer, significantly softer | | **3** |
| 5,75 - 6,15 | lighter rusty-brown color, hard consistency | | **3** |
| 6,15 - 6,28 | sandstone of greenish color (absence of Fe pigmentation), hard, non-compact | | **3** |
| 6,28 - 6,70 | lighter rusty-brown silty claystone, hard cosnistency | | **3** |
| 6,70 - 7,00 | aquiferous layer, disintegrated to small plates and small scraps | | **3** |
| 7,00 - 7,10 | rusty-brown silty claystone of lighter color | F 1792 - 93 | **3** |
| 7,10 - 7,15 | light rusty-brown silty claystone | | **3** |

| | | | |
|---|---|---|---|
| 7,15 - 7,50 | soft-plastic layer, sharply disintegrated silty claystone, soft consistency (probably due to drilling) | | **3** |
| 7,50 - 7,70 | consistency solid to hard, - harder plates with softer filling  (probably due to drilling) | | **3** |
| 7,70 - 7,95 | soft-plastic layer, with hard fragments (probably due to drilling) | | **3** |
| 7,95 - 8,00 | rusty-brown silty claystone, solid to hard consistency | > 500 kPa | **3** |
| 8,00 - 8,14 | soft-plastic consistency, very wet, hrader cores, soter filling matter | 100 - 500 kPa | **3** |
| 8,14 - 8,70 | green color (thanks to the clay minerals), solid to hard consistency | | **3** |
| 8,70 - 8,80 | soft-plastic consistency (probably due to drilling) | | **3** |
| 8,80 - 9,00 | light grey-green color, solid to hard consistency | | **3** |
| 9,00 - 9,55 | sharply disintegrated core, 10mm fragments max. | | **3** |
| 9,55 - 10,00 | light rusty-brown core, disintegrated to stone fragments of maximum size 80*25 mm | | **3** |
| 10,00 - 10,23 | as above, copmact core, hard consistency | | **3** |
| 10,23 - 10,36 | light grey-brown silty claystone, easy to disintegrate by hand, hard consistency, probably dominantly silty particles | F1794 | **3** |
| 10,36 - 10,57 | as above - compact core, hard consistency | > 500 kPa | **3** |
| 10,57 - 10,83 | significantly softer consistency, horizotal layeres of 2 - 3 cm thickness, soft filling matter (silty clay) | | **3** |
| 10,83 - 10,95 | grey-rusty-brown silty claystone, thin layers of green color, hard, lighter color then surrounding | | **3** |
| 10,95 - 11,36 | lighter rusty-brown color, silty claystone, hard consistency | 11,25 - F1795 | **3+** |
| 11,36 - 11,45 | rusty-gray-brown silty claystone + greenish layers, few sandy fraction, very fine to silty character | | **3+** |
| 11,45 - 11,50 | as above, lighter rusty-brown color, hard consistency | | **3+** |
| 11,50 - 11,65 | disintegrated core - light colored, layered, grey-rusty-brown, disintegrated to silt, easy to disintegrate by hand | F1796 - 97 | **3+** |
| 11,65 - 12,00 | dark grey silty claystone, compact, hard consistency | | **3+** |

**Table 15 - Borehole data at East Borehole**

| Distance from surface (m) | Description | Note | |
|---|---|---|---|
| 0,00 - 0,20 | red-brown, slightly sandy calcareous soil with small stone fragments | HCl reaction | |
| 0,20 - 0,40 | compact core of red-brown calcareous soil with fragments of paleoryolite and ignimbrite with fragments of claystone to siltstone, easy to break down by hand (not the stone fragments), green-grey concretions without Fe pigmentation | HCl reaction | |
| 0,40 - 0,60 | compact core of red-brown calcareous soil with fragments of paleoryolite and ignibrite with fragments of claystone to siltstone, easy to break down by hand (not the stone fragments) | HCl reaction | |
| 0,60 - 1,00 | red-brown fragments of ignibrite, hard | | |
| 1,00 - 1,60 | red-brown fragments of ignibrite, hard | | |
| 1,60 - 2,00 | compact pieces of grey-red mortar with stone fragments of different petrographical character (fragments size to 5 mm) | | |
| 2,00 - 2,50 | comapct fragments of hard grey calcareous siltstone to clay-silty limestone | | |
| 2,50 - 3,00 | compact pieces of grey-red mortar with stone fragments of different petrographical character (fragments size to 5 mm), piece of straw detected inside the sample | | |
| 3,00 - 3,60 | compact pieces of grey-red mortar with stone fragments of different petrographical character (fragments size to 5 mm) | Footing Level at 1.80 m below ground | |
| 3,60 - 4,30 | fragments of red-brown clay siltstone ca 8 cm x 3 cm, hard | | **1+** |
| 4,30 - 4,70 | layer of grey-green siltstone (lightly red colored), relatively hard, easy to break down to to small plates of 1 cm thickness | | **1+** |
| 4,70 - 5,30 | red-brown siltstone, fragments | | **1+** |
| 5,30 - 5,50 | red-brown siltstone, bigger fragments | in pieces | **2** |
| 5,50 - 5,80 | red-brown siltstone, spilled | | **2** |
| 5,80 - 6,30 | red-brown clay siltstone, hard fragments ca 5 cm | | **3** |
| 6,30 - 6,40 | red-brown claystone with grey streaks, comapact, solid, it is possible to berak down by hand | | **3** |
| 6,40 - 6,45 | red-brown claystone with grey streaks, comapact, solid, it is possible to berak down by hand | in piece | **3** |
| 6,45 - 6,90 | incoherent red-brown claystone with fragments of siltstone, grey smudged | spilled | **3** |
| 6,90 - 7,40 | compact core of red-brown caystone, grey smudged, easy to break down by hand to smaller pieces | | **3** |
| 7,40 - 8,00 | red-brown calcareous claystone to siltstone, hard | HCl reaction | **3** |

| | | | |
|---|---|---|---|
| 8,00 - 8,20 | compact core of red-brown caystone, grey smudged, easy to break down by hand to smaller pieces | | 3 |
| 8,20 - 8,40 | red-brown calacreous claystone to siltstone, hard | HCl reaction | 3 |
| 8,40 - 9,40 | red-brown claystone with portion of silt fraction, gre to green-grey smudged (thanks to clay minerals, without Fe pigmentation) | HCl reaction | 3 |
| 9,40 - 10,60 | layer of grey-brown claystone with siltstone fragments (size ca 2 - 3 cm), easy to break down by hand | | 3 |
| 10,60 - 12,00 | compact core of red-brown claystone with siltstone ragments, easy to break down by hand to smaller pieces | | 3+ |

# APPENDIX D
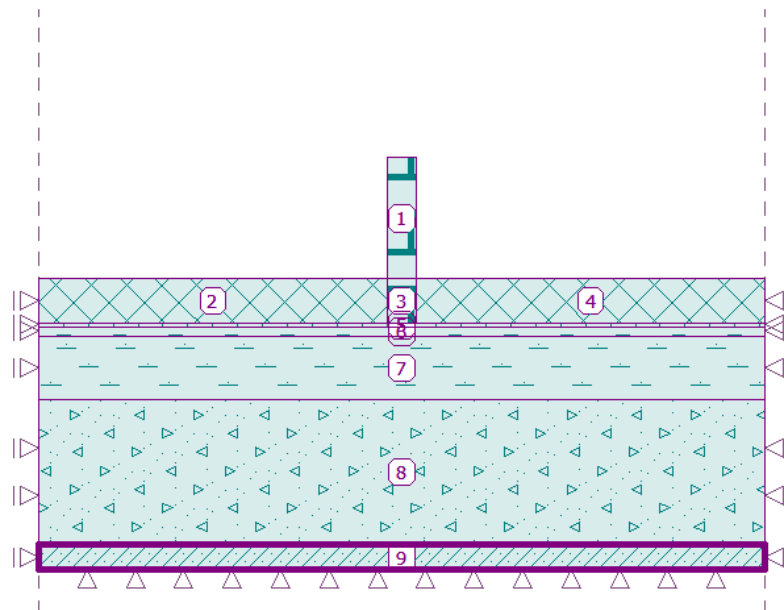


**Figure D.1 - Model Considered for Sacristy Wall**
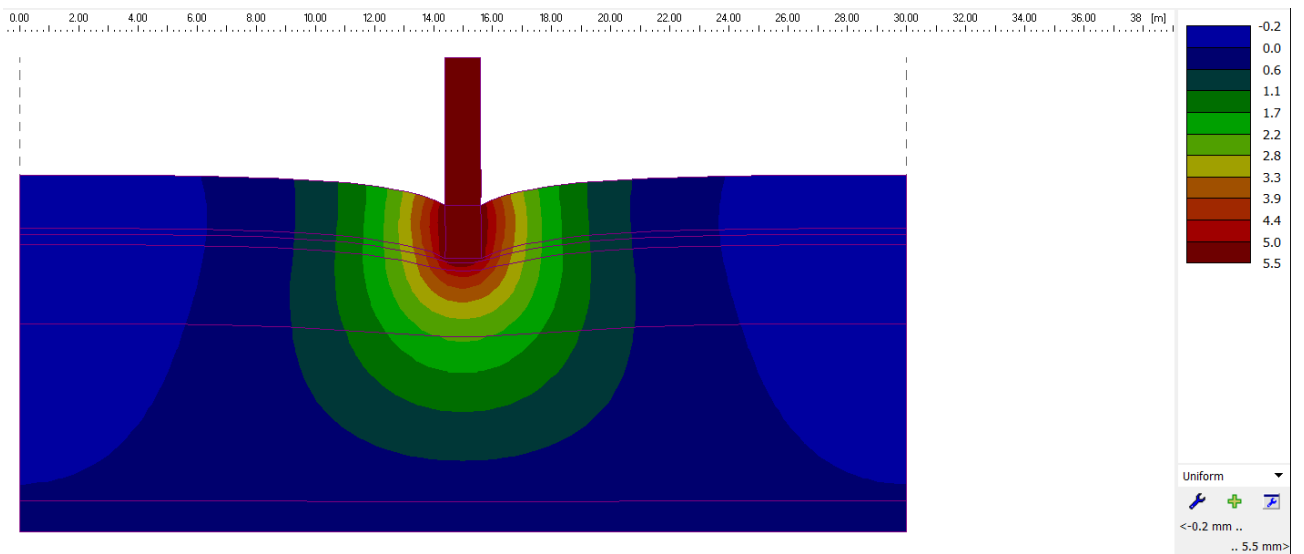


**Figure D.2 - Settlement Results of Sacristy Wall**
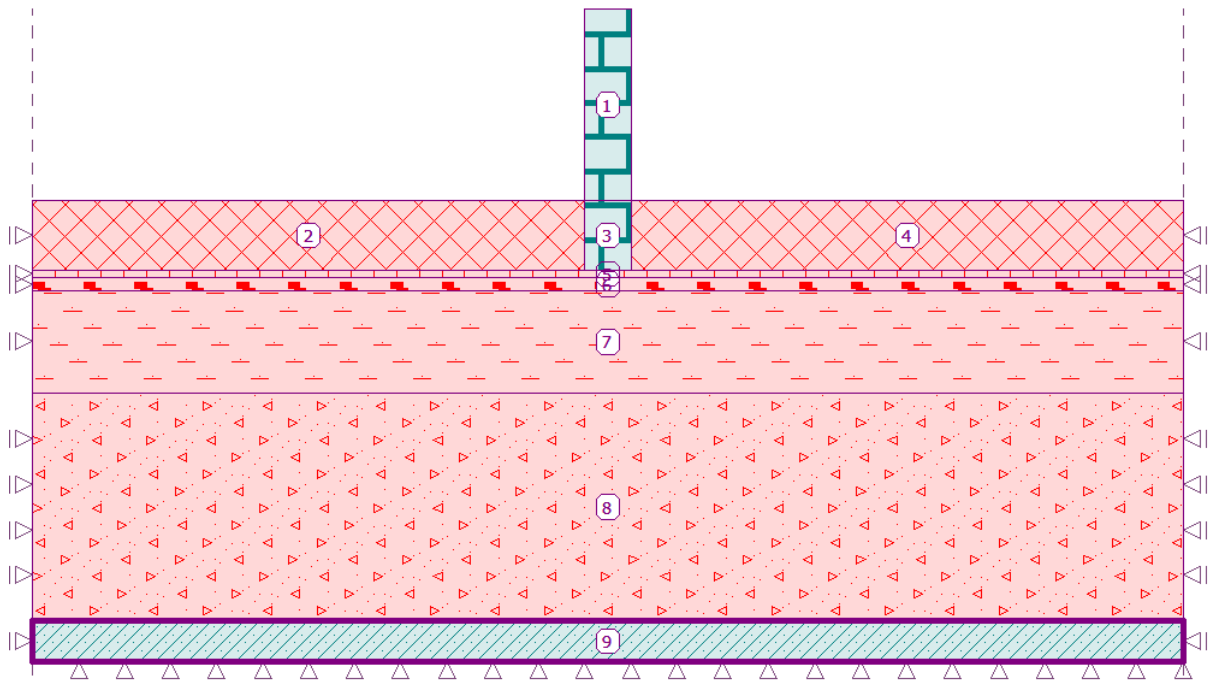
**Figure D.3 - Model Considered for Sacristy Wall in degraded condition**
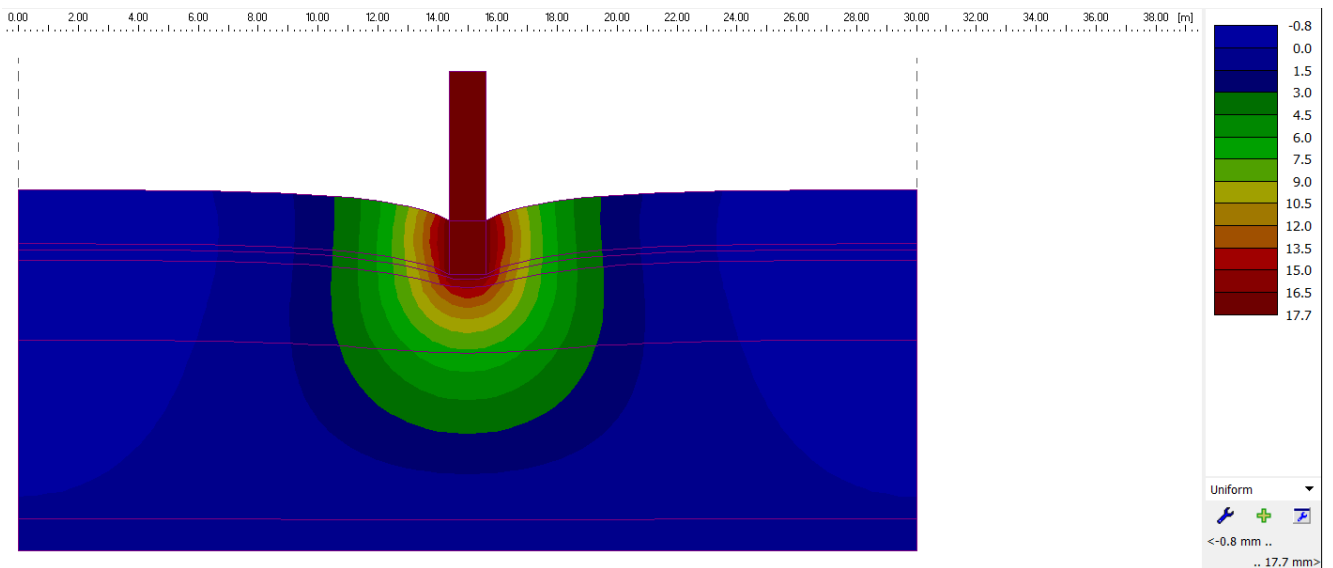


**Figure D.4 - Settlement results for Sacristy Wall in degraded condition**
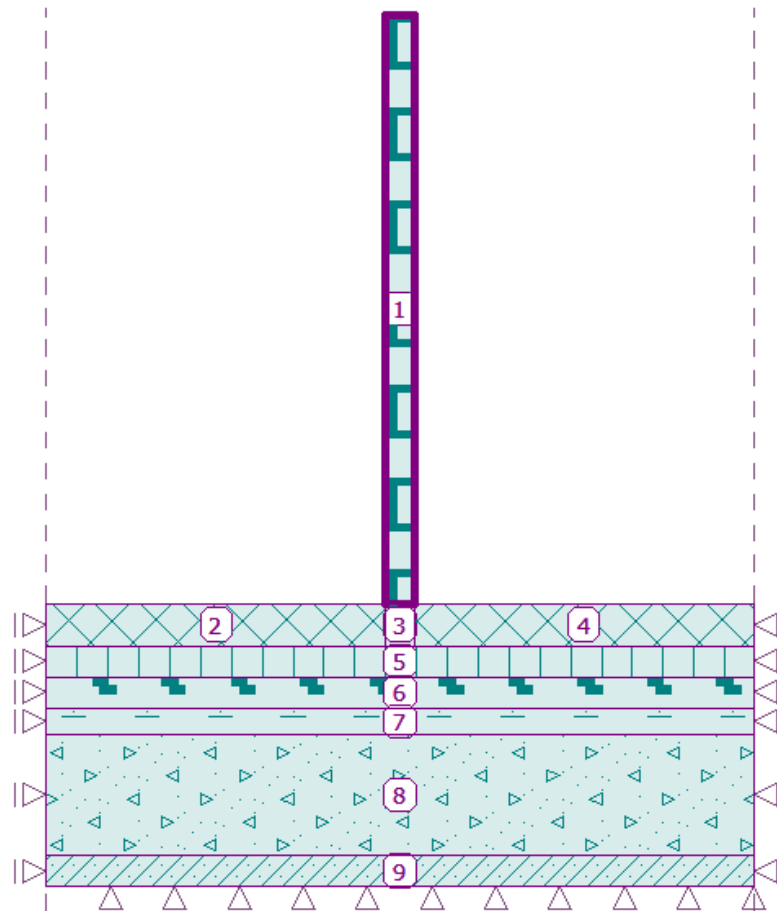
**Figure D.5 - Model considered for the Tower Wall**
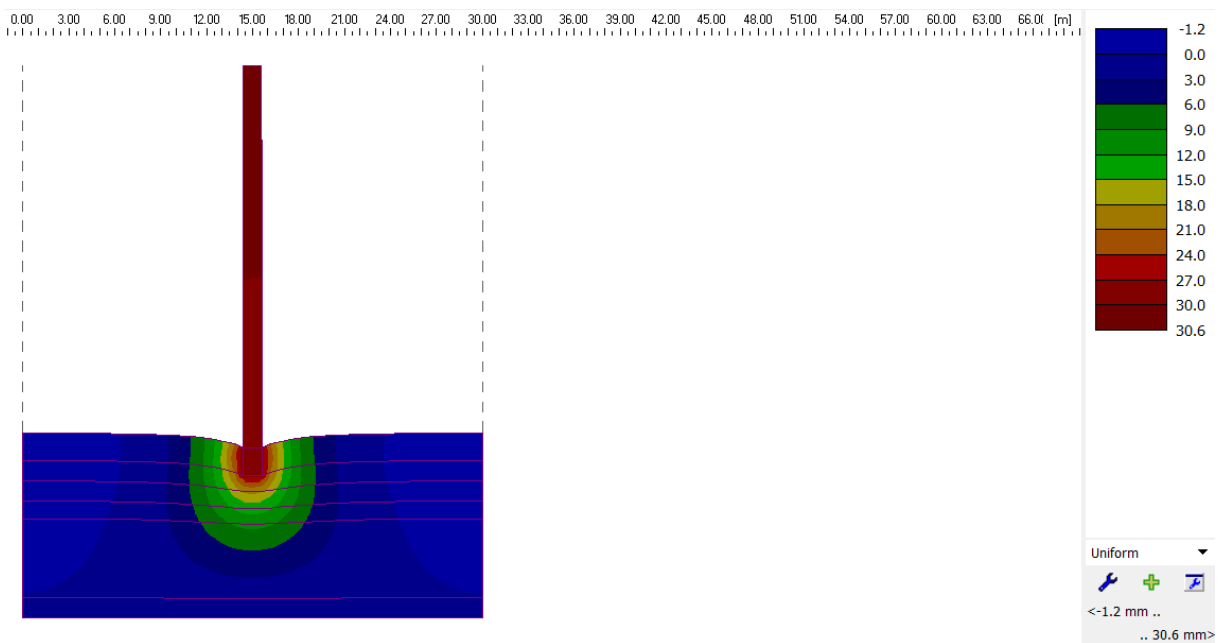


**Figure D.6 - Settlement results for Tower Wall**
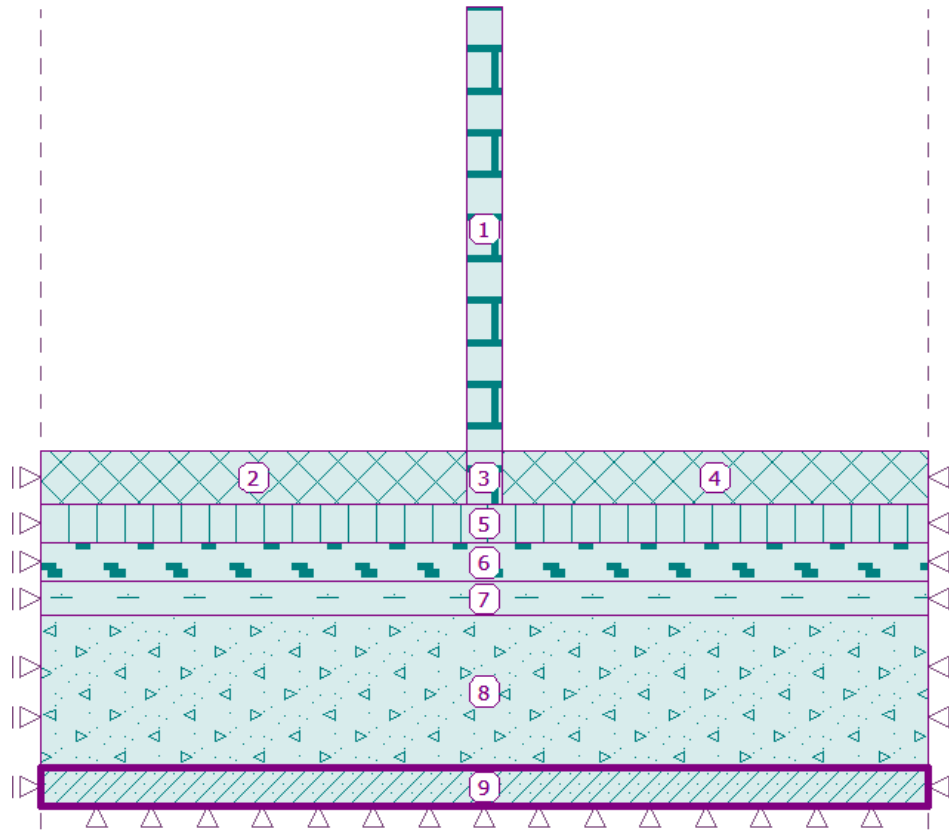
**Figure D.7 - Model Considered for the Front Main Nave Wall**
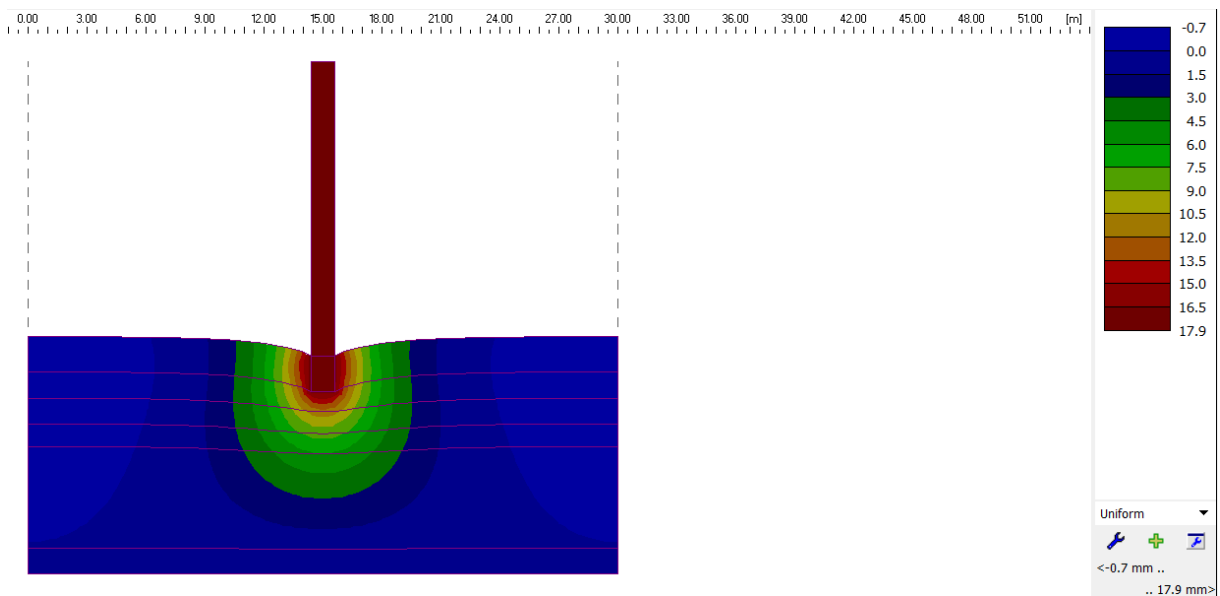


**Figure D.8 - Settlement results for the Front Main Nave Wall**
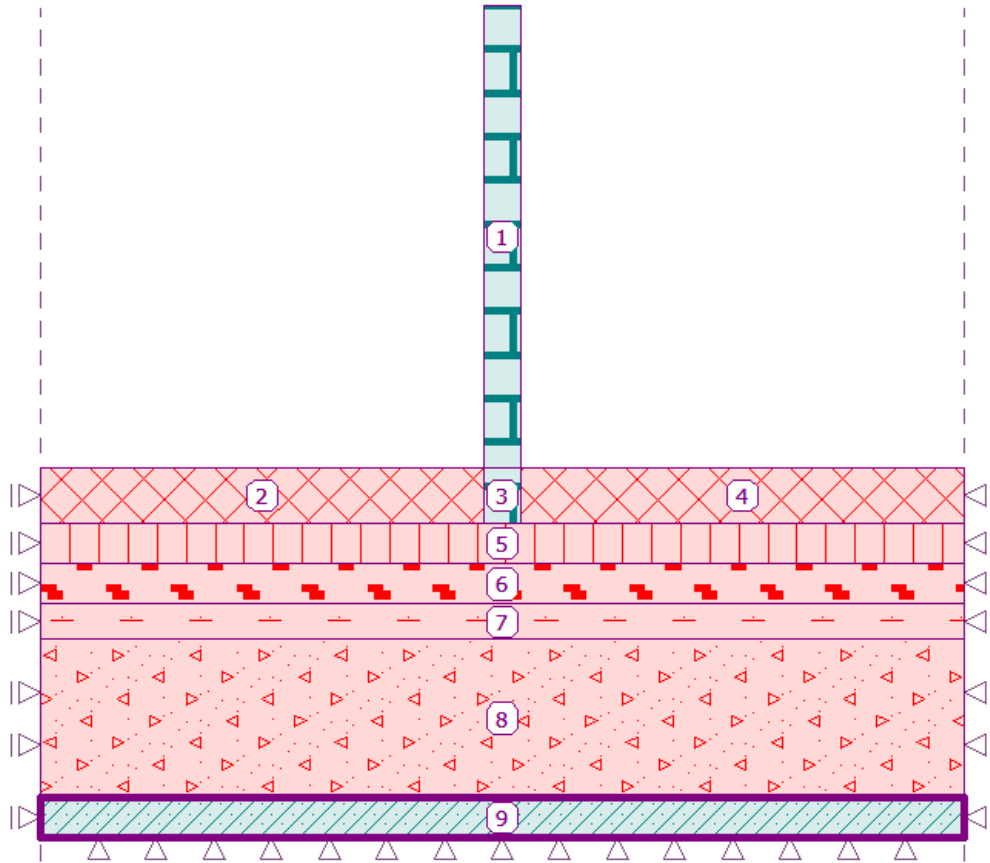
**Figure D.9 - Model Considered for the Front Main Nave Wall in degraded condition**
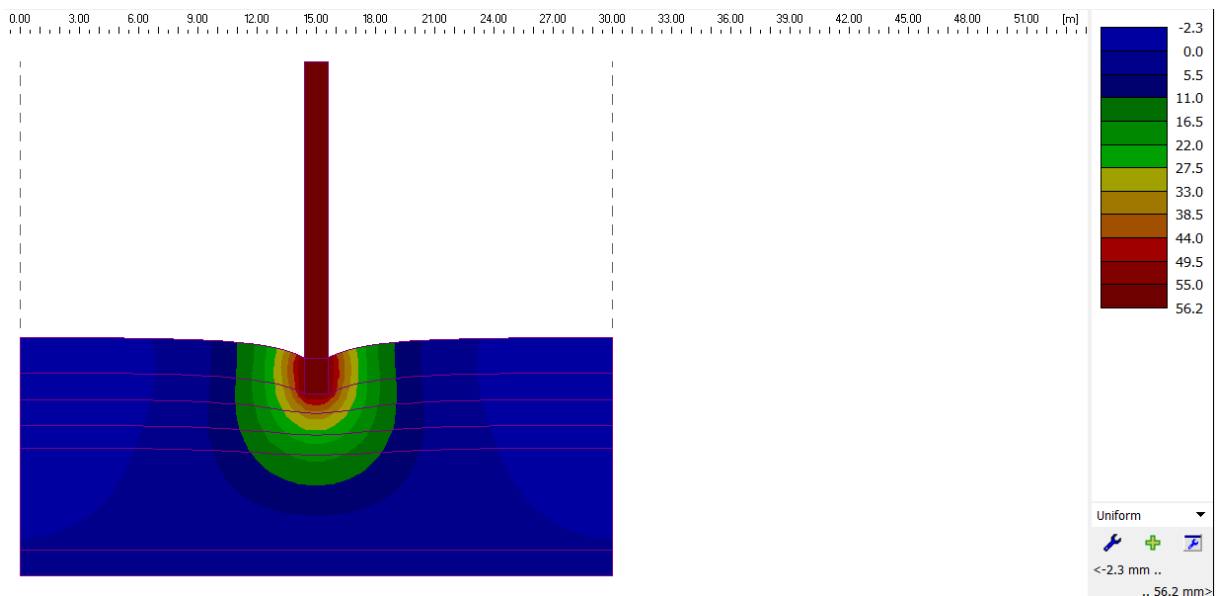


**Figure D.10 - Settlement results for the Front Main Nave Wall in degraded condition**